INTERACTIONS BETWEEN ADSORBED MACROMOLECULES

MEASUREMENTS ON EMULSIONS AND LIQUID FILMS

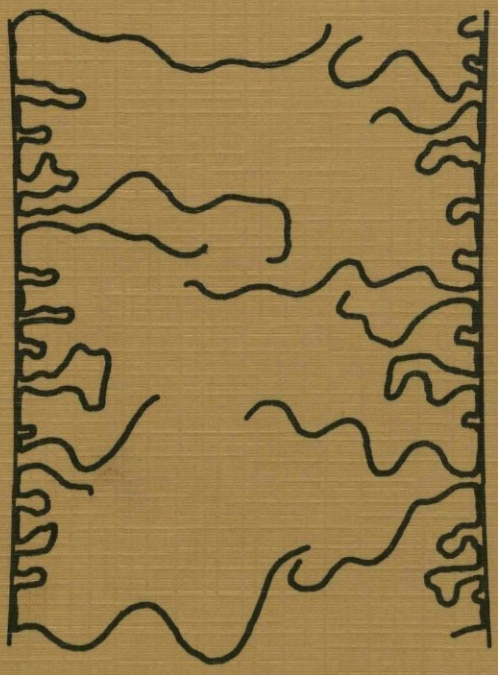

T. VAN VLIET

541.64–148:541.57
541.183.23

T. VAN VLIET

INTERACTIONS BETWEEN ADSORBED MACROMOLECULES

MEASUREMENTS ON EMULSIONS AND LIQUID FILMS

PROEFSCHRIFT

TER VERKRIJGING VAN DE GRAAD
VAN DOCTOR IN DE LANDBOUWWETENSCHAPPEN
OP GEZAG VAN DE RECTOR MAGNIFICUS,
DR. IR. J. P. H. VAN DER WANT, HOOGLERAAR IN DE VIROLOGIE,
IN HET OPENBAAR TE VERDEDIGEN OP VRIJDAG 18 MAART 1977
DES NAMIDDAGS TE VIER UUR IN DE AULA VAN DE
LANDBOUWHOGESCHOOL TE WAGENINGEN

H. VEENMAN & ZONEN B.V. – WAGENINGEN – 1977

STELLINGEN

1

De sterische wisselwerking tussen twee geadsorbeerde lagen van macromolekulen wordt vooral bepaald door de eigenschappen van de buitenste delen van de geadsorbeerde laag.

Dit proefschrift, hoofdstuk 5.

2

Reologie van sterisch gestabiliseerde dispersies is een uitstekende methode om wisselwerkingen tussen geadsorbeerde macromolekulen te bestuderen.

Dit proefschrift, hoofdstukken 4 en 6.

3

De bijdrage van staarten tot de eigenschappen van geadsorbeerde lagen van macromolekulen wordt vaak onderschat.

Dit proefschrift, hoofdstuk 5.

4

In tegenstelling tot zijn reputatie is het zeer de vraag of ureum hydrofobe bindingen verbreekt.

A. BEN-NAIM en M. YAACOBI, J. Phys. Chem. **78**, 170–175 (1974).

5

Graham en Phillips concluderen dat de splijtdruk en de dikten van de films tussen twee emulsiedruppels vooral de stabiliteit tegen coalescentie van door eiwitten gestabiliseerde emulsies bepalen, terwijl daarentegen bij schuimen de stabiliteit met name bepaald zou worden door de reologische eigenschappen van de geadsorbeerde eiwitlagen. Het is echter zeer wel mogelijk dat dit door hen gesuggereerde verschil een gevolg is van de door hen gekozen meetomstandigheden.

D. E. GRAHAM en M. C. PHILLIPS, in: Theory and Practice of Emulsion Technology, A. L. SMITH, Ed., Academic Press, London/New York (1976a); D. E. GRAHAM and M. C. PHILLIPS, in: Foams, R. J. AKERS, Ed., Academic Press, London/New York (1976b).

6

De door Dennis en medewerkers voorgestelde combinatie van stripping-voltammetrische experimenten ter bepaling van bromide, chloride en lood in stofdeeltjes uit de lucht is nodeloos ingewikkeld. Vermoedelijk is één enkel pulspolarografisch experiment minstens even doelmatig.

B. L. DENNIS, G. S. WILSON en J. L. MOYERS, Anal. Chim. Acta **86**, 27–34 (1976); J. A. TURNER, R. H. ABEL en R. A. OSTERYOUNG, Anal. Chem. **47**, 1343–1347 (1975).

7

De mogelijkheden voor toepassing van natuurlijke rode kleurstoffen ter vervanging van synthetische bij de bereiding van levensmiddelen, dienen niet overschat te worden.

8

Bij de productie van microbiëel eiwit dient bij voorkeur geen fossiele brandstof als koolstof- en energiebron te worden gebruikt, maar materiaal dat jaarlijks in grote hoeveelheden door de natuur geproduceerd wordt.

J. L. SHENNAN en J. D. LEVI, in: Progress in Industrial Microbiology, D. J. D. HOCKENHULL, Ed., Churchill Livingstone, Edinburgh/London **13**, 1–59 (1974); J. T. WORGAN, in: The Biological Efficiency of Protein Production, J. G. W. JONES, Ed., Cambridge University Press **20**, 339–361 (1973).

9

Propagandisten van het gebruik van wateronoplosbare minerale meststoffen leggen veelal te zeer de nadruk op de wisselwerking tussen een actief microbiologisch bodemleven en de opname van voedingselementen door de plant.

Commissie Onderzoek Biologische Landbouwmethoden, Alternatieve landbouw, Inventarisatie evaluatie en aanbevelingen voor onderzoek, Interimrapport november 1973, Pudoc, Wageningen (1974); B. MOSSE, C. Ll. POWELL and D. S. HAYMAN, New Phytol **76**, 331–343 (1976).

10

De wijze waarop Sekiguchi, Fujisawa en Ando de verschillen verklaren die 1-gesubstitueerde 2,4-dinitronaftelenen bij de vorming van anionische σ-complexen met alkoxyde-anionen te zien geven, is aan bedenkingen onderhevig.

S. SEKIGUCHI, S. FUJISAWA en Y. ANDO, Bull. Chem. Soc. Japan **49**, 1451–1452 (1976).

11

Aangezien de suggestie vermeden moet worden dat een bepaalde politiek christelijk is, omdat ze is uitgewerkt door mensen die het evangelie als richtsnoer van hun politiek handelen nemen, dienen de naam, de statuten en het huishoudelijk reglement van het CDA gewijzigd te worden.

12

Het verdient aanbeveling om de plaats van de inhoudsopgave van wetenschappelijke tijdschriften te normaliseren.

T. VAN VLIET
Wageningen, 18 maart 1977

VOORWOORD

Het doen van een onderzoek en het schrijven van een proefschrift erover is gelukkig veel meer het resultaat van een samenwerking tussen vele personen dan de titelpagina doet vermoeden. Zo heeft zowel de samenwerking met de mensen op het Laboratorium voor Fysische en Kolloidchemie als het samenwerken en leven met mensen daarbuiten het tot stand komen van dit proefschrift positief beïnvloed. Veel dank aan allen.

Toch wil ik enkele personen hier in het bijzonder noemen.

Willemien, jouw directe bijdrage aan dit proefschrift is moeilijk te quantificeren, maar daarom voor mij niet minder wezenlijk.

Vervolgens gaat mijn dank uit naar mijn ouders en zusters die thuis een zodanig klimaat schiepen dat de overgang van de boerderij naar het scheikundig onderzoek verrassend eenvoudig was.

Zonder de inspanningen van de leraren verbonden aan de Marnix M.U.L.O. te Maassluis en de Hogere Landbouwschool van het K.N.L.C. te Dordrecht was dit proefschrift nooit tot stand gekomen.

Beste Hans, hooggeleerde promotor, ik prijs me gelukkig dat je ruim negen jaar geleden gelijk had, toen je bij de uitslag van het propaedeutisch examen voorspelde dat we elkaar nog wel eens weer zouden zien. Het kunnen samenwerken met een zo kritische en mede daardoor sterk stimulerende persoonlijkheid als jij bent, is een groot genoegen. Dit zeker niet alleen om wetenschappelijke redenen. Hans, ik heb het als een voorrecht beschouwd om drie jaar onder jouw begeleiding bezig te kunnen zijn met een van mijn grootste hobby's.

Zeergeleerde van den Tempel, de vele keren dat we over interacties tussen geadsorbeerde macromolekulen en andere zaken konden praten werden door mij als leerzaam en genoeglijk ervaren. Daarvoor mijn hartelijke dank.

Het onderzoek naar de eigenschappen van door polymeer gestabiliseerde vrije vloeistoffilms kon gedaan worden dankzij het electronisch vernuft van Ronald Wegh en het technisch kunnen van Simon Maasland en Henny van Beek. Ik dank jullie voor de bouw van de benodigde apparatuur. Ook de studenten die in het kader van hun ingenieursstudie aan het onderzoek hebben bijgedragen ben ik zeer erkentelijk.

H. Chabot van Unilever Research Laboratory bedank ik voor het corrigeren van de Engelse tekst. De figuren werden zeer nauwgezet getekend door Gert Buurman, terwijl Marian Heitkamp-Rijckaert op onnavolgbare wijze het geschreven manuscript wist om te zetten in een net getypte tekst.

Het in dit proefschrift beschreven onderzoek was mogelijk door financiële steun van Unilever Research. De wijze waarop de samenwerking tussen het Laboratorium voor Fysische en Kolloidchemie van de Landbouwhogeschool en Unilever Research was geregeld moge model staan voor andere samenwerkingsverbanden.

CONTENTS

1. INTRODUCTION

1.1. INTERACTIONS BETWEEN ADSORBED MACROMOLECULES

Interactions between adsorbed macromolecules are responsible for several well known facts. Not only do they determine to a large extent the properties of products such as milk, but they also play an important role in processes such as paper production and water purification. Use of it is made in the stabilization of the foam layer on beer, but also in the destabilization of solid dispersions in liquids. By bringing about relatively minor alterations in the properties of adsorbed macromolecules, the ensuing interaction changes can be so dramatic that originally fluid systems become almost solid or vice versa.

For the study of the properties of adsorbed macromolecules it is expedient to distinguish between nonionic macromolecules (or nonionic polymers) and ionic macromolecules (or polyelectrolytes). The last mentioned class includes, for instance, the often relatively simple synthetic polyelectrolytes, most carbohydrates and derivatives of them and the usually more complex proteins. Because of the charged groups in the ionic macromolecules, the interactions between them are sensitive to the presence of electrolytes and to the pH of the solution. A well known example of this is the reaction of milk to the addition of Ca^{++} and/or to a lowering of pH.

Interactions between adsorbed macromolecules depend to a large extent on the way in which these macromolecules are adsorbed at an interface. JENKEL and RUMBACH (1951) were the first to propose that only a part of the segments of an adsorbed macromolecule are really in contact with the interface (train segments). The other segments protrude into the solvent as loops and tails. Because of this last phenomenon, the intra- and intermolecular interactions between the segments of adsorbed macromolecules are to a large extent also determined by the solvent quality. The direct influence of the nature of the adsorbent is, as a rule, much less pronounced than that of the solvent. In general the adsorption of macromolecules depends on the properties of the interface, the solvent quality and on the molecular weight and specific properties (like the flexibility) of the macromolecule. Reviews have been given by PATAT et al. (1964); STROMBERG (1967) and VINCENT (1974).

As yet, theories on macromolecular adsorption have been almost exlusively restricted to nonionic flexible homopolymers. FRISCH and SIMHA (1954; 1955 and 1957) developed the first theory of any consequence. More modern theories, based on the concept of trains and loops and/or tails have been developed by SILBERBERG (1962a, b; 1967 and 1968) and HOEVE (1965; 1966; 1970 and 1971). These theories do not only give an expression for the adsorbed amount, but they also describe the segment density distribution. All these theories presuppose the attainment of equilibrium. In general, the main experimental effects are qualitatively rather well described. Quantitative comparison with

experiments is still difficult, partly because it is not easy to measure the segment distribution unambiguously and partly because in practice equilibrium is seldom attained. A first extension of the polymer adsorption theories to the adsorption of polyelectrolytes has been given by HESSELINK (1972).

A first theoretical explanation for the interactions between macromolecules (steric interaction) adsorbed on different interfaces, has been given as long ago as 1951, by MACKOR and VAN DER WAALS (1951; 1952). It is based on the concept, that the conformational entropy of an adsorbed macromolecule is reduced on the approach of a second interface (the volume restriction effect). This effect is always repulsive, it counteracts the approach of both interfaces. FISCHER (1958) was the first, to point out that when two adsorbed layers of macromolecules interpenetrate the increased polymer segment concentration between the interfaces leads to a local 'excess osmotic pressure' (osmotic effect or mixing term). The mixing term can be either repulsive or attractive, depending on the solvent quality. A more elaborated theory based on this concept has been given by EVANS and NAPPER (1973b). MEIER (1967) and later HESSELINK et al. (1971b) combined the volume restriction effect and the mixing term in one theory. EVANS and NAPPER claimed that the mixing term, if correctly elaborated, already includes the volume restriction term. Reviews on steric interaction have been given by VINCENT (1974) and, especially for non-aqueous systems, by LYKLEMA (1968).

As shortly indicated, there is no generally accepted steric repulsion theory at the moment. Experiments on the direct determination of the steric repulsion as a function of the distance between two interfaces covered by adsorbed polymer layers are scarce. For instance, DOROSZKOWSKI and LAMBOURNE (1971 and 1973) measured directly the steric repulsion forces between polymer layers, adsorbed on spherical lates particles. They made compression studies with these particles spread at different interfaces, using a surface balance technique. Although the agreement between their experimental results and the theoretical predictions was encouraging, more experimental results are necessary in order to test the present theories and to indicate ways to improve them.

By studying interactions between adsorbed macromolecules one has to take into account more specific interactions between the polymer segments, for instance electrostatic and hydrophobic interactions. They are in a complicated way incorporated in the mixing term. In special cases they can dominate over the other terms. Hydrophobic interactions are specific for aqueous solutions (TANFORD, 1973). They can occur between non-polar groups in a macromolecule. The importance of electrostatic and hydrophobic interactions in determining the properties of adsorbed proteins has been emphasized by for instance NORDE (1976). Interactions between different macromolecules are still more complicated.

Although such interactions are of great practical interest (for instance SHERMAN, 1968; ROBERTS, 1976), there are only a few basic studies on it with well-defined macromolecular systems (for instance BÖHM and LYKLEMA, 1976). Attention must be paid to both interactions between the segments in

one adsorbed macromolecule *(intramolecular)* and those between different macromolecules in one adsorption layer or adsorbed on different particles *(intermolecular)*.

The aim of the present study is to gain more insight in the factors, determining the inter- and intramolecular interactions between adsorbed macromolecules. To that order, several experimental and theoretical approaches will be followed using well-defined systems.

In this study interactions between adsorbed macromolecules will be studied by measurements on thin free liquid films and emulsions. Two different macromolecules will be used: a nonionic one, polyvinyl alcohol (PVA) and an ionic one, a copolymer of methacrylic acid and the methyl ester of methacrylic acid (PMA-pe). The well known nonionic polymer PVA can be used in order to check the predictions of the steric interaction theories. The weak polyelectrolyte PMA-pe is a much more complicated macromolecule. In bulk solution it shows a conformational transition as a function of the charge density on the chain. This is a result of the prominence of special attraction forces between the methyl groups (MANDEL and STADHOUDER, 1964). Therefore this polyelectrolyte is especially suitable for the study of the influence of specific interactions between segments, on the interaction between two adsorbed layers of macromolecules. In a provisional publication (VAN VLIET and LYKLEMA, 1975) it was shown that the intramolecular interaction in free polymethacrylates and the intermolecular interaction between adsorbed polyelectrolytes are very similar.

There are a few workable ways to investigate interactions between adsorbed macromolecules. Their strong influence on the flow properties of dispersed systems (BÖHM and LYKLEMA, 1976) immediately point to one possibility, namely through rheological measurements. In these kinds of measurements the reaction of a system upon application of a stress or a strain on it, is recorded as a function of time. The interpretation of rheological properties of dispersed systems in terms of particle interactions has been elaborated by, for instance VAN DEN TEMPEL (1961; 1963); PAPENHUIZEN (1972) and STRENGE and SONNTAG (1974). BÖHM and LYKLEMA (1976) showed that in the case of polyelectrolyte stabilized emulsions, the interactions between the adsorbed macromolecules determine to a large extent the rheological properties of these emulsions. In an analogous experiment, the interactions between the macromolecules adsorbed at one liquid-liquid or liquid-gas interface can be studied by surface rheology.

The same factors that govern the stability of dispersed systems, influence the behaviour of free liquid films. Therefore soap films are used as a tool to study double layer repulsion and VAN DER WAALS attraction (LYKLEMA et al. 1965a; SHELUDKO, 1967). In the same way polymer stabilized thin free liquid films can be used, to study the steric interaction between two adsorbed layers of macromolecules.

1.2. Outline of this study

As indicated above the aim of this study is to gain more insight in the interactions between adsorbed macromolecules. To that purpose measurements have been done on free liquid films and emulsions stabilized by macromolecules (PVA and PMA-pe).

In the first part of this study the interactions (Coulombic, van der Waals and hydrophobic ones) between the segments in the PMA-pe molecules will be examined. Their influence on the conformation of PMA-pe molecules in the bulk solution and adsorbed at an interface will be investigated. Extensive attention will be paid to the relation between intra- and intermolecular segment-segment interactions and the rheological properties of emulsions, stabilized by PMA-pe. In the rheological measurements, pH, salt concentration and bivalent cation concentration are important variables.

The properties of thin free liquid films, stabilized by PVA and PMA-pe, will be discussed in the second part. The equilibrium thickness and the drainage behaviour of the films will be determined. For PVA films, the free energy of steric repulsion will be calculated as a function of the overlap between the adsorbed polymer layers and compared with theoretical predictions by the Hesselink et al. (1971b) theory. The results lead to new ideas on the density distribution of the segments of adsorbed PVA at an aqueous solution-air surface.

The influence of the interactions between the segments in the PMA-pe molecule on the properties of the films stabilized by this polyelectrolyte, will be discussed.

The rheological properties of viscoelastic emulsions stabilized by PMA-pe, are studied in the last part. Dynamic and creep measurements will be reported. A semiquantitative model is discussed, relating the shear modulus of the emulsions with the interaction forces between the emulsion droplets.

It will appear that the information, derived from the various techniques fits well together to further our insight in the interaction forces in the macromolecules studied.

2. CHARACTERIZATION OF MATERIALS

2.1. GENERAL

All chemicals used were analytical grade. Solutions were prepared with distilled water.

2.2. PARAFFIN

For the emulsion experiments, paraffin, which is virtually insoluble in water, was selected as the oil phase. Liquid paraffin from Merck A. G., Darmstadt, Germany, with a density of 880 $kg.m^{-3}$ was used. Its viscosity at 25 °C was about 0.08 $N.s.m^{-2}$.

2.3. GLYCEROL

To the polymer solutions, which were used in case of the free liquid film experiments, 1 M glycerol was added. We used glycerol from Merck A. G., Darmstadt, Germany, twice distilled, with a water content of 12–14%. Its density was about 1230 $kg.m^{-3}$.

2.4. COPOLYMER OF METHACRYLIC ACID AND THE METHYL ESTER OF METHACRYLIC ACID

2.4.1. *Synthesis and properties*

In this study, a copolymer of methacrylic acid and its methyl ester in the molar ratio 2:1, further abbreviated as PMA-pe, was used. The structural formula is shown schematically in fig. 2–1. The polyelectrolyte was manufactured by Röhm A. G., Darmstadt, Germany, and commercially available as Rohagit S, low viscosity grade. The polyelectrolyte has been prepared by a pearl polymerisation of a mixture of the two monomer components, as described by DBP 947115 (1956). A detailed description of the manufacture and the properties of the used PMA-pe has been given by BÖHM (1974) and VÖLKER (1961a; 1961b). The composition has been checked by titration and elementary analysis (BÖHM, 1974). The most relevant properties characterizing the poly-

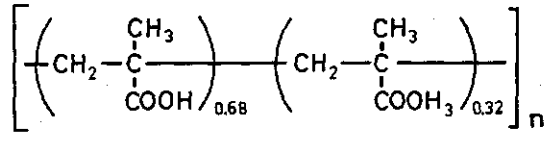

FIG. 2-1. Structural formula of the copolymer of methacrylic acid and the methyl ester of methacrylic acid (schematic).

TABLE 2-1. Properties of PMA-pe.

Degree of polymerization	~1000
Viscosity average molecular weight M_v	$\sim 10^5$
Percentage acid groups	67.6%
Percentage ester groups	32.4%

electrolyte are summarized in table 2–1. The distribution of the ester groups is supposed to be random.

The polyelectrolyte does not dissolve in water, but only in alkaline solutions. In order to prepare Na-PMA-pe solutions, the following procedure was adopted: to a weighed amount of the polyelectrolyte, the alkaline solution was slowly added under constant stirring. The addition of the alkaline solution was stopped when complete neutralization was reached. It is possible to decrease the degree of neutralization α of the dissolved PMA-pe by adding HCl, without precipitation. The lowest degree of neutralization which can be obtained depends on the ionic strength, for instance $\alpha_{min} = 0.00$ in 0.02 M NaCl and $\alpha_{min} = 0.08$ in 0.2 M NaCl. In order to avoid degradation of the PMA-pe, the dissolution procedure should be carried out in the dark (VÖLKER, 1961a; 1961b). Ca-PMA-pe solutions were prepared following a different procedure. Weighed amounts of PMA-pe and dry $Ca(OH)_2$ were mixed, after which water was slowly added to the mixture under constant stirring. After dissolution of the polyelectrolyte, α can be reduced to about 0.10 by the addition of HCl.

2.4.2. *The conformational transition of polymethacrylates*

Polyelectrolytes of the polymethacrylate type have the interesting property that as a function of the pH they occur in two different conformations. This is in contrast with most other polyelectrolytes. At low pH, polymethacrylates occur in a compact form: the hyper-coiled or a-conformation. At a pH above ~ 5 (the precise value depends on the nature and the concentration of the counterions), the molecule expands rapidly towards the common, more extended b-conformation. This conformational transition has been found by several authors, employing a wide variety of experimental techniques, among which: potentiometric titration (ARNOLD and OVERBEEK, 1950; KATCHALSKY, 1951b; LEYTE and MANDEL, 1964; MANDEL et al., 1967), viscometry (ARNOLD and OVERBEEK, 1950; KATCHALSKY and EISENBERG, 1951a; KATCHALSKY, 1951b; GREGOR et al., 1957b; SILBERBERG and MIJNLIEFF, 1970), calorimetry (CRESCENZI et al., 1972; DELBEN et al., 1972), dye-binding (MANDEL and STORK, 1974), spectrophotometry (MANDEL et al., 1967) and diffusion (KEDEM and KATCHALSKY, 1955).

LANDO et al. (1973) concluded from laser-excited Raman spectroscopy that the conformational transition of polymethacrylic acid (further abbreviated as PMA) involves two superimposed phenomena: (1) the tertiary conformational transition (from the hyper-coiled or a-conformation towards the exten-

ded coiled or b-conformation), and (2) the randomization of the local conformation (the secondary structure except the stereoregularity), as evidenced by the Raman spectra. Since the randomization of the local conformation of syndiotactic and atactic PMA occurs gradually over a relatively wide range of α, it was concluded that the overall transition of these polymethacrylic acids cannot be a strictly cooperative process. On the other hand, the overall conformational transition of the isotactic polyelectrolyte may be cooperative. In connection with this, LEYTE et al. (1972) found that the potentiometric titration curve for isotactic PMA is irreversible in contradistinction to the corresponding curves for syndiotactic and atactic PMA. NAGASAWA et al. (1965) reported another difference between the potentiometric titration results of syndiotactic and isotactic PMA: at given pH and ionic strength, isotactic PMA had a higher charge density than the syndiotactic one, a fact that was explained by assuming different local conformations. Probably, the overall transition is rather abrupt in isotactic PMA, but more gradual in syndiotactic and atactic PMA. KAY et al. (1976) found a sharp decrease in the linewidths of side chain resonances at $\alpha \backsimeq 0.2$ from linewidth measurements on the ^1H NMR spectra of D_2O solutions of PMA. It was shown by ^{13}C nuclear spin-lattice relaxation and nuclear Overhauser enhancement that the segmental motions are more free at high pD (8.0) than at low pD (2.8) (CUTNELL and GLASEL, 1976). Both results agree with the concept of a kind of conformational transition of PMA in aqueous solution. LEYTE (1966) and ANUFRIEVA et al. (1968) calculated from potentiometric data that the number of monomeric units transforming cooperatively in atactic PMA is about 30. This conclusion seems to be in conflict with that of LANDO et al. (1973). Perhaps the relatively small cooperativeness in the transition of the tertiary structure of atactic PMA is reflected in the secondary structure in such a way that it cannot be detected by Raman spectroscopy. A second possibility is that the PMA used by LEYTE (1966) and ANUFRIEVA et al. (1968) contained a certain amount of isotactic triades. They did not check the stereoregularity.

OKAMOTO and WADA (1974) concluded from viscoelastic measurements of dilute aqueous solutions of PMA, that the transition occurs in two steps. The compact structure of PMA was thought to be stabilized by methyl-methyl bonds between adjacent groups as well as by methyl-methyl bonds between groups spatially close, but situated far from each other along the chain contour. In the initial stage of the transition, the latter type would primarily break up, resulting in expansion of the overall chain dimensions (change of tertiary conformation), and subsequently the former type of bonds would break, resulting in a change of the local chain conformation.

We conclude that the exact nature of the conformational transition is not clear in every respect. Below, we shall ignore these subtleties and use the current term: 'conformational transition', meaning a transition of the tertiary structure of the polyelectrolyte, except where explicitly mentioned otherwise.

A conformational transition has also been observed for a few other synthetic polyelectrolytes, e.g. for a copolymer of ethylacrylate and acrylic acid in the

molar ration 3:1 (TAN et al., 1974; 1975), a copolymer of maleic acid and alkyl vinyl ether (DUBIN and STRAUSS, 1970) and a polycondensate between L-lysine and 1,3-benzene disulfonyl chloride (FENYO et al., 1974; MULLER, 1974).

MANDEL and STADHOUDER (1964) and BÖHM (1974) mentioned the presence of a conformational transition for PMA-pe. Hydrophobic bonding (ELIASSAF, 1965; DELBEN et al., 1972) and VAN DER WAALS attraction (MANDEL et al., 1967) have been suggested as the main factor in the establishment of the hyper-coiled conformation at low pH of polyelectrolytes of the polymethacrylate type.

The conformation of free and adsorbed PMA-pe and the nature of the underlying interaction forces are discussed further in chapter 4.

2.4.3. *Quantitative determination in solution*

PMA-pe can be determined quantitatively in solution by potentiometric titration if the amounts of base, necessary to neutralize 1 g of the polyelectrolyte (7.59 mg eq.) and α are known. Prior to titration, the PMA-pe solutions were diluted 1:1 with 1 M NaCl in order to obtain a sharper equivalence point at $\alpha = 1.0$ (GREGOR and FREDERICK, 1957a). The titrations were performed under a nitrogen atmosphere. NaOH was used as titrant. It is not possible to use this procedure if $\alpha = 1.0$.

2.5. POLYVINYL ALCOHOL

2.5.1. *Synthesis and properties*

Polyvinyl alcohol (PVA) is a nonionic water soluble polymer, with a relatively simple chemical structure. The properties and applications have been described in a few monographs (FINCH, 1968; PRITCHARD, 1970 and FINCH, 1973).

Polyvinyl alcohol is prepared by polymerization of vinyl acetate into polyvinyl acetate (PVAc). Subsequently this polymer is partially hydrolysed to give polyvinyl alcohol, containing a certain percentage of acetate groups. The polymer obtained may be considered as a copolymer of vinyl alcohol and vinyl acetate. The structural formula is shown in fig. 2–2.

Most samples of PVA, used in this study were manufactured by KURARAY, Japan. They were prepared by a solution polymerization, followed by an alkaline hydrolysis in methanol. Detailed descriptions of the manufacture and the properties of the PVA's used are given by SCHOLTENS (1977) and

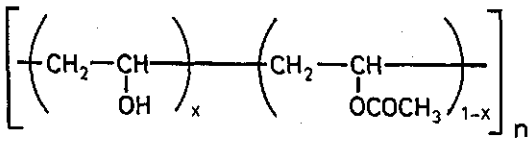

FIG. 2-2. Structural formula of polyvinyl alcohol (schematic). x = fraction hydrolyzed.

TABLE 2-2. Properties of PVA samples used.

sample code	degree of hydrolysis	viscosity average molecular weight M_v	degree of polymerization*	ash content %
205	87–89	27,000	550	0.7
217	87–89	86,000	1750	0.7
224	87–89	120,000	2450	0.7
R-2	83.4	89,000	1750	

* Calculated by dividing M_v by the mean segment weight.

BELTMAN (1975). One sample, PVA R-2, was kindly supplied by SCHOLTENS of our laboratory. The most relevant properties which characterize the polymer are summarized in table 2–2. The molecular weight distribution is rather wide. It is approximately of the FLORY-SCHULZ type, probably the 'most probable' or FLORY-distribution (PRITCHARD, 1970; SCHOLTENS, 1977). In the KURARAY PVA'S the distribution of the acetate groups is more or less of the block-type (TOYOSHIMA, 1968; SCHOLTENS, 1977). The distribution of acetate groups is expected to influence the adsorption characteristics of the PVA's to a large extent. In PVA R-2, the acetate distribution is random. The polymers used contain no detectable structural irregularities (UV and IR spectroscopy).

PVA with a degree of hydrolysis lower than 90% dissolves in water at room temperature, but at higher temperatures ($\sim$ 70°C) phase separation occurs.

2.5.2. *Conformational parameters of polyvinyl alcohol*

The solvent quality is one of the important parameters, determining the conformation of a polymer at an interface. Because in the free liquid film experiments polymer solutions in a 1 M aqueous glycerol solution are used, the conformational parameters have been determined in such a solution. The effect of the addition of 1 M glycerol can be found, by comparing the conformational parameters with those obtained previously in aqueous solution.

A convenient way of studying the conformational parameters is by using viscosity experiments. Viscosities were measured in a Viscomatic M.S. type 53,000, manufactured by FICA, France, with a photo-electric elution time determination. Ubbelohde capillaries were used. They were thermostatted at 25 $\pm$ 0.05°C. The elution times for water were about 100 s. COUETTE-HAGENBACH corrections were applied in accordance with the values, determined by SCHOLTENS (1977). The instrumental inaccuracy in the viscosity measurements is less then $1^0/_{00}$.

Intrinsic viscosities were obtained by extrapolation of the viscosity ratio excess η_{re} ($= \eta_{solution}/\eta_{solvent}-1$) to infinite dilution. Several extrapolation procedures to obtain the intrinsic viscosity and the HUGGINS constant k' are available, of which the MARTIN equation most satisfactorily describes the relation between the viscosity and the concentration over a wide range of this last parameter, for poor solvent systems (SAKAI, 1968). However, for good

solvents SAKAI suggested to use arithmetic averages of the values, calculated from a HUGGINS plot and those from a MARTIN plot. Because we consider a 1 M glycerol solution to be a rather poor or moderate solvent for the PVA samples used (see discussion below), the MARTIN equation was applied for extrapolation. This equation reads:

$$\ln \frac{\eta_{re}}{c_p} = \ln [\eta] + k' [\eta] c_p \qquad (2.1.)$$

where c_p is the polymer concentration, $[\eta]$ the intrinsic viscosity and k' the HUGGINS constant. The two last mentioned properties are obtained from a MARTIN plot according to equation 2.1. by linear regression. The results are tabulated in table 2-3. The inaccuracy in the obtained $[\eta]$ is $< 1\%$ and in k' $\leqslant 2\%$. A more extensive discussion of the reproducibility in the $[\eta]$ and k' determination is given by SCHOLTENS (1977). In the case of aqueous solutions the viscosities were measured at 30°C. The differences in $[\eta]$ for the two solvents cannot be attributed to the temperature difference, since a raise in temperature of 5°C would result in a decrease of $[\eta]$ of about 3% (PRITCHARD, 1970). Values of $[\eta]$ which have been calculated with the HUGGINS equation, are slightly lower (3% at most) than those tabulated. In water $[\eta]$ is somewhat higher than in a 1 M glycerol solution, whereas k' is much lower. These facts indicate that water is a slightly better solvent for the PVA samples, than a 1 M aqueous glycerol solution.

The tabulated values can be used to calculate constants k_1 and a in the MARK-HOUWINK relation

$$[\eta] = k_1 M_v^a \qquad (2.2.)$$

The results for a 1 M glycerol solution are $k_1 = 7.1\ 10^{-4}$ dl/g and $a = 0.62$ (25°C) and for water $k_1 = 5.3\ 10^{-4}$ and $a = 0.65$ (30°C). Because the inaccuracy in M_v is not known, nothing can be said about the absolute accuracy of these values. However, the differences in a and k_1 for the two solutions are marginally significant. The values for PVA in water are in good agreement with those, listed by KURATA et al. (1975).

The values of the HUGGINS constant k' and of a indicate, that both water and a 1 M aqueous glycerol solution are moderate solvents for PVA. They indicate also that probably the solvent power of 1 M aqueous glycerol solution is somewhat lower than for water.

TABLE 2-3. Intrinsic viscosity and HUGGINS constants for PVA samples of different molecular weight.

sample	1 M glycerol solution (25°C)		water (30°C)	
	$[\eta]$/dl g^{-1}	k'	$[\eta]$/dl g^{-1}	k'
205	0.393	0.52	0.395	0.40
217	0.823	0.48	0.847	0.35
224	0.976	0.49	1.035	0.38

The conformation of a polymer can be described by several parameters. The most important ones are the root mean square end-to-end distance, $(\overline{r^2})^{1/2}$, and the r.m.s. radius of gyration $(\overline{s^2})^{1/2}$. For a branched polymer only $(\overline{s^2})^{1/2}$ can be used. For linear random polymers the two quantities are related by:

$$\overline{r^2} = 6\,\overline{s^2} \tag{2.3.}$$

The simplest model of a linear polymer is a volumeless freely jointed chain, composed of m links, each with a length of l. Then the r.m.s. end-to-end distance can be calculated from random flight statistics (FLORY, 1953; TANFORD, 1961). Next a fixed valence angle θ and restriction in rotation can be built in. The result is:

$$\overline{r_0^2} = \sigma^2\, m\, l^2\, \frac{1 + \cos\theta}{1 - \cos\theta} \tag{2.4.}$$

where σ accounts for the steric hindrance to rotation around a C-C bond. The subscript zero indicates that the net effect of both the excluded volume effect, due to the finite volume of the chain segments and contraction or expansion due to segment-segment and segment-solvent interaction, is zero. The dimension $(\overline{r_0^2})^{1/2}$ (the unperturbed r.m.s. end-to-end distance) is independent of or unperturbed by the nature of the solvent. For a polymethylene chain $\cos\theta = 0.333$, hence equation (2.4.) reduces to:

$$\overline{r_0^2} = 2\sigma^2\, m\, l^2 \tag{2.5.}$$

It is possible to correct for the finite volume of the chain segments and for the interaction of the segments with the solvent by introducing a linear expansion factor α, which increases with increasing solvent quality. The dimension increase that follows from the finite volume of the segments, can be counteracted by dissolving the polymer in a poorer solvent. When the contraction, which results from the poorer solvency exactly cancels the expansion due to the excluded volume effect, the solvent is termed a theta (Θ) solvent. The dimension of a real chain can be related to its unperturbed dimension or its dimension in a Θ solvent by:

$$\overline{r^2} = \alpha^2\, \overline{r_0^2} \tag{2.6.}$$

KUHN (1934) has pointed out, that in order to calculate chain dimensions, a polymer chain with fixed valence angles and restricted rotation around the bonds may be replaced by an equivalent chain of the same contour length L'. This equivalent chain consists of i statistical chain elements of length l_s freely jointed together. Then the r.m.s. end-to-end distance can be written as:

$$\overline{r_0^2} = i\, l_s^2 \tag{2.7.}$$

Usually the contour length L' is assumed to correspond to the planar zig-zag of the all-trans conformation, with a distance of 0.253 nm between alternate carbon atoms (MORAWETZ, 1965, p. 120). Following FLEER (1971), it can then

be deduced from equations (2.5.) and (2.7.) and taking $l = 0.154$ nm, that l_s is given by:

$$l_s = 4\sigma^2 \frac{0.154^2}{0.253} = 0.375\,\sigma^2 \text{ nm} \tag{2.8.}$$

Then the number of segments per statistical chain element (s.c.e.)[1] is:

$$\frac{m}{2i} = \frac{l_s}{0.253} = 1.48\,\sigma^2 \tag{2.9.}$$

If it is accepted that a linear flexible polymer can be described as a statistical coil, its chain dimensions can be calculated from viscosity measurements using (FLORY, 1953, p. 611):

$$[\eta] = \Phi \frac{(\overline{r^2})^{3/2}}{M} \tag{2.10.}$$

In the original theory of FLORY Φ should be a dimensionless universal constant. However it appears that Φ depends slightly on the solvent quality. It varies from about 2.0×10^{21} for a very good solvent ($[\eta]$ expressed in dl g^{-1} and $(\overline{r^2})^{1/2}$ in cm), to 2.55×10^{21} for a Θ solvent (TANFORD, 1961, p. 401).

The linear expansion factor can also be obtained from viscometry. However, the expansion factor found by viscometry is lower because upon expansion of the coil the segment density decreases. This promotes the ability of the solvent to flow through the outer parts of the coil. The viscometric expansion factor α_η is defined by (YAMAKAWA, 1971, p. 364):

$$\alpha_\eta^3 \equiv [\eta]/[\eta_\Theta] \tag{2.11.}$$

KURATA and YAMAKAWA (YAMAKAWA, 1971, p. 302) proposed the next semi empirical relation between α_η and α:

$$\alpha_\eta^3 = \alpha^{2.43} \tag{2.12.}$$

Then equation (2.10) can be modified to read (YAMAKAWA, 1971, p. 364):

$$[\eta] = K_0 \alpha_\eta^3 M^{1/2} \tag{2.13.}$$

with

$$K_0 = \Phi_0 \left(\frac{\overline{r_0^2}}{M}\right)^{3/2} \tag{2.14.}$$

The subscript zero implies that the constants K_0 and Φ_0 are independent of the solvent quality. It can be deduced that the constants Φ and Φ_0 are related by:

$$\Phi = \Phi_0 \left(\frac{\alpha_\eta}{\alpha}\right)^3 \tag{2.15.}$$

[1] Following FLEER (1971) the term *segment* will be used to denote a monomer unit of PVA, whereas an *element* refers to a statistical chain element, consisting of several segments.

The value of Φ_0 depends only on polymer properties such as the nature of the molecular weight distribution. The values of the expansion factors α and α_η depend both on the solvent quality and on the molecular weight. This complication for determining K_0 and $(\overline{r_0^2})^{1/2}$ can be eliminated, by formulating a relation between α_η and an excluded volume parameter z. KURATA and YAMAKAWA (YAMAKAWA, 1971, p. 301) derived the next relation:

$$\alpha_\eta^3 = 1 + 1.55\, z + \ldots\ldots \tag{2.16.}$$

with

$$z = \left(\frac{3}{2\pi\, \overline{r_0^2}}\right)^{3/2} BM^2 \tag{2.17.}$$

where B is B'/M_s^2, in which M_s is the molecular weight of a segment and B' is the binary cluster integral for a pair of segments. It represents the effective volume, excluded to one segment by the presence of another (YAMAKAWA, 1971, p. 80). Elimation of α_η between equation (2.13.) and equations (2.16.) and (2.17.) results in (STOCKMAYER and FIXMAN, 1963):

$$\frac{[\eta]}{M_v^{1/2}} = K_0 + 0.51\, \Phi_0\, BM_v^{1/2} \tag{2.18.}$$

The STOCKMAYER-FIXMAN equation is one of the simplest to apply and gives good results, except for high molecular weights ($M > 10^6$) in good solvents. The better known quantity Φ_0 should be used for calculations rather than Φ because in order to estimate Φ, the solvent quality must be known. A few alternative equations are available, enabling one to find the conformation parameters of PVA (YAMAKAWA, 1971, p. 364).

By plotting $[\eta]/M_v^{1/2}$ against $M_v^{1/2}$ (fig. 2–3), K_0 can be calculated from the intercept. The data listed in table 2–3 are used. Next α_η and α follow from

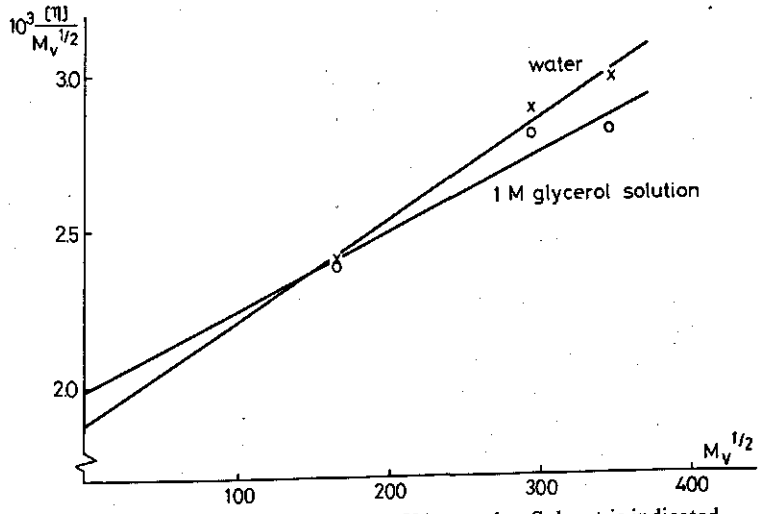

FIG. 2-3. STOCKMAYER-FIXMAN plot for three PVA samples. Solvent is indicated.

TABLE 2-4. Solution parameters of the used KURARAY PVA samples.

solvent	$10^3 K_0$	σ	l_s (nm)	$m/2i$	a	$10^4 k_1$
water	1.9 ± 0.07	2.19	1.80	7.1	0.65	5.3
1 M glycerol	2.0 ± 0.1	2.23	1.86	7.4	0.62	7.1

TABLE 2-5. Dimensions of PVA molecules in solution.

solvent	sample	M_v	$(\overline{r_0^2})^{1/2}$/nm	$(\overline{r^2})^{1/2}$/nm	α
water	204	27,000	15.8	17.2	1.09
	217	86,000	28.3	32.8	1.16
	224	120,000	33.4	39.7	1.19
1 M glycerol	204	27,000	16.1	17.5	1.09
	217	86,000	28.8	33.1	1.15
	224	120,000	34.0	39.1	1.15

equations (2.13.) and (2.12.) respectively. A value for Φ_0 must be chosen, in order to calculate the other parameters. KURATA et al. (1975) gave as a reasonable value in the case of a poorly fractionated polymer ($M_w/M_n \sim 2$), $\Phi_0 = 2.1 \times 10^{21}$ if $[\eta]$ is expressed in dl/g and $(\overline{r^2})^{1/2}$ in cm. Then $(\overline{r_0^2})^{1/2}$ and σ can be calculated. The results are represented in tables 2–4 and 2–5. The units in table 2–4 are based on the value of $[\eta]$ in dl/g. The r.m.s. end-to-end distance of PVA R-2 in water is ca 10% lower than that for PVA 217 (SCHOLTENS, 1977). The corresponding data in a 1 M aqueous glycerol solution are not available.

KURATA et al. (1975) gave as a mean value $K_0 = (2.2 \pm 0.25)\ 10^{-3}$ for PVA, measured by several authors. This is in reasonable agreement with the values found by us for PVA with 12% acetate groups. For σ these authors give 2.04 and 2.12 for fully-hydrolyzed PVA and PVAc respectively, indicating more resticted rotation in PVAc. The length of a statistical chain element l_s and the number of segments per statistical chain element have been calculated from σ, using equations (2.8.) and (2.9.). The results are almost equal to those mentioned by FLEER (1971). Table 2–4 includes also the constants of the MARK-HOUWINK equation.

The coil dimensions are listed in table 2–5. Within experimental accuracy no difference is found between the values for PVA in water and in a 1 M aqueous glycerol solution. The inaccuracy in K_0, resulting from the extrapolation procedure, is about 5%. Because the accuracy of M_v is not known no definite conclusion can be drawn on the inaccuracy in $(\overline{r^2})^{1/2}$ and α. As expected α increases with increasing molecular weight. Of course, in view of the large inaccuracy (see e.g. fig. 2–3) the tabulated results can be used only for semi-quantitative calculations. This is also the reason why we did not try to calculate the interaction parameter B' from the slope of the STOCKMAYER-FIXMAN plot.

The end conclusion can be that maybe a 1 M aqueous glycerol solution is a slightly poorer solvent for PVA than water. However, possible differences are hardly significant.

3. EXPERIMENTAL PART

3.1. PREPARATION OF THE EMULSIONS

Because the properties of emulsions depend substantially on the way of preparation, a standard method has been adopted. The method was essentially identical to the one described by LANKVELD and LYKLEMA (1972c) and BÖHM and LYKLEMA (1976). A 250 cm^3 glass beaker (diameter $\sim$ 7 cm) was filled with polyelectrolyte solution and paraffin to a total volume of 100 cm^3. A volume fraction of paraffin $\phi = 0.5$ was chosen for the rheological experiments. In other experiments ϕ varied. The contents of the beaker were emulsified with a type T45 Ultra-Turrax, ex Janke & Kunkel K. G., Germany. The time of emulsification was 2 minutes, except where otherwise stated. With an emulsification time of 2 minutes, the temperature of the emulsions rose to between 55 and 65°C, depending on ϕ and the polyelectrolyte concentration. Finally, the emulsions were cooled to room temperature.

The rheological properties of the emulsions were determined between 14 and 24 hours after preparation. The specific interfacial area S and the amount Γ adsorbed at the interface were also measured for a few emulsions. This was done between 14 and 20 hours after preparation of the emulsions.

3.2. DETERMINATION OF THE SPECIFIC AREA OF THE EMULSIONS

Interfacial areas of the emulsions per cm^3 oil phase were determined using the turbidity spectra technique, elaborated by GOULDEN (1958) and WALSTRA (1965; 1968). WALSTRA (1968) and LANKVELD and LYKLEMA (1972c) used this technique already for paraffin in water emulsions, whereas BÖHM and LYKLEMA (1976) applied it to PMA-pe stabilized emulsions. The principle of the technique and the method followed have been described extensively by LANKVELD (1970) and BÖHM (1974). Here follows only a very short description.

The attenuation of a light beam passing through a diluted colourless emulsion is due to scattering. This attenuation was measured as a function of wavelength. From these data, the turbidity spectra could be calculated. Theoretical turbidity spectra have been computed for some globule-size distributions. Truncated log-normal distributions were found to be most satisfactory for PMA-pe stabilized emulsions (BÖHM, 1974). By matching the experimental and the theoretical spectra, the volume-surface diameter $\bar{d}_{32}$ was obtained, defined through:

$$\bar{d}_{32} = \frac{\sum_i N_i d_i^3}{\sum_i N_i d_i^2} \tag{3.1.}$$

where d_i is the diameter of the i-th emulsion droplet and N_i the number of emulsion droplets i per unit volume. The specific interfacial area S could then be calculated from:

$$S = 6\,V/\bar{d}_{32} \tag{3.2.}$$

where V is the volume of the dispersed phase.

The inaccuracy in S in less than 5% for the higher specific areas. It is within 10% if S is smaller than 1.0 $m^2.cm^{-3}$.

3.3. Determination of the polyelectrolyte adsorption

The amount Γ adsorbed in $mg.m^{-2}$ of the polyelectrolyte at the interface was calculated from material balance. The amount added is known. Before determination of the remaining bulk concentration of PMA-pe, the oil phase must be removed. To that end the emulsion was centrifuged for 30 minutes in a Beckman J-21B centrifuge at 4000 till 15,000 rev/min. The number of revolutions was higher at higher α-values and polyelectrolyte concentrations. It was verified that centrifugation did not cause desorption (Böhm, 1974). The amount of PMA-pe in the aqueous phase was determined in duplicate by titration (see section 2.4.3.).

The inaccuracy in the adsorption determination was found to be within 2% for $\alpha \leqslant 0.7$. For higher α, it could be as high as 10% depending on α and the polyelectrolyte supply. This poorer reproducibility was caused by the short titration length to $\alpha = 1.0$ and the relatively low adsorption of the polyelectrolyte.

3.4. Titration of free and adsorbed PMA-pe

The potentiometric titrations have been carried out with a Schott combined glass electrode. All titrations were performed in a titration vessel, containing 100 cm^3 of polyelectrolyte solution, under nitrogen at room temperature (22°C). NaOH and $Ca(OH)_2$ were used as titrants. Their molarity was adapted to the concentration of the polyelectrolyte.

In addition to dissolved PMA-pe, paraffin in water emulsions stabilized by the same polyelectrolyte were titrated. The emulsions contained also some dissolved PMA-pe, which prior to titration, was removed by subjecting the emulsions twice to centrifugation and subsequent redispersion in 0.05 M NaCl. The emulsions obtained in this way contained approx. 150 mg PMA-pe in 300 cm^3 emulsion. The volume fraction of paraffin was ca. 0.25. These emulsions were titrated with HCl towards $\alpha \sim 0$ and back to $\alpha = 1.0$ with NaOH. Emulsions prepared at high pH were used because for them the desorption of polymer during the titration can be neglected (Böhm, 1974). The titration procedure was the same as for dissolved PMA-pe. One single titration took 8 hours.

3.5. Rheological measurements

3.5.1. *General*

Several techniques were used to study the rheological properties of PMA-pe solutions and those of emulsions stabilized by this polyelectrolyte.

PMA-pe solution viscosities at various temperatures were measured in Ubbelohde-type viscometers. The viscometers were mounted in a water bath, thermostatted at T $\pm$0.05 °C. The elution times for water at 10 °C were about 500 s and at 70 °C about 200 s. Intrinsic viscosities $[\eta]$ were obtained by extrapolation of η_{re}/c to c = 0. Dilutions were done isoionically in 0.05 M Na^+.

Emulsion viscosities were measured in a Haake Rotovisko at a shear rate $D = 7.05\ s^{-1}$ and a shearing time ($t \sim 10$–40 min) taken long enough so that the observed viscosity did not change any more. The observed viscosity was independent of the way in which the emulsions were brought into the apparatus. The temperature was 20 $\pm$ 0.2 °C except where otherwise stated.

The viscoelastic properties of the emulsions were studied by dynamic- and creep measurements. In this way it is possible to obtain the deformation of the emulsions as a function of time, which is not possible with the viscosity measurements. A second advantage of dynamic methods is that, if the deformations are small enough, no irreversible breakdown of the emulsion structure occurs during the measurements. These two properties are essential prerequisites for the calculation of the elastic- and the viscous part of the deformation of the system.

The apparatus for the dynamic and the creep measurements is described in sections 3.4.2. and 3.4.3. respectively.

3.5.2. *Dynamic measurements with the rheometer*

The rheometer is an apparatus that has been developed by Duiser and den Otter, TNO Delft (Netherlands). It has been described extensively by Duiser (1965); den Otter (1967) and Beltman (1975). Essentially, the apparatus consists of two coaxial cylinders (see fig. 3–1) between which the sample is brought. The inner one is brought in harmonic oscillation by means of a torsion

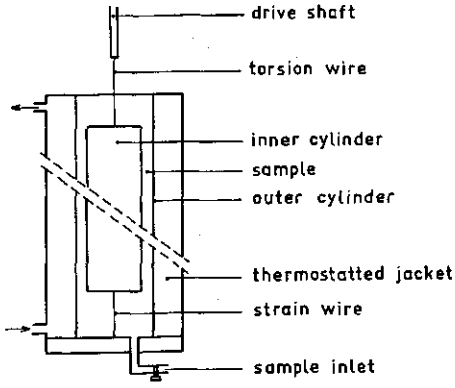

Fig. 3-1. Principle of the rheometer.

wire and a driving system. The amplitude of the drive shaft can be varied between 0–0.25 rad and the frequency between 3.2×10^{-5} and 50 Hz. The latter corresponds with an angular frequency ω of 2×10^{-4} and $3 \times 10^{2}\ s^{-1}$. The amplitude difference and the phase shift between the drive shaft and the inner cylinder can be measured by means of two light bundles and a special mirror system. The storage and loss moduli, G' and G'' respectively, can be calculated from the observed phase shift and amplitude difference, provided the amplitude is low enough to ensure linear viscoelasticity. Equations (3.3.) and (3.4.) were used for the calculation of the dynamic moduli (DEN OTTER, 1967).

$$G' = (D_1/E)(\varepsilon_{ao}/\varepsilon_{co})\{1-(\varepsilon_a/\varepsilon_{ao})^2\}^{1/2}-(D_1 + D_2)/E + I\omega^2/E \qquad (3.3.)$$

$$G'' = (D_1/E)(\varepsilon_a/\varepsilon_{co}) \qquad (3.4.)$$

in which D_1 torsion constant of torsion wire
D_2 torsion constant of strain wire
E cylinder constant $= 4\pi H/(R_i^{-1}-R_o^{-2})\ m^3$
R_o radius outer cylinder (4.5 mm)
R_i radius inner cylinder (3.75 mm)
H height of inner cylinder (15.0 cm)
I moment of inertia of inner cylinder
ε_{ao} amplitude of the drive shaft
ε_{co} amplitude of the inner cylinder
ε_a $\varepsilon_{ao} \sin Q$
Q phase shift between drive shaft and inner cylinder
ω angular frequency (s^{-1})

The calculation of the constants has been described by BELTMAN (1975) and DUISER (1965). G' and G'' were calculated with a Wang-700B table computer. The temperature was 20.0 ± 0.2 °C, except in the experiments where T was variable.

3.5.3. *Creep measurements*

Some creep measurements have been done with an apparatus developed and built in the Laboratory of Physical and Colloid Chemistry, Agricultural University, Wageningen, Netherlands. The apparatus has been described

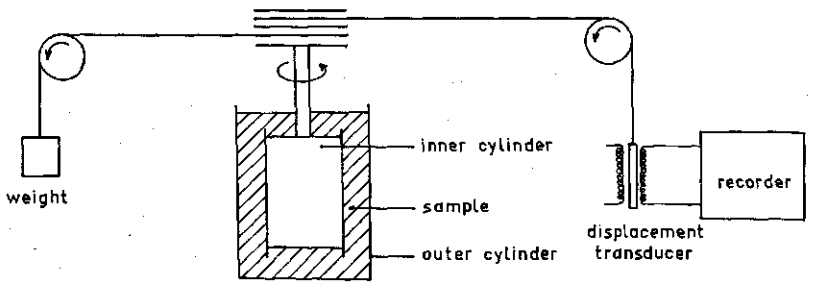

FIG. 3-2. Coaxial cylinder viscometer for creep measurements.

extensively by BELTMAN (1975). A scheme is given in fig. 3–2. The displacement transducer is from Hewlett Packard (Palo Alto, California, U.S.A.). The radius R_p of the pulley is 2.00 cm. The inner cylinder radius R_1 is 1.45 cm and the outer cylinder radius R_2 is 2.50 cm. The height of the inner cylinder is 4.50 cm. It is possible to calculate the shear modulus G and shear compliance J from the mass of the weight and the displacement of the inner cylinder as follows (BELTMAN, 1975):

$$1/J = G = \frac{\sigma}{\gamma} = \frac{0.98\, g\, Rp\, (R_2 - R_1)}{2\pi H \Delta R_1^3} \text{ (N.m}^{-2}\text{)} \qquad (3.5.)$$

in which g is the mass of the weight (kg), Δ the angular displacement of the inner cylinder (rad), σ the shear stress and γ the shear strain.

3.6. THICKNESS MEASUREMENTS OF POLYMER STABILIZED FREE LIQUID FILMS

3.6.1. *Apparatus*

3.6.1.1. Mechanical part

The mechanical part was a modified form of a cell developed at the Van 't Hoff Laboratory, State University of Utrecht, The Netherlands. The cell (see fig. 3–3) was made in the Laboratory for Physical and Colloid Chemistry, Agricultural University, Wageningen, The Netherlands by S. MAASLAND.

The films were formed in a glass ring with an inside diameter of 3.7 mm and a height of 3 mm. The horizontal films had a diameter of 1.5 to 3.0 mm, depending on the disjoining pressure. They were formed by bringing a droplet of the polymer solution in the ring through a needle. The two surfaces could be brought together by sucking away the surplus of solution. The extent of suction could be controlled by raising or lowering the container, with the polymer solution supply. The height difference between the horizontal film and the level of the polymer supply was measured with a cathetometer. The films could be visually inspected by flash light.

The whole was built in a water-thermostatted (25.00 $\pm$0.02 °C) brass box. This box was surrounded by a perspex box, which was placed, together with the optical part, in an air-thermostatted (26 $\pm$1 °C) container. The latter temperature was slightly higher than that of the brass box, in order to prevent condensation on the glass windows of the box. The box could be moved in the horizontal plane. It was possible to set the glass ring in a more or less horizontal position by changing the position of the whole box by means of a three point adjustment.

3.6.1.2. Optical and electronic part

A scheme of the optical and electronic part of the apparatus is given in fig. 3–4. The light source was a 0.5 milliwatt helium neon laser of Spectra-Physics, model 155, wavelength 632.8 nm. The attenuated (65 times) and chopped light

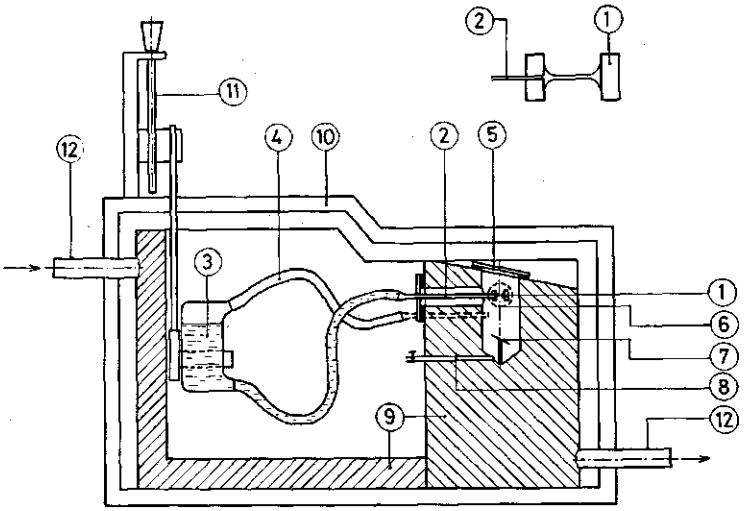

FIG. 3-3. Apparatus for the measurement of the thickness of free liquid films. Mechanical part. Insert: glass ring with film.

1 Glass ring in which the film is formed
2 Needle
3 Polymer solution supply
4 Connection between the atmosphere in the container with the polymer solution and the chamber with the film
5 Glass window through which the light beams pass
6 Window through which the height of the horizontal film can be measured
7 Light trap
8 Outlet for polymer solution
9 Water thermostatted brass box
10 Perspex box
11 Adjustment device for raising or lowering the container with polymer solution
12 Inlet and outlet for thermostatting liquid

(about 180 Hz) was converged by a lens (f = 30 cm). By a prism half of it was directed perpendicular (90° ±4°) onto the film. The other half was used as the reference beam. The light spot on the film had a diameter of about 0.5 mm. The reflected and the reference beams were directed by light guides to the photodetectors. The light guides were manufactured by Rank Precision Industries Ltd., Leeds, England. These guides consist of a bundle of glass fibers, randomly grouped together. These bundles are protected by a flexible metallic armouring, covered by a PVC sheathing. The ends of the guides are ground and optically polished. The optical diameter of the guides is 3 mm and the spectral transmission ranges from 400 to 1300 nm. PIN photodiodes (5082–4204) from Hewlett Packard were used as photodetectors. The signals of the photodiodes were preamplified and then directed to the electronic part by coaxial cables.

The electronic part was also developed and built by the Laboratory for Physical and Colloid Chemistry, Agricultural University, Wageningen, The Netherlands by R. WEGH. In this part, the film signal and the reference beam

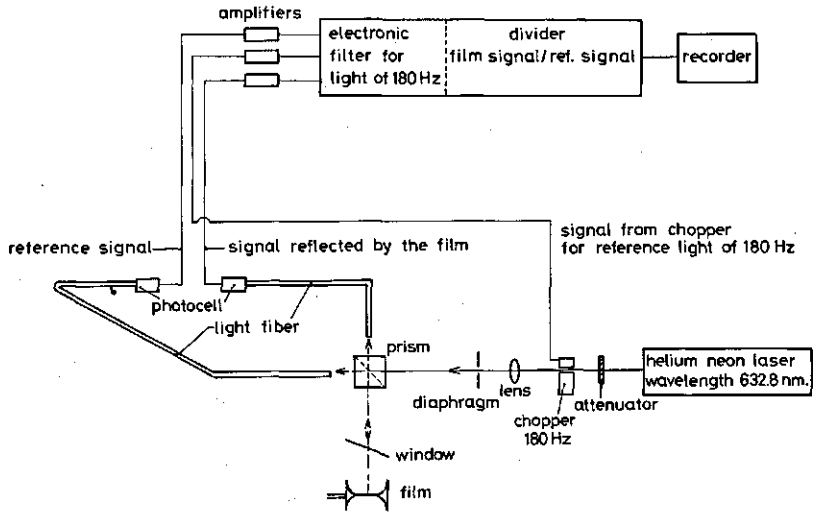

FIG. 3-4. Apparatus for the measurement of the thickness of polymer films. Optical and electronic part.

signal could be amplified independently. After that, the signals were filtered in order to select the part with the same frequency as a second reference signal coming directly from the chopper. The two alternating current signals were transformed into direct current signals. The direct currents could be amplified in such a way, that they were of the same order of magnitude. Subsequently the film signal was divided by the reference beam signal and the current coming from the divider (Intech, A 733), registered by a Servogor recorder (RE 511).

3.6.2. *Experimental procedure*

The glass container and the tube to the glass ring were filled with the polymer solution and then thermostatted in the brass box at 25.00 $\pm$ 0.02 °C for at least fifteen hours. A few drops of the solution were also brought into the room with the glass ring, in order to promote faster equilibriation between the solution and the atmosphere. The polymer solutions contained 1 M glycerol. This lowers the water vapour pressure and in that way reduces the evaporation of water from the film (AGTEROF, 1975). Prior to use the solutions were filtered over a G 5 glass filter.

The inaccuracy in the thickness measurements was about 5%.

The films were formed by raising the glass container with the polymer solution. After a droplet of the solution had been placed in the glass ring, the container was lowered to such a height, that the suction for forming a film was just too low. After a waiting time (1 hour, except where otherwise stated) the two surfaces were brought together, by lowering the container. The hydrostatic suction could be varied between 0 and 15 mm water pressure. Upon formation of the film in the ring, some compression and/or expansion of the surface may occur. It is difficult to assess the extent to which this occurs and its

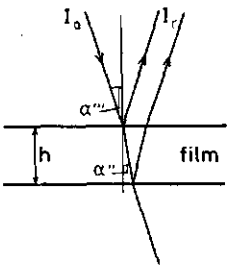

FIG. 3-5. Reflection of light by a homogeneous film.

effect on the final properties of the film if any. The film formation and the influence on it of factors such as waiting time are further discussed in chapter 5.

3.6.3. *Calculation of thicknesses from the intensity of reflected light*

For more than one century optical properties of thin liquid films have been used as a tool for the measurement of their thickness (see for a bibliography MYSELS et al., 1959). For the simple case of a transparent, homogeneous and isotropic film in air the relation between the intensity of the reflected light I_r and the thickness of the film h (VAŠIČEK, 1960) (fig. 3–5) is given by the formula:

$$\frac{I_r}{I_o} = \frac{4r^2 \sin^2 \Delta}{1 - 2r^2 + 4r^2 \sin^2 \Delta + r^4} \tag{3.6.}$$

where I_o = intensity of the incident beam

r = FRESNEL coefficient; for non-polarized light and angles $< 30°$ given by:

$$r = \frac{n_f - n_o}{n_f + n_o}$$

n_o = refractive index of air

n_f = refractive index of the film material

Δ = phase difference between the beam reflected at the two sides of the film. It is given by the expression:

$$\Delta = \frac{2\pi\, n_f\, h \cos \alpha''}{\lambda} \tag{3.7.}$$

λ = wavelength in vacuum of the light used

α'' = angle of refraction

The film thickness h_s at which maximum reflection occurs (silvery films) is given by:

$$h_s = \frac{p\lambda}{4\, n_f \cos \alpha''} \tag{3.8.}$$

where $p = 1, 3, 5 \ldots$.

In equation (3.6.) the term r^4 can be neglected in our case (BRUIL, 1970).

Realizing that for silvery films $\sin^2 \Delta = 1$, one finds for the relation between film thickness, the reflected intensity I_r of that film and that of the silvery film I_s the following equation (BRUIL, 1970):

$$\frac{I_r}{I_s} = \frac{1 + 2r^2}{1 - 2r^2 + 4r^2 \sin^2 \frac{2\pi n_f h \cos \alpha''}{\lambda}} \sin^2 \frac{2\pi n_f h \cos \alpha''}{\lambda} \qquad (3.9.)$$

This equation applies to a homogeneous film. However, polymer films are not homogeneous. They rather consist of two polymer monolayers either or not separated by an aqueous core. The structure of a polymer monolayer has been described by for instance SILBERBERG (1968, 1975) and HOEVE (1971) (section 5.2.3.1.). For soap films a three layer sandwich-like structure has been accepted, formed by two surfactant monolayers and an aqueous core with essentially bulk concentrations. A correction has been worked out for the difference in reflection between such a film and a homogeneous one (VAŠIČEK, 1960; DUYVIS, 1962; LYKLEMA et al., 1965b; FRANKEL and MYSELS, 1966). It accounts for the differing optical properties of the surface layers and the ensuing multiple reflections. The correction h^* applied to the equivalent aqueous solution thickness h_f (that is the thickness, calculated by equation (3.9.) where n_f is the refractive index of the bulk solution) is negative if n (surface layers) $> n$ (aqueous core) and independent of the thickness of the aqueous core.

The more general theory of FRANKEL and MYSELS can be extended to cover reflection from multilayer systems. In the derivation of the correction they assumed, that the thickness of the interface layers is small in comparison to the wavelength of the reflected light. This assumption is not justified for an adsorbed polymer layer as a whole. One can overcome this difficulty by considering a polymer monolayer as if consisting of a collection of parallel sheaths of gradually changing index of refraction. The equation derived by FRANKEL and MYSELS (1966) reads:

$$h_f = (n_f^2 - 1)^{-1} \sum_{i=1}^{i=k} h_i (n_i^2 - 1) \qquad (3.10.)$$

where n_i is the refractive index of the i th layer, with thickness h_i and k is the number of layers with a different refractive index. Now it is possible to calculate the effect of replacing the continuous polymer layer by a one step (block) or multi step distribution. It is assumed that the refractive index in the multi step distribution decends exponentially with the distance from the interface. The difference calculated between the correction for a one step distribution and that for a thirteen step distribution was found to be less than 10%, corresponding to 0.3 nm. This is far below the inaccuracy of the total film thickness measurement, amounting to about 3 nm. Therefore, we calculated the correction to be applied to the equivalent water thickness, by replacing the smeared out polymer segment layer by a block distribution. As a result we worked for optical purposes with a kind of three layer sandwich-like structure, similar to that used for soap films, but with much thicker surface layers (fig. 3–6) and lower refractive

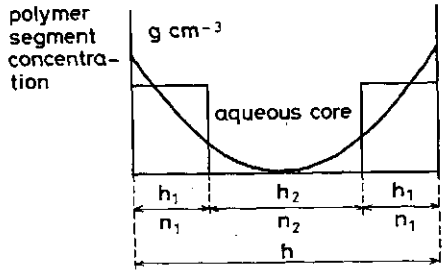

FIG. 3-6. Schematic model of a polymer film, used for the optical determination of thicknesses.

index. Equation (3.10.) can now be transformed into:

$$h^* = 2\,h_1\,\frac{n_2^2 - n_1^2}{n_2^2 - 1} \tag{3.11.}$$

where h^* is the correction to be applied to the equivalent aqueous solution thickness (h_f) of the film, h_1 the thickness and n_1 the refractive index of the equivalent polymer surface layer and n_2 the refractive index of the aqueous core of the film. The latter is assumed to be indentical to the refractive index of the bulk polymer solution (from which it follows that $n_2 = n_f$).

The thickness h_1 of the equivalent polymer surface layer can to a large extent be chosen arbitrarily. The concentration of polymer in that layer was found by means of ellipsometry. The refractive index n_1 was calculated, considering $(dn/dc)_T$ to be a constant for a given polymer (see for instance: KLENIN et al., 1974). Then the correction h^* is for reasonable values of the relevant parameters (Γ (adsorbed amount) = 1–5 mg m^{-2}, $(dn/dc)_T = 0.15$ cm^3 g^{-1} and $h_1 = 5$–25 nm) within a few per cent independent of the choice of h_1. The result is that for a given polymer, the correction h^* depends on Γ only. The constant $(dn/dc)_T$ was measured with an Abbe refractometer. It was assumed that any error arising from a non-linearity in $n(c)$ at very high polymer concentrations in the first layers near the interface, can be ignored. The refractive indices of the two equivalent polymer surface layers were much lower than the corresponding ones for soap films. As a result the *relative* corrections of the total film thickness are much smaller than the corresponding ones in the case of surfactant films.

Another difficulty arising with polymer stabilized films is that normally the FRESNEL coefficient is supposed to be independent of the film thickness and only a function of the structure of the surface layers. However, for thin polymer films there must be a kind of overlap between the two polymer layers adsorbed at the two opposing surfaces. This changes the refractive indices of the adsorbed polymer layers, at least in the region of overlap, with respect to those in thick films. If the polymer concentrations are not too high $(dn/dc)_T$ is constant. Because of the low concentrations in the overlap region (KOOPAL and LYKLEMA, 1975; section 5.4.) the difference in the mean refractive indices of the adsorbed layers of thin and thick films is probably small. Upon an average concentration rise of 1% over the entire film, the thickness of a correctly calculated film is

about 0.6% lower than when the correction is not applied. Since the concentration change will mostly be less than 1%, we neglect this difference.

4. CONFORMATION OF FREE AND ADSORBED POLYMETHACRYLATE

4.1. INTRODUCTION

In section 2.4.2. it has been described, that polyelectrolytes of the polymethacrylate type occur in two different conformations, as a function of pH. In this chapter we shall show that, under suitable conditions, this conformational transition can also be observed if the polymethacrylate is adsorbed at a liquid-liquid interface. Indications of this fact are found in work by BÖHM and LYKLEMA (1974; 1975; 1976). Firstly the conformational transition will be studied by potentiometric titration. It will be shown that the occurrence of the transition in PMA-pe layers, adsorbed on paraffin drops, emulsified in aqueous solution, can be monitored rheologically. This phenomenon in turn can be exploited advantageously to obtain additional information on the nature of the underlying interaction forces (v. VLIET and LYKLEMA, 1975).

4.2. INTERACTION FORCES DETERMINING THE CONFORMATION OF POLYMETHACRYLATES

The conformation of a polyelectrolyte in a dilute solution depends on intramolecular solute-solute, solvent-solute and solvent-solvent interactions. The presence of a second solute, for instance low molecular weight electrolyte, can also exert influence. In the case of polyelectrolytes, the COULOMBIC interaction between the segments is a major factor. This interaction is influenced by the presence of salt. From the fact that polymethacrylates occur in an uncommon compact form at low pH, it can be concluded that there must be an attractive force between the polyelectrolyte segments. MANDEL and STADHOUDER (1964) found that esterification of PMA does not influence the range of the degree of ionization α' over which the conformational transition occurs, if α' was related to the total number of segments. It means that the occurrence of the compact or a-conformation is neither due to the carboxyl groups nor to the ester groups. The latter affect the transition only in an indirect way, namely by decreasing the electrostatic repulsion between the carboxyl groups. A second conclusion of these experiments was, that intramolecular hydrogen bonds between the carboxyl groups are excluded as a major factor in establishing the compact conformation. MANDEL et al., concluded that the methyl groups in the main chain must be the main factor for the stabilization of the compact conformation. These conclusions were supported by comparison of the properties of polyacrylic acid (PAA) and partially esterfied polyacrylic acid (PAA-pe) with those of PMA and PMA-pe (BÖHM, 1974). Hydrophobic bonding (ELIASSAF, 1965; DELBEN et al., 1967) and VAN DER WAALS attraction (MANDEL et al., 1967)

between the methyl groups have been put forward as explanations for the formation of the compact conformation at low pH. These two kinds of interaction forces and COULOMBIC interaction will be discussed more fully in the next three sections.

Besides the mentioned interaction forces other factors, as e.g. steric ones, play a part. In the case of adsorbed polyelectrolytes, the nature of the interface and the interaction with it, is also important. The influence will be both from enthalpic (e.g. the adsorption energy) and entropic (e.g. a part of the volume is excluded for the polyelectrolyte by the interface) origin. Besides, concentration effects can play an indirect part.

The ultimate conformation will be the result of the complicated sum of all forces. Their relative influence can be changed by varying the solvent properties.

4.2.1. VAN DER WAALS *attraction*

VAN DER WAALS attraction between the methyl groups in the main chain has been suggested as the important factor determining the compact conformation of polyelectrolytes of the polymethacrylate type (MANDEL et al., 1967).

The LONDON-VAN DER WAALS attraction energy V_{A11} between two atoms (molecules) of the same material is given by (LONDON, 1930):

$$V_{A11} = -\frac{\beta_{11}}{r^6} \tag{4.1.}$$

where β_{11} is the LONDON constant and r the distance between the centres of the two atoms. The constant β_{11} depends on the polarizability of the atoms and on the frequency of the outer shell electrons. The order of magnitude of β_{11} is 10^{-77} Jm^6 (LONDON, 1937) which results in an attraction energy V_{A11} of around 4×10^{-20} J and 10^{-23} J respectively for $r = 0.25$ nm and 1 nm.

The attractive force F_{A11} is found by differentiating equation (4.1.).

$$F_{A11} = -\frac{6\beta_{11}}{r^7} \tag{4.2.}$$

For the LONDON constant between atoms (molecules) of different materials it has been found that (BERTHELOT's principle):

$$\beta_{12} = \sqrt{\beta_{11}\beta_{22}} \tag{4.3.}$$

For a calculation of the VAN DER WAALS attraction between the methyl groups in the main chain of PMA, dissolved in water, the following factors must also be taken into account. Firstly, the interaction between the water molecules and the methyl groups. Besides dispersion effect DEBIJE-VAN DER WAALS attraction (induction effect) will also play a part. The induction effect is ca. $\frac{1}{4}$ of the dispersion effect (calculated from data of LONDON, 1937, for $r = 0.35$ nm 0.6 and 2.4 kJ/mol respectively). Secondly, a possible change in the coordination number of the methyl groups and the water molecules. The volume of a CH_3 group and a H_2O molecule is of the same order. Therefore difficulties

arise only with the H_2O molecule as a result of the particular properties of water (NÉMETHY and SCHERAGA, 1962a). The dispersion effect between water molecules is only a part ($\pm 1/5$) (LONDON, 1937) of the total VAN DER WAALS attraction.

The problem can now be approached from different angles:

a. Calculation of the H_2O–H_2O, CH_3–CH_3 and CH_3–H_2O VAN DER WAALS interaction in vacuum and then trying to arrive at a nett CH_3–CH_3 interaction in an aqueous solution. For reasonable r the H_2O–H_2O interaction seems to be larger than the other contributions resulting in a nett CH_3–CH_3 attraction. Sometimes (e.g. HOWARTH, 1975) the assumption is made that water has an almost zero enthalpy of cavity formation. The insertion of a small solute molecule in such a cavity is energetically favourable. Now if the assumption is made that the enthalpy of cavity formation for one or two -CH_3 groups is nearly the same, the nett CH_3–CH_3 interaction in aqueous solution depends on the balance between the CH_3–CH_3 and CH_3–H_2O interactions. Those are of the same order of magnitude.

b. The HAMAKER constant for hydrocarbons in water is ca. 0.5×10^{-20} J (VISSER, 1972). The corresponding LONDON constant would then be ca. 0.5×10^{-78} Jm^6. Mathematically it is now possible to calculate V_A between two methyl groups in water (e.g. for $r = 0.35$ nm $V_A = 0.17$ kJ/mol). However the physical picture behind this type of calculations becomes unrealistic on molecular scale. For instance it is not possible to pose that there is water between two methyl groups at a distance of 0.35 nm.

BORN repulsion must be considered only at very short distances between the atoms (of the order of the sum of the atomic radii). The effect of it on the calculated interactions is ignored.

The conclusion is that in principle VAN DER WAALS attraction can be the major factor determining the compact conformation. However, it is not possible to arrive at the conclusion that VAN DER WAALS attraction is the main factor. We shall return to this problem in section 4.5.

4.2.2. *Hydrophobic bonding*

The term hydrophobic bonding is used to describe the tendency of nonpolar groups in water to aggregate, thereby decreasing the extent of the interaction with the surrounding water. In fact the attraction of nonpolar groups for each other plays only a minor part in the hydrophobic effect. The effect arises primarily from the influence of the nonpolar group on the structure of the adjacent water (TANFORD, 1973). Consequently, the effect is correlated with the structure of water. This is the reason why a quantitative description of the effect requires the choice of a water-model (FRANKS, 1973). Although some criticism on the term 'hydrophobic bonding' is possible (HILDEBRAND, 1968), we shall use this common term, realizing that probably the effect is better described by 'lipophobic bonding'.

Thermodynamically, hydrophobic bonding is characterized by a positive enthalpic effect (of the order of 1.5 kJ/mol, 25 °C) and a bigger positive entropy

effect (ca. 3 kJ/mol, 25 °C); which results in a negative free energy of formation of the order of 1.5 kJ/mol (0.6 kT per methyl group) (NÉMETHY and SCHERAGA, 1962b; OAKENFULL and FENWICK, 1975). Usually the entropy gain is attributed to the decreased number of water molecules, which are ordered by the nonpolar solutes, i.e. to a decrease in hydrogen bonding, after clustering of the solutes. The positive enthalpy term would then arise from the decrease in hydrogen bonding of the water molecules.

The free energy of the formation of hydrophobic bonds at moderate temperatures becomes more negative by raising the temperature. NÉMETHY and SCHERAGA (1962b) predicted an interaction maximum between aliphatic and aromatic groups at 331 K and at 315 K respectively.

The importance of the concept of hydrophobic bonding for the conformation of proteins and other macromolecules was first pointed out by KAUZMAN (1959). Hydrophobic bonding as a factor in determining the conformation of polymethacrylates was put forward by ELIASSAF (1965) and later mentioned by ANUFRIEVA et al. (1968); DELBEN et al. (1972) and BÖHM (1974). We shall return to the role of hydrophobic bonding in determining the conformation of PMA-pe in section 4.5.

4.2.3. COULOMBIC *interaction*

The interaction between two charged groups is of a long range nature. The interaction force is inversely proportional to the second power of the distance. In the case of PMA-pe it is possible to change the extent of dissociation of the carboxyl groups by varying the pH of the solution. Hence, it is possible to vary the COULOMBIC interaction between the polyelectrolyte segments. This interaction also depends on the concentration and nature of the added electrolyte. The ions screen the charges and in that way lower the intra- and inter-molecular electrostatic repulsion and attraction.

According to OOSAWA (1971), counterions, bound to a polyelectrolyte can be divided into the following three groups: 1. mobile in the region of the macroion; 2. mobile bound in the potentional valley along the chain contour; 3. bound to individual charged groups of the macroion, forming ion pairs (not important for monovalent ions). The difference between group 1 and 2 is not so pronounced. We will only make a distinction between mobile bound in the region of the macroion (class 1 and 2) and bound as an ion pair. The distribution over free and bound (condensed) ions and over the different classes of bound ions depends on the charge density of the polyelectrolyte under consideration and on the nature and valency of the counter ions.

In the case of bivalent counterions a kind of bridge can be formed between two carboxyl groups. This can influence the conformation of the polyelectrolyte to a large extent (KATCHALSKY, 1971).

In this chapter measurements will be reported of the influence of the NaCl concentration on the interaction between PMA-pe segments. Moreover, the importance of Ca^{++} ions in stabilizing the compact conformation of PMA-pe will be studied.

4.3. CHARACTERIZATION OF FREE AND ADSORBED PMA-PE BY POTENTIOMETRIC TITRATION

4.3.1. *Principle of the method*

Potentiometric titration is a common technique for studying conformational properties of polyelectrolytes in solutions. For instance, by this method the helix-random coil transition can be detected in proteins (NAGASAWA, 1971). Several authors (e.g. ARNOLD and OVERBEEK, 1950; KATCHALSKY, 1951b; LEYTE and MANDEL, 1964; MANDEL et al., 1967) reported potentiometric data for synthetic polyelectrolytes, such as PMA and PAA. In distinction to most other polyelectrolytes, including polyacrylates, the titration curve of PMA indicates a conformational transition. MANDEL and STADHOUDER (1964) and BÖHM (1974) reported potentiometric data for PMA-pe, also indicative of a conformational transition.

The titration behaviour of a weak polyacid in aqueous solution deviates from that of a carboxylic acid. In the latter case the negative logarithm of the ionization constant K_0 is given by:

$$pK_0 = pH + \log [(1-\alpha')/\alpha'] \tag{4.4.}$$

$$\text{with } pK_0 = 0.434\, \Delta G^0/RT \tag{4.5.}$$

α' = degree of ionization (the prime is used to distinguish this quantity from the degree of neutralization).
where ΔG^0 is the standard free energy change of the dissociation process and RT has the usual meaning.

However, for a polyelectrolyte that is already charged, an additional amount of work ΔG_{el} is required to remove a H^+ ion against the electrostatic forces of the charges, which are already present in the molecule. It is customary to define an apparent ionization constant K (OVERBEEK, 1948; KATCHALSKY and GILLIS, 1949).

$$pK \equiv pH + \log[(1-\alpha')/\alpha'] = 0.434\, (\Delta G^0 + \Delta G_{el}(\alpha'))/RT \tag{4.6.}$$

where $\Delta G_{el}(\alpha')$ is the additional electrostatic free energy per carboxyl group. Apart from charge interactions all other interactions are neglected in (4.6.). Thus, equation (4.4.) must be modified to read:

$$pH = pK_0 - \log[(1-\alpha')/\alpha'] + 0.434\, (\Delta G_{el}(\alpha'))/RT \tag{4.7.}$$

One can obtain pK_0 from a plot of pK versus α' by extrapolation to $\alpha' = 0$. Then the electrostatic free energy G_{el} of the polyelectrolyte can be calculated from the area under the graph of $pK - pK_0$ versus α'. LEYTE and MANDEL (1964) demonstrated that it is possible to calculate from the peculiar form of the $pK(\alpha')$ curve of polymethacrylates, the non-electrostatic part of the standard free energy change $(G^0_\beta - G^0_\alpha)_{\alpha'=o,T}$ of the conformational transition. In that case the pK_b versus α' curve of the more extended b-conformation was obtained by extrapolation to $\alpha' = 0$ with the aid of the empirical HENDERSON-HASSELBALCH (H–H) equation.

$$pH = pK_{av} - n \log [(1-\alpha')/\alpha'] \qquad (4.8.)$$

in which K_{av} (averaged ionization constant) and n are constants depending on the nature and concentration of the polyacid and the ionic strength of the solution (MANDEL, 1970). It has been observed experimentally (e.g. FISHER and KUNIN, 1956), that the titration behaviour of many polyelectrolytes conforms to this equation over a wide range of α'. Usually a straight line is obtained. Deviations from linearity, e.g. the occurrence of an inflection point, indicate conformational transitions in the polyelectrolyte.

Assuming (4.8.) to apply pK ($= pK_{av} - (n-1) \log [(1-\alpha')/\alpha']$) versus α' can be calculated for the two conformations of the polymethacrylate. As has been shown by LEYTE and MANDEL (1964), $(G_b^0 - G_a^0)_{\alpha'=o,T}$ is then readily calculated from the area included between the experimental pK versus α' curve and the one extrapolated to $\alpha' = 0$ for PMA-pe in the b-conformation.

In the following sections we shall show that the conformational transition of PMA-pe in solution can also be observed at a paraffin-aqueous solution interface. Besides, the influence of Ca^{++} ions on the transition in solution will be studied. The experimental procedure is described in section 3.4.

4.3.2. *Results and discussion*

Titration results are presented as H–H plots in fig. 4–1. In fig. 4–1a the plots for free and adsorbed PMA-pe in a Na^+ environment are given and in fig. 4–1b those for free PMA-pe in a Ca^{++} solution. Clearly, in each titration two regions are found conforming to the H–H equation. The two dashed straight lines represent the two conformations.

The H–H plot for the adsorbed PMA-pe was obtained by titrating an emulsion (see section 3.4.) with HCl to $\alpha' \sim 0$ and back to $\alpha' = 1.0$ with NaOH. (The degree of ionization of the original PMA-pe solution, before emulsification, was 0.7 or 0.9.) The exact value of α' at the lower end of the titration could not be established: α' of adsorbed PMA-pe is not identical to α' of the original solution, used for the stabilization of the emulsion. Moreover, not all the adsorbed polyelectrolyte was titrated. Nevertheless, it appeared possible to establish the entire H–H plot using the following tricks. A small range of values of α' could be extablished by equilizing the pH of the emulsions titrated with HCl, to that of emulsions stabilized by PMA-pe with α' near 0.05. The region of $\alpha' \sim 0$ could also be established from the shape of the titration curve. These two methods gave the same results. Next it was found, that by allowing the value of α' in this small range to vary (for instance between $\alpha' = 0.03$ and 0.06) only with one particular value the characteristic H–H plots were obtained. This feature was used as an additional means of positioning the curves. The value of α' obtained in this way is used in following calculations. Some indications of hysteresis effects have been found upon titration of adsorbed PMA-pe. This deserves further experimental investigation.

At the high pH side of the H–H plot of Ca-PMA-pe neutralized by $Ca(OH)_2$ (fig. 4–1b), two straight lines are found. WOJTCZAK (1966) reported only the

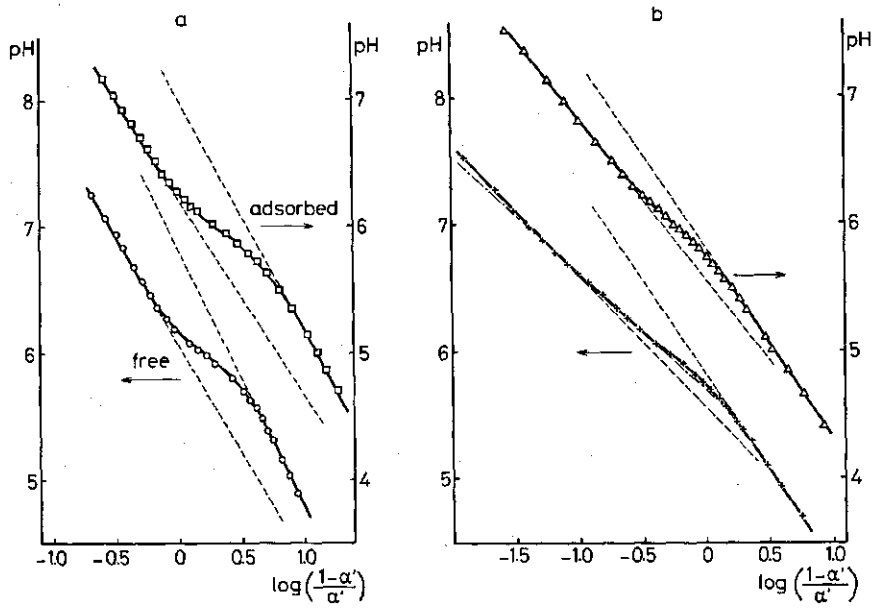

FIG. 4-1. HENDERSON-HASSELBALCH plots for PMA-pe.
a. ○ Na-PMA-pe solution. Electrolyte 0.05 M NaCl. $c_p = 2000$ ppm.
□ Na-PMA-pe adsorbed at the paraffin-aqueous 0.05 M NaCl solution interface. Adsorption ca. 1.3 mg m^{-2}. Volume fraction of paraffin ϕ 0.23.
b. Ca-PMA-pe solution. Cation 0.0038 M Ca^{++}. $c_p = 1000$ ppm.
△ titrated with 0.1076 N NaOH.
+ titrated with 0.0338 N $Ca(OH)_2$.

line between log $(1 - \alpha'/\alpha') = -0.4$ and -1.0. He did not show the plot for higher α'. Although the application of a H–H plot at high α' is limited, we assumed considering the good reproducibility of the graphs that the results are realistic. We supposed, after comparison of the H–H plot with that of Ca-PMA-pe titrated by NaOH, that the conformational transition occurs between the two outer straight lines. In that case the third line reflects the character of the transition which is much more complicated than in the presence of monovalent cations.

The slope n of the dashed straight lines in fig. 4–1 is slighter in the case of Ca-PMA-pe than for Na-PMA-pe. MANDEL (1970) found that in a limited range of α' values around $\alpha' = 0.5$ the next equation applied:

$$n = 1 + \frac{0.4343}{4} (\delta pK/\delta\alpha')_{\alpha'=0,5} \qquad (4.9.)$$

Combination of equation (4.9.) with (4.6.) and (4.8.) shows as expected that Ca^{++} ions screen the charge of the carboxyl groups to a larger extent than Na^+.

To calculate the transition standard free energy at $\alpha' = 0$, it is necessary to obtain the area between the experimental pK versus α' curve and the extrapolated one for PMA-pe in the b-conformation. However, pK values at $\alpha' = 0$

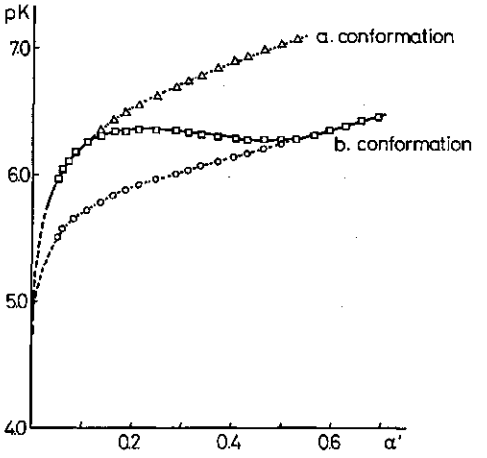

FIG. 4-2. Apparent pK as a function of α' for PMA-pe adsorbed at the paraffin-aqueous 0.05 M NaCl solution interface. Adsorption ca. 1.3 mg m^{-2}. Volume fraction of paraffin 0.23.
□ calculated points from experimental curve
△, ○ points as extrapolated from H-H plot (fig. 4-1a).

cannot be calculated exactly. An extrapolation must be made. The method adapted by LEYTE and MANDEL (1964) could not be applied, because we found a bend in the pK versus $(\alpha')^{1/3}$ curve. The values of pK_0 obtained in this way were scattered between 4.0 and 5.0. Therefore we chose the same value as LEYTE and MANDEL. Fortunately it is not so important to locate exactly the position of pK_0, because at low α' the p$K(\alpha')$ curves almost coincide (fig. 4–2). For the same reason as a first approximation the pK_0 values of the two conformations were taken as identical. The results of the calculations are presented in table 4–1. P is the degree of polymerization. There is no difference in the transition free energy at $\alpha' = 0$ between free and adsorbed Na-PMA-pe, demonstrating their similarity. The following values per monomeric unit of Na-PMA have been reported in the literature: 0.32 kT (MANDEL et al., 1967), 0.31 kT (CRESCENZI et al., 1972) and 0.37 kT (CONIO et al., 1976). The agreement is satisfactory since the polyelectrolytes used are not identical. The values for Ca-PMA-pe are clearly lower than those for Na-PMA-pe. Maybe the Ca^{++} ions influence the attractive forces responsible for the compact conformation.

TABLE 4-1. Standard free energy of the process (uncharged compact conformation) → (uncharged more extended b-conformation).

	$(1/PkT)(G_2^{\beta} - G_2^{\alpha})_{\alpha'=0,T}$
PMA-pe solution, 0.05 M NaCl, c_p = 2000 ppm	0.36
PMA-pe adsorbed at the paraffin-aqueous 0.05 M NaCl solution interface, adsorption ca. 1.3 mg m^{-2}	0.38
Ca-PMA-pe solution, cation 0.0038 M Ca^{++}, c_p = 1000 ppm	
titrated with NaOH solution	0.19
titrated with $Ca(OH)_2$ solution	0.21

It is not allowed to interpret this kind of data directly in terms of attraction energy between the polyelectrolyte segments at low pH. Besides the energy effects mentioned, other factors contribute to the observed values of $(G_g^0 - G_a^0)_{\alpha'=0,T}$. These factors include: (a) the change in the conformational energy of PMA-pe chains passing from the compact state to the more extended one; (b) the associated change in the free energy of the water molecules. Lack of information on these points makes it impossible to arrive at a definite conclusion about the nature of the attractive forces in this way. Probably the only tentative remark that can be made in this direction is, that it is hardly imaginable that the Ca^{++} ion effect found can be explained as VAN DER WAALS attraction being the main or sole factor in establishing the compact conformation.

The titration data can be replotted (LEYTE and MANDEL, 1964) to give the fraction f_b of PMA-pe in the extended or b-conformation as a function of α'. To that end the assumption had to be made, that in the transition region the following linear combination holds:

$$\alpha' c_p = \alpha'_a(c_p - c_b) + \alpha'_b c_b \qquad (4.10.)$$

in which c_p = total polyelectrolyte concentration
c_b = polyelectrolyte concentration in the b-conformation
α'_a = degree of ionization in the a-conformation
α'_b = degree of ionization in the b-conformation

Since α'_a and α'_b can be found as a function of α' from the lower and upper linear parts of the H–H plots f_b can be calculated as a function of α'. The results are summarized in fig. 4–3. From these plots, and also from previous ones, it can be concluded, that:

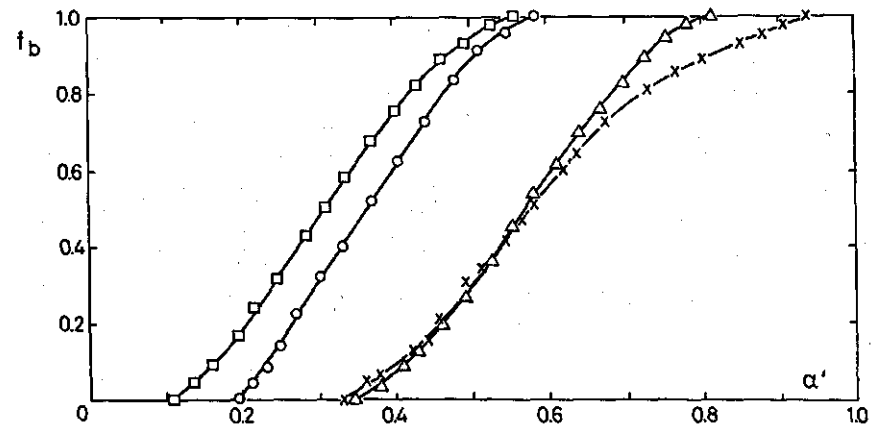

FIG. 4-3. Fraction f_b of PMA-pe in the expanded or b-conformation.
○ Na-PMA-pe solution. Electrolyte 0.05 M NaCl. c_p = 2000 ppm.
□ Na-PMA-pe adsorbed at the paraffin-aqueous 0.05 M NaCl solution interface. Adsorption ca. 1.3 mg m^{-2}. Volume fraction of paraffin 0.23.
△, × Ca-PMA-pe solution. Cation 0.0038 M Ca^{++}. c_p = 1000 ppm. Titrated with 0.1076 N NaOH (△) or with 0.0338 N $Ca(OH)_2$ (×).

TABLE 4-2. Titration data of adsorbed PMA-pe.

	emulsion	I	II	III
α' PMA-pe solution used as emulgator		0.70	0.70	0.90
α' adsorbed PMA-pe layer		0.51	0.50	0.75
Amount PMA-pe initially added	mg	338	345	230
Amount PMA-pe in supernatant	mg	179	168	143
Amount PMA-pe adsorbed	mg m^{-2}	1.17	1.28	0.72
Amount PMA-pe titrated	mg m^{-2}	0.66	0.71	0.51
Non-titrable amount	mg m^{-2}	0.52	0.57	0.22

1. The conformational transition occurs also in adsorbed PMA-pe. As compared with free PMA-pe, the transition region is somewhat broadened and shifted to lower α'. In connection with our findings, we note that CASPERS et al. (1974) observed a conformational transition as a function of pH in polypeptides, spread at the air-water interface. The total number of titratable groups was calculated from the amount of NaOH, necessary for the back titration from $\alpha' \backsimeq 0.0$ to $\alpha' = 1.0$. Then α' of the adsorbed layer can be calculated from the added amount of HCl. The total amount adsorbed is known (see section 3.3.). It follows from a balance count of the total number of titratable groups, that in the region of pH 4.5–9 a small part of the adsorbed PMA-pe is not titrated. The results of the calculations are summarized in table 4–2. The 'lost' amount corresponds roughly with the amount that can be accommodated in the first segment layers near the interface (0.3–0.5 mg m^{-2} depending on the pH, BÖHM, 1974). This is not surprising in view of the negative field at the interface.
2. The presence of Ca^{++} ions influences the conformational transition of PMA-pe. The transition region is shifted to higher α'. The width of the transition region depends on the hydroxide used. Calcium ions can form a complex with two carboxylate ions (KATCHALSKY, 1971). The forming of Ca^{++} bridges between two adjacent carboxyl groups is unlikely (BEGALA and STRAUSS, 1972), because then 8 member rings had to be formed. Therefore Ca^{++} bridges will be formed mainly between carboxyl groups, situated more or less far away from each other along the chain contour. The extent to which this happens depends on the degree of ionization and the local conformation of carboxyl groups. Such bridges can be effective in stabilizing the compact conformation. It should be pointed out that the effect of Ca^{++} will be cooperative.

We will return to the importance of Ca^{++} in stabilizing the compact form of PMA-pe in section 4.5.3.

4.4. CHARACTERIZATION OF ADSORBED PMA-PE BY RHEOLOGICAL MEASUREMENTS OF EMULSIONS STABILIZED BY THIS POLYELECTROLYTE

The interaction between liquid droplets dispersed in a continuous phase is reflected in the rheological properties of the system (e.g. VAN DEN TEMPEL, 1963; PAPENHUIZEN, 1972; STRENGE and SONNTAG, 1974). Likewise the interaction

between polyelectrolyte molecules adsorbed on emulsion droplets, is reflected in the rheological properties of the emulsions (BÖHM and LYKLEMA, 1976). In this section we shall try to correlate the rheological properties of emulsions stabilized by PMA-pe, with the interaction forces between the polyelectrolyte segments. A second goal will be to determine the relationship between these intermolecular interaction forces and the intramolecular forces which are responsible for the conformational transition of the polyelectrolyte.

The experimental procedures are described in sections 3.1. and 3.5. A more extensive description of the measurement of dynamic moduli will be given in section 6.5.

4.4.1. *Dynamic moduli and viscosity of emulsions stabilized by PMA-pe*

The results of the measurements of emulsions stabilized by Na-PMA-pe are represented in fig. 4–4. It can be concluded, both from the viscosity and the dynamic data, that strong attraction between the emulsion droplets occurs only at low α. In that case, a substantial part of the adsorbed PMA-pe is in the a-conformation. At high α, the emulsions are very fluid, with little or no attraction between the adsorbed polyelectrolyte layers. Comparison of the obtained data with the viscosity of emulsions stabilized by a copolymer of acrylic acid and the methyl ester of acrylic acid (PAA-pe) (data of BÖHM, 1974), shows that the results cannot be explained with the DLVO theory (VERWEY and OVERBEEK, 1948) only. Since the polyelectrolyte adsorption in mg m^{-2} is almost equal and that neither the dispersity did vary, this cannot cause the difference.

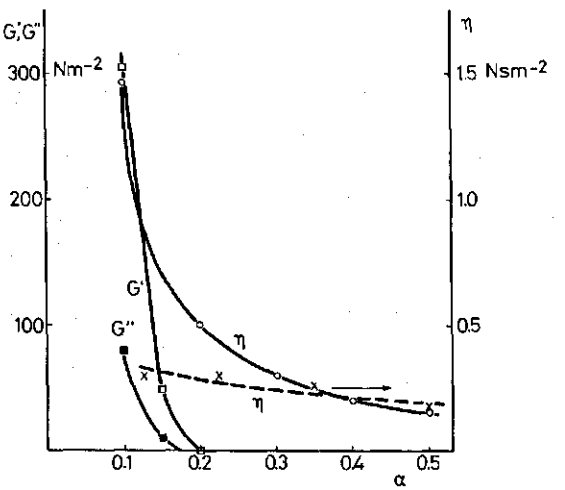

FIG. 4-4. Dynamic moduli and viscosities of emulsions stabilized by PMA-pe as a function of the degree of neutralization. Electrolyte 0.05 M NaCl. $\phi = 0.5$. Polyelectrolyte supply 2 mg per cm^3 of paraffin.
○ Viscosity η. $D = 7.05\ s^{-1}$.
× Viscosity of emulsions stabilized by PAA-pe. $D = 7.05\ s^{-1}$, according to BÖHM (1974).
□ Storage modulus G'.
■ Loss modulus G''.

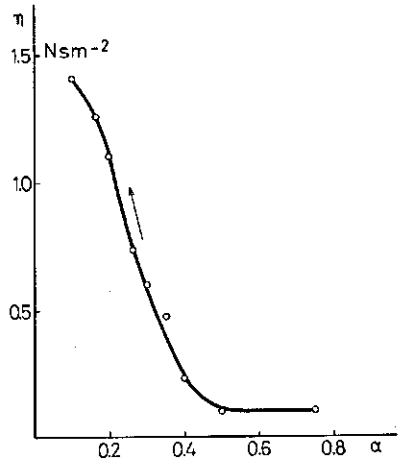

FIG. 4-5. Influence of lowering α on the viscosity of paraffin in water emulsions stabilized by PMA-pe originally at $\alpha = 0.75$. Electrolyte 0.05 M NaCl. ϕ = ca. 0.5. $D = 7.05\ s^{-1}$.

Emulsions prepared at high α, from which dissolved PMA-pe was removed by centrifugation and redispersion in 0.05 M NaCl, became viscous by lowering α to $\alpha < 0.4$ (fig. 4–5). The transition from fluid to a viscous emulsion was completely reversible. The values of α are not very accurate. However, we think it is justifiable to conclude again, that the transition from a fluid to a viscous emulsion occurs in the same region of α, as the conformational transition of PMA-pe. A second conclusion is, that the strong attraction between the emulsion droplets does not follow from multilayer formation. Namely at high α the repulsion between the polyelectrolyte segments dominates, so that then multilayer adsorption will not occur. Because no polyelectrolyte is present in the continuous phase, adsorption in a second layer cannot occur when lowering α. It was checked that no desorption of PMA-pe takes place during that operation.

The addition of salt to emulsions manufactured with an electrolyte concentration of 0.025 M NaCl, raised the viscosity and the dynamic moduli (fig. 4–6). In our picture this can be interpreted as follows: the ions screen the charge of the carboxyl groups and lower in that way their electrostatic repulsion. At a given α, the expansion becomes less pronounced and the a-conformation can persist till higher α values. These findings agree with those of BÖHM (1974) and CRESCENZI et al. (1972). These authors measured an upward shift (towards higher α) of the transition region, in which the conformational transition of free PMA-pe takes place with increasing concentration of NaCl.

Anticipating the discussion in section 5.4., it is interesting to note that the interaction between adsorbed Na-PMA-pe layers is also reflected in the drainage behaviour of free liquid films, stabilized by this polyelectrolyte. At $\alpha \geq 0.5$ the films are mobile and drain relatively rapidly, whereas at $\alpha \sim 0.1$ the films are rigid and drain towards equilibrium only over days.

The results of the dynamic moduli and viscosity measurements of emulsions

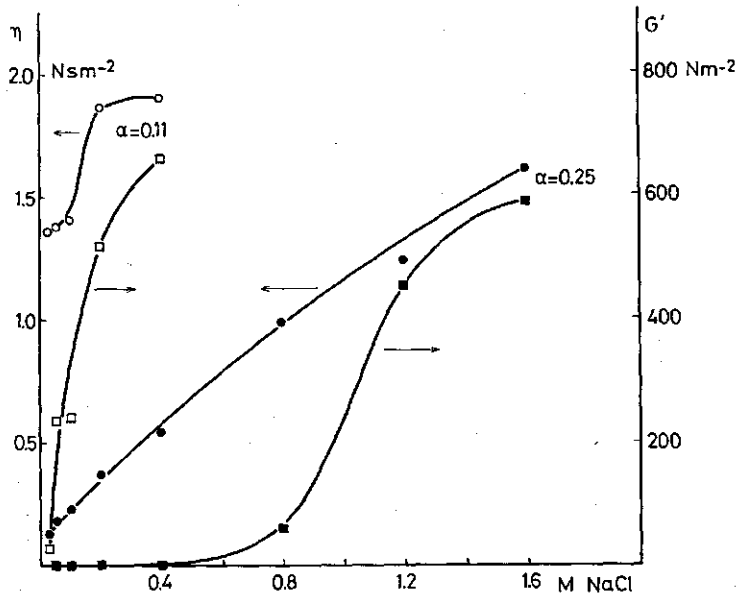

FIG. 4-6. Influence of the addition of salt on the storage moduli and the viscosities of paraffin in water emulsions stabilized by PMA-pe. Degree of neutralization is given. Electrolyte originally 0.025 M NaCl. $\phi = 0.5$. Polyelectrolyte supply 2 mg per cm^3 of paraffin.
○, ● Viscosities, $D = 7.05\ s^{-1}$.
□, ■ Storage moduli.

stabilized by Ca-PMA-pe, are shown in fig. 4–7. A part of the viscosity line is dotted. The viscosity values in that region are qualitative only, as a consequence of slip along the wall of the cylinders during the measurements. The shapes of the curves are much more complex than in the case of Na-PMA-pe. The adsorption and the specific surface area are but little dependent on α (BÖHM, 1974). A first tentative explanation of the sharp rise in the viscosity and the moduli between $\alpha = 0.1$ and 0.4 can be, that it represents the growing importance of Ca^{++} bridges between carboxyl groups. The sharp fall between $\alpha = 0.4$ and 0.6 correlates with the conformational transition (fig. 4–3). We return to the influence of Ca^{++} on the conformation of PMA-pe in section 4.5.3. Anticipating this we want to draw attention firstly to the second maximum at $\alpha = 0.8$; and secondly to the fact that comparison of the data of fig. 4–7 with those of fig. 4–4 shows, that at $\alpha = 0.1$ the viscosity and the dynamic moduli are lower than the corresponding data for Na-PMA-pe stabilized emulsions.

Now we arrive at some conclusions.

1. The occurrence of the compact conformation at low α in dissolved PMA-pe reflects some intramolecular attraction between the polyelectrolyte segments.
2. It follows from the titration data of adsorbed PMA-pe, that this attraction occurs also intermolecularly between the loops and/or trains adsorbed on one emulsion droplet.

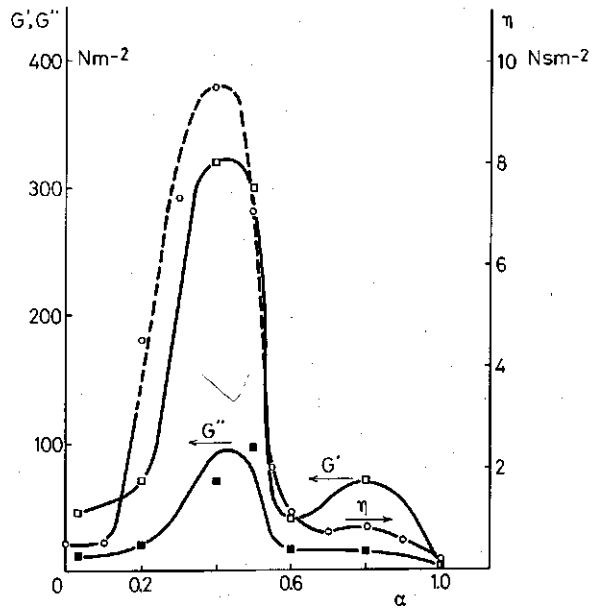

FIG. 4-7. Dynamic moduli and viscosities of emulsions stabilized by PMA-pe as a function of the degree of neutralization. Cation 0.0076 M Ca^{++}. $\phi = 0.5$. Polyelectrolyte supply 2 mg per cm^3 of paraffin.
○ Viscosity η, $D = 7.05\ s^{-1}$.
□ Storage modulus G'.
■ Loss modulus G''.

3. The high values of the viscosity of PMA-pe stabilized emulsions at low α are due to attraction between extending loops and/or tails, anchored onto different droplets.
4. The final conclusion is that the *intramolecular* interaction in free polymethacrylates and the *intermolecular* interaction between adsorbed polyelectrolytes are very similar.

4.5. NATURE OF THE ATTRACTIVE FORCES BETWEEN THE POLYELECTROLYTE SEGMENTS

As already mentioned before, there has hitherto been no consensus of opinion over the nature of the attractive forces, that are responsible for the compact conformation at low pH. VAN DER WAALS attraction (MANDEL et al., 1967) and hydrophobic bonding (ELIASSAF, 1965; DELBEN et al., 1967) have both been put forward as explanations.

In the next sections we shall describe a few sets of experiments, performed to obtain more information on the nature of the attractive forces. To that end we used the finding, formulated at the end of section 4.4.2. that rheological mea-

surements with emulsions are an easily accessible tool to verify the nature of these forces. Successively the influence of the addition of methanol on Na-PMA-pe stabilized emulsions, and the effect of variation of the temperature, will be described. The influence of Ca^{++} has also been further investigated.

The experimental procedures are described in sections 3.1. to 3.3. and in 3.5.

4.5.1. *Influence of the addition of methanol on the viscosity of emulsions stabilized by Na-PMA-pe*

The results are shown in fig. 4–8. In this set of experiments the emulsification time was limited to 1 minute in order to prevent evaporation of methanol (Me OH) because of the temperature rise during emulsification.

The effect of the addition of MeOH on the viscosity of an emulsion depends very strongly on α. If a major part of the adsorbed polyelectrolyte is in the b-conformation, η is low and MeOH has virtually no effect. At low α (that is the region of enhanced viscosity), the viscosity passes through a maximum at a mole fraction of methanol $X_{MeOH} \sim 0.13$–0.17.

Before the results at low α were interpreted, it was verified that the maximum could not be attributed to a variation in the adsorbed amount Γ at the paraffin-aqueous solution interface or by variation in the emulsion droplet diameter (or specific area S). As shown in fig. 4–9, both depend on X_{MeOH}. A larger specific area (or smaller mean emulsion droplet diameter) would raise η (SHERMAN, 1968, Ch. 4), whereas a reduction of the adsorbed amount would result in a

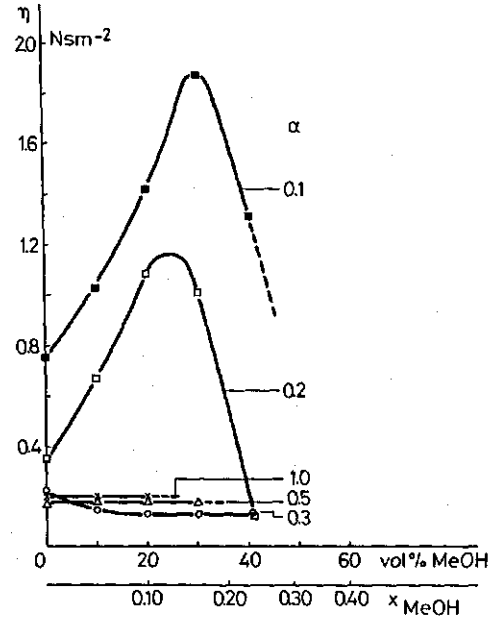

FIG. 4-8. Viscosities of paraffin emulsions in water-methanol mixtures. $D = 7.05\ s^{-1}$. Stabilizer Na-PMA-pe. Degree of neutralization is given. Electrolyte 0.05 M NaCl. $\phi = 0.5$. Polyelectrolyte supply 2 mg per cm^3 of paraffin. Emulsification time 1 min.

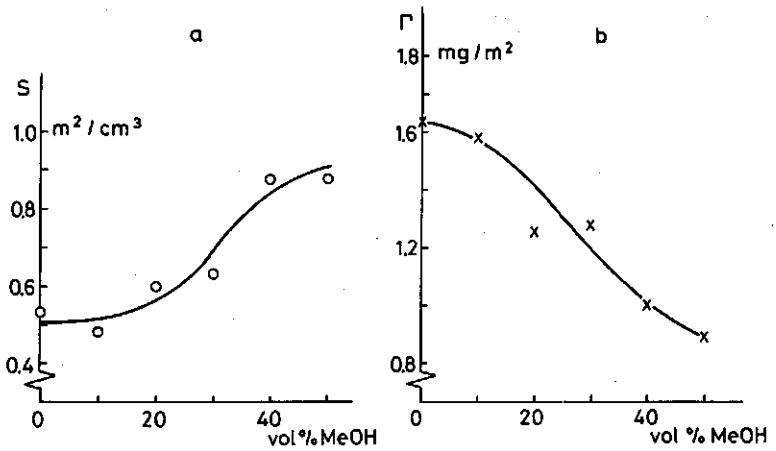

FIG. 4-9. Properties at $\alpha = 0.1$ of paraffin emulsions inwater-methanol mixtures. Stabilizer Na-PMA-pe. Electrolyte 0.05 M NaCl. $\phi = 0.5$. Polyelectrolyte supply 2 mg per cm³ of paraffin.
a Specific area S (m^2/cm^3 paraffin).
b Adsorbed amount Γ of polyelectrolyte.

lowering of η (BÖHM, 1974). However, addition of 10–20% MeOH has only a small influence on S, whereas η increases drastically in that region.

A second indication that the variation of S and Γ does not cause the maximum is found in intrinsic viscosity $[\eta]$ measurements of polymethacrylic acid in 2×10^{-3} N HCl by PRIEL and SILBERBERG (1970b). These authors observed that $[\eta]$ as a function of X_{MeOH} first decreased, then passed through a minimum at $X_{MeOH} \sim 0.1$, and finally increased till a maximum at $X_{MeOH} \sim 0.4$. It is good to realize that an increase in the attractive force between the polyelectrolyte segments, which in our case is measured between different adsorbed layers, leads to an enhanced emulsion viscosity, whereas in bulk the same force acts only inside the molecule (provided the solution is dilute) and hence leads to compaction and subsequent reduction of $[\eta]$. Thus, our maximum is in perfect qualitative agreement with the minimum, observed by PRIEL and SILBERBERG (1970b). It might even be assumed, that the extremes are not far apart, which would indicate the great similarity between the types of interaction in free and adsorbed polymethacrylate. A conclusion at which we also arrived at the end of section 4.4.2. Obviously, exact agreement may not be expected since the polyelectrolytes used were not identical. Realizing that the maximum in η and the minimum in $[\eta]$ are both attraction maxima, it is permissible to conclude, that the addition of a small amount of MeOH increases the attraction between the polyelectrolyte segments, that give rise to the a-conformation, whereas large amounts of MeOH disrupt such bonds.

The disrupture of bonds by MeOH has been used as an argument, that these bonds are due to hydrophobic interaction (KAUZMAN, 1959; MANDEL et al., 1967; ANUFRIEVA et al., 1968). Perhaps this may apply to large volume fractions

of MeOH and hence explain the reduction of η beyond the maximum (fig. 4–8) or the increase of $[\eta]$ beyond the minimum (PRIEL and SILBERBERG, 1970b). However, smaller MeOH contents behave in a different way. A similar interaction maximum as in water-methanol mixtures has been found by intrinsic viscosity measurements in mixtures of water with ethanol, 1.2-ethanediol and n-propanol respectively (HUPPENTHAL, 1963; PRIEL and SILBERBERG, 1970a, b). Experimentally, these trends have been established for the influence of ethanol (EtOH) on hydrophobic bonding (YAACOBI and BEN-NAIM, 1973; OAKENFULL and FENWICK, 1974). These authors concluded from a conductometric study of ion-pair formation by doublelong-chain electrolytes that hydrophobic interaction initially became stronger with increasing ethanol concentration. The interaction reached its maximum at $X_{EtOH} = 0.10$. In a study on the solubilities of methane and ethane in ethanol-water mixtures YAACOBI and BEN-NAIM found that hydrophobic interaction reaches its maximum at X_{EtOH} = ca. 0.15.

Our insight into the structural details of the influence of alcohol molecules has not been developed enough to arrive at a definite molecular picture. Nevertheless, it appears justifiable to conclude that our results and those of the authors cited above support each other, and that they are not in conflict with hydrophobic bonding as a main factor in producing the a-conformation at low α.

4.5.2. *Effect of the variation of the temperature*

The temperature dependence of the intrinsic viscosity $[\eta]$ of dissolved PMA-pe is shown in fig. 4–10. The minimum at $T \sim 325$ K corresponds very well with a similar minimum in $[\eta]$ of PMA dissolved in 0.02 N HCl, found by SILBERBERG et al. (1957). On the other hand, the emulsion viscosity and the storage modulus pass through a maximum (fig. 4–11) at a temperature somewhat depending on the properties of the emulsions. Following the same way of reasoning as in the previous section, we concluded that the extremes found reflect maxima in the attraction between polyelectrolyte segments. NÉMETHY and SCHERAGA (1962b) predicted such an interaction maximum for hydro-

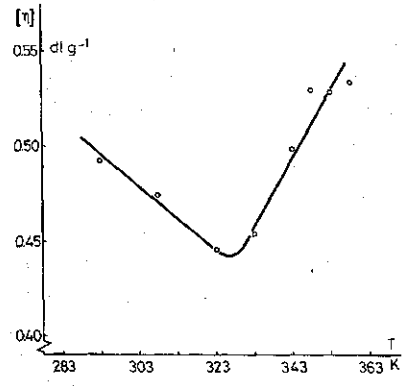

FIG. 4-10. Influence of temperature on the intrinsic viscosity of dissolved PMA-pe at $\alpha = 0.1$. Cation 0.05 M Na^+.

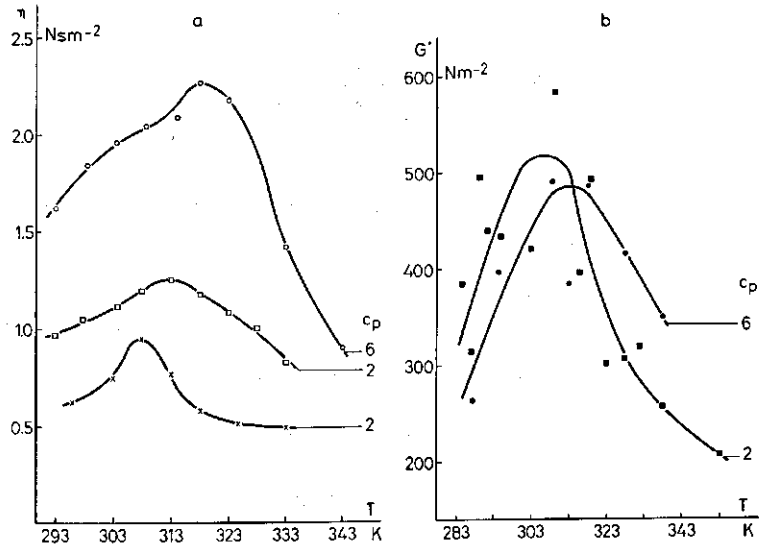

FIG. 4-11. Influence of temperature on the viscosity and the storage modulus of PMA-pe stabilized emulsions. $\alpha = 0.1$. Electrolyte 0.05 M NaCl. $\phi = 0.05$. The polyelectrolyte supply c_p in mg per cm³ of paraffin is given.
× Emulsification time 1 min.
○, □, ■, ● Emulsification time 2 min.
a Viscosity. $D = 7.05\ s^{-1}$.
b Storage modulus.

phobic bonding between aliphatic and aromatic groups at 330 K and at 315 K respectively.

According to NÉMETHY and SCHERAGA, the total standard free energy $\Delta_{hb}F^v$ of formation of a hydrophobic bond can be written as:

$$\Delta_{hb}F^v = \Delta F_w^v + \Delta F_s^v \tag{4.11.}$$

Where ΔF_w^v is the contribution from the change of the water structure and ΔF_s^v the contribution from the change in the state of the solute. By forming a hydrophobic bond between two solute molecules or two parts of a molecule, an equal number of water molecules totalling ΔY^s are removed from the two shells around them. They become part of the bulk water. The value to be substituted for ΔY^s depends on the arrangement of the hydrophobic groups in the bond and the number of groups participating in it. Then, the contribution of the water molecules to $\Delta_{hb}F^v$ is:

$$\Delta F_w^v = \Delta Y^s(F_w^v - F_w^c) \tag{4.12.}$$

where $F_w^v - F_w^c$ is the standard free energy change per mole of water undergoing the change. For the contribution of the solute (chain molecules) to $\Delta_{hb}F^v$, NÉMETHY and SCHERAGA derived:

$$\Delta F_s^v = -(\tfrac{1}{2})E_{RW}\Delta Y^s + Z_R E_R + \Sigma\Delta F_{rot} \tag{4.13.}$$

where $\Delta Y^s E_{RW}$ is the energy loss as a result of breaking ΔY^s water-solute interactions. The formation of Z_R hydrocarbon-hydrocarbon interactions is accompanied by an energy gain $Z_R E_R$. The two terms represent VAN DER WAALS attraction. The last term of equation (4.11.) represents the increase in the free energy arising from the reduction in the internal C–C bond rotation in the molecules, accompanying the formation of a hydrophobic bond.

The values of $\Delta_{hb}F^o$ calculated with equations (4.11.) to (4.13.) can be represented as a function of the temperature by an equation having the form:

$$\Delta_{hb}F^o = a + bT + cT^2 \qquad (4.14.)$$

The values to be substituted for the coefficients a, b and c depend on the nature of the interacting groups. The other thermodynamic parameters can be derived from $\Delta_{hb}F^o$ as:

$$\Delta_{hb}H^o = a - cT^2 \qquad (4.15.)$$

$$\Delta_{hb}S^o = -b - 2cT$$

At room temperature, $\Delta_{hb}F^o$ is < 0, $\Delta_{hb}H^o$ and $\Delta_{hb}S^o$ are > 0. At higher temperatures, both $\Delta_{hb}H^o$ and $\Delta_{hb}S^o$ approach zero. The enthalpy of formation becomes even negative above about 330 *K* (315 *K* for aromatic side chains). This occurs because the water structure breaks down at elevated temperatures. Then, the solubility of aliphatic compounds will be determined mainly by interaction energies. The endothermic nature of the formation of hydrophobic bonds causes them to become stronger with increasing temperature to a certain temperature above which the water structure breakdown prevails, leading to a reduction in the extent of hydrophobic bond formation.

Now we return to the results shown in figs. 4–10 and 4–11. The semiquantitative analogy with the more theoretically found interaction maxima is good enough to point again to hydrophobic interaction as a main factor in the establishment of the a-conformation. A quantitative agreement may not be anticipated, neither with the semitheoretically found interaction maxima nor between the different sets of experiments. Anyway, if VAN DER WAALS attraction would be the only factor in the establishment of the a-conformation, the interaction would not show a maximum.

An explanation for the discrepancy between the temperature at which the attraction is at its maximum, found by intrinsic viscosity measurements and by storage modulus and emulsion viscosity measurements can be sought in the difference between adsorbed and free polyelectrolytes. A strong indication that the discrepancy is connected with the adsorption can be obtained from table 4–3. The data are taken from figs. 4–10 and 4–11a. The results shown in fig. 4–11b are too much scattered to obtain a reliable maximum attraction temperature.

The lowering in T_{max} for adsorbed PMA-pe as compared with free PMA-pe must be an effect of a decrease in the temperature, whereby $\Delta_{hb}H^o$ becomes negative. In other words, $\Delta_{hb}H^o$ will be less endothermal at every temperature

TABLE 4-3. Maximum attraction temperature of free and adsorbed PMA-pe.

	amount adsorbed at the interface/mg m^{-2} (BÖHM, 1974)	T_{max} K
free PMA-pe		326
adsorbed PMA-pe	3.9	318
adsorbed PMA-pe	2.1	312
adsorbed PMA-pe	1.6	308

or the value of it is the same at e.g. room temperature but decreases with increasing temperature more rapidly.

Starting from the other side, adsorption influences the amount of intermolecular hydrophobic interactions formed and the effectivity of the interactions. Next we assume that the influence of the temperature on $\Delta_{hb}H^o$ is determined only by the properties of the individual bonds and not by the total number. Factors determining the effectivity of the hydrophobic interactions are (see eq. (4.11.)):

1. The ordering of water around the methyl groups and in the bulk. An influence of the paraffin-aqueous solution interface on the water structure in the overlap region can be neglected, because the adsorbed polyelectrolyte layer is rather thick (LYKLEMA et al., 1965b). Neither is it likely that the adsorption would influence the ordering of the water around the methyl groups relatively far away from the interface.
2. The area of the contact region and the intensity of the contact between two or more hydrophobic groups per methyl group. The assumption is, that the adsorption of the polyelectrolyte would lower the number of possible conformations of the polyelectrolyte. By this the location of the methyl groups, cooperating in a bond, with respect to each other will not be in optimum every time. Besides, it is imaginable that the number of bonds in which three or more methyl groups are concerned, diminishes. So, ΔY^s and $Z_R E_R$ in equation (4.12.) and (4.13.) and the relation between them will be influenced. Also $\Sigma\Delta F_{rot}$ will be influenced, but this factor is not so important in the enthalpy calculation (NÉMETHY and SCHERAGA, 1962b). Then, the speculative conclusion is that ΔY^s and $Z_R E_R$ are the crucial factors in the shift of the maximum attraction temperature after adsorption. However an influence of a change in $\Delta\Sigma F_{rot}$ cannot be excluded. As nothing is known about the temperature influence on the shift of ΔY^s and $Z_R E_R$ by adsorption, no conclusion can be drawn about the decrease of $\Delta_{hb}H^o$ with increasing temperature. The only conclusion about $\Delta_{hb}H^o$ which seems to be justified is, that part of the effect follows from the fact that the enthalpy effect is less endothermic after adsorption of the PMA-pe.

4.5.3. *Importance of Ca^{++} ions in stabilizing the compact conformation*

The results of the rheological measurements of emulsions stabilized by Ca-PMA-pe are represented in fig. 4–7 (section 4.4.1.). Viscosity data are also

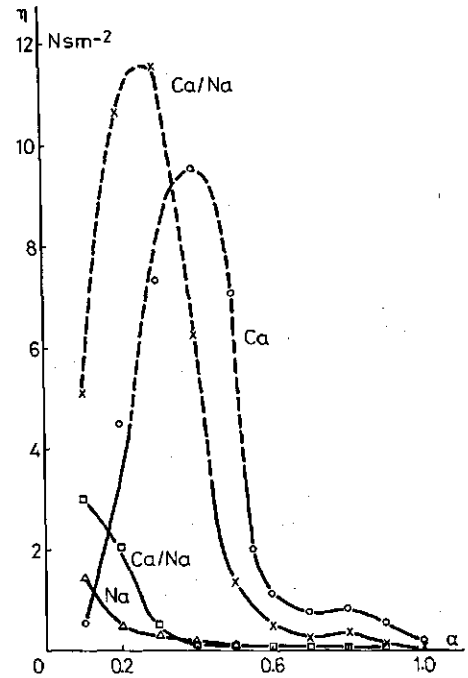

FIG. 4-12. Viscosity of emulsions stabilized by PMA-pe as a function of the degree of neutralization. $\phi = 0.5$. Polyelectrolyte supply 2 mg per cm³ of paraffin. $D = 7.05\ s^{-1}$. Cation: ○ 0.0076 M Ca^{++}. × 0.0076 M Ca^{++} and 0.0152 M Na^{+}. □ 0.0038 M Ca^{++} and 0.0402 M Na^{+}. △ 0.0652 M Na^{+}.

shown in fig. 4–12. In fig. 4–12 data are shown for various concentrations of Ca^{++} and Na^{+} ions. If besides Ca^{++} ions also Na^{+} ions are present, a shift in the maximum to lower α occurs. The extent of the shift depends on the Ca^{++}/Na^{+} ratio. Addition of 0.0038 M $CaCl_2$, before emulsification, to the Ca-PMA-pe solution did not influence the measured viscosities essentially. Only a small broadening of the large maximum was observed.

The viscosity of emulsions prepared with 0.0076 M Mg^{++} and 0.0152 M Na^{+} was the same as that for the corresponding Ca-PMA-pe stabilized emulsions. MICHAELI (1960) reported that the interaction between PMA and Ca^{++}, Ba^{++} or Mg^{++} ions is almost identical. This agrees with our findings for Ca-PMA-pe and Mg-PMA-pe stabilized emulsions. Therefore, below, no distinction between these two ions has to be made.

In previous sections it was shown, that hydrophobic interaction between the methyl groups and electrostatic repulsion between charged carboxyl groups determines to a large extent the viscosity of Na-PMA-pe stabilized emulsions. In the presence of bivalent cations one has to take into account in addition: a. the formation of a complex of the bivalent cations with two carboxylate ions, b. a more effective screening of the negative charges than in the case of monovalent ions.

Because of practical reasons the curves with 0.0076 M Ca^{++} as the cation are dealt with first.

The sharp rise in the viscosities and the dynamic moduli between $\alpha = 0.1$ and 0.4 corresponds with an increase in the number of carboxyl groups. Potentiometric titration experiments show that in this α region free PMA-pe occurs in the compact or a-conformation. It follows from the experiments in the present of sodium ions that it is hardly imaginable that hydrophobic interaction between the two adsorbed polyelectrolyte layers increases so strongly in this α region. Therefore only a growing importance of Ca^{++} bridges remains as a possible explanation. BEGALA and STRAUSS (1972) argued that the forming of Ca^{++} bridges between adjacent carboxyl groups is unlikely, because then highly strained eight-member rings must be formed. On the other hand, O'NEILL et al. (1965) pointed out that this is not a decisive argument against eight-member rings in the case of PMA, since it is well known that all conformations of the highly substituted polymethacrylate chain are already highly strained, on the basis of its spatial structure. However, in PMA-pe the ester groups, distributed along the chain cause the major part of the carboxyl groups to be solitary. So even if eight-member rings can be formed there are only few of them. Therefore Ca^{++} bridges are formed mainly intermolecularly and intramolecularly between non-vicinal carboxyl groups. Perhaps it is even allowed to conclude from the temperature influence on the storage modulus (fig. 4–13a) that, besides the Ca^{++} bridges, hydrophobic interaction also plays some role at $\alpha = 0.4$. If only Ca^{++} bridges were responsible a more continuous descent of η with increasing temperature would be expected.

At $\alpha > 0.45$ a drastic fall in the viscosities and the dynamic moduli was observed. The conformational transition occurs in the same α region (section 4.3.).

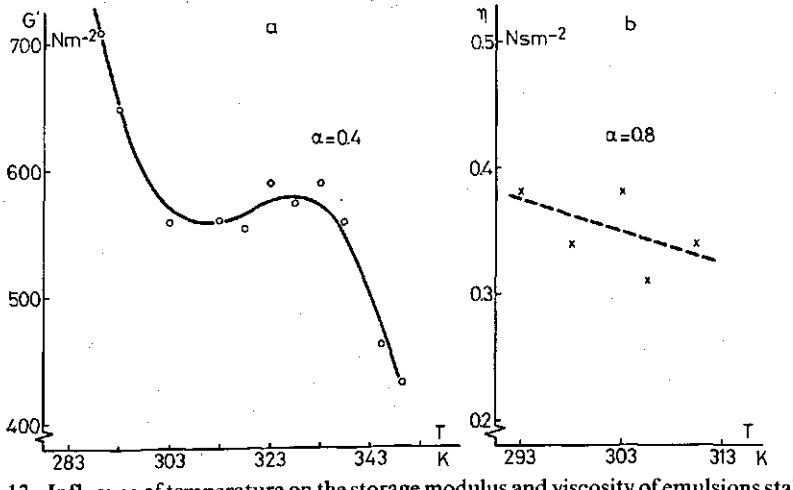

FIG. 4-13. Influence of temperature on the storage modulus and viscosity of emulsions stabilized by PMA-pe. Degree of neutralization is given. Cation 0.0076 M Ca^{++}. $\phi = 0.5$. Polyelectrolyte supply 2 mg per cm^3 of paraffin.

Apparently, there the electrostatic repulsion between the negatively charged carboxyl groups starts to dominate. The fact that it occurs, indicates that not all the dissociated carboxyl groups form bonds with Ca^{++} ions. WOJTCZAK (1965) concluded from conductometric titrations of PMA with $Ca(OH)_2$, that the fractional charge of the polyelectrolyte is between 0.05 to 0.10 over almost the entire range of α. On the other hand, both O'NEILL et al. (1965) and MORAWETZ et al. (1966) found that the binding of Mg^{++} ions to PMA depends on α. For syndiotactic PMA the binding of Mg^{++} per carboxylate group is higher at $\alpha = 0.5$ than at $\alpha = 0.25$ or 0.75, while for the isotactic polymer the binding is the same at $\alpha = 0.25$ and 0.50, but lower at $\alpha = 0.75$. As a corollary to our measurements it may be mentioned that WOJTCZAK (1965) found that the viscosity ratio excess divided by c_p of PMA solutions, increases strongly between $\alpha = 0.3$ and 0.7.

At $\alpha > 0.6$ the viscosities and the dynamic moduli are relatively low. The small maximum around $\alpha = 0.8$ is not easily explained. It is possibly connected with the balance between intra- and intermolecular Ca^{++} bridges. Also the temperature influence on the viscosity of the emulsions at $\alpha = 0.8$ (fig. 4–13b) agrees with the fact that Ca^{++} bridges are the origin of the higher viscosity. Perhaps at $\alpha = 1.0$ the Ca^{++} bridges are mainly intramolecular.

The observed broadening of the large maximum upon addition of 0.0038 M $CaCl_2$ could result from the formation of a few more Ca^{++} bridges and/or from increased screening of the negative charges.

The $\eta(\alpha)$ curve is influenced in two ways if, besides Ca^{++} ions, Na^+ ions are added: a. replacement of Ca^{++} ions by Na^+ ions. MORAWETZ et al. (1966) reported that the binding of Mg^{++} ions to PMA with $\alpha = 0.5$ decreases if the concentration of NaBr raises. Probably, the same occurs with Ca^{++} ions by addition of NaCl. b. a change in the specific area of the emulsion and/or a change in the adsorbed amount. Emulsions, stabilized by Ca-PMA-pe, have a specific area lower than that of Na-PMA-pe stabilized emulsions, whereas the adsorbed amount is higher (BÖHM, 1974). A larger specific area would raise η (SHERMAN, 1968, Ch. 4), whereas a reduction of the adsorbed amount would result in a lowering of η (BÖHM, 1974).

At the moment, it is not feasible to estimate both effects quantitatively. It must be mentioned that a change in the viscosity through effect b is caused indirectly by effect a. Probably the observed changes in the $\eta(\alpha)$ curves are caused by a combined action of the direct and indirect effect of the replacement of bound Ca^{++} ions by bound Na^+ ions.

Finally, a remark must be made on the fact that the viscosity at $\alpha = 0.1$ and 0.2 goes through a maximum as a function of the Ca^{++}/Na^+ ratio. A relatively simple change in the balance between intra- and intermolecular Ca^{++} bridges cannot explain everything. At $\alpha = 0.1$, the viscosities and dynamic moduli of Na-PMA-pe emulsions are higher than in the case of Ca-PMA-pe emulsions, whereas, then, the adsorbed amount per m^2 is much higher (BÖHM, 1974). In the presence of Na^+ ions, the high viscosities and dynamic moduli at $\alpha = 0.1$ are due to hydrophobic interactions (section 4.5.2.). If the Ca^{++} ions would not

influence the interaction between the adsorbed polyelectrolyte layers, a raise of η,G' and G'' would have to be expected due to the increased adsorbed amount per m^2 (section 6.5.1.). Apparently, the Ca^{++} ions influence the adsorbed layers in such a way, that the hydrophobic interaction between two layers adsorbed on different droplets is diminished. Perhaps the Ca^{++} ions influence the flexibility of the extended loops and tails and diminish in that way the hydrophobic interaction. In section 6.6.2., it will be argued that the hydrophobic interaction between the Na-PMA-pe molecules adsorbed on different droplets is a cooperative process. Such a process would be quite sensitive to factors such as chain flexibility. Hence, at $\alpha = 0.1$, Ca^{++} ions do play a role in the interaction, although this role is indirect.

4.6. Summary

In this chapter, the conformation of free and adsorbed PMA-pe was discussed. It was shown that under suitable conditions the conformational transition occurring in free polymethacrylates can also be observed in the adsorbed state. This transition in PMA-pe layers, adsorbed on paraffin drops emulsified in aqueous solution, can be monitored rheologically. This feature, in turn, can be advantageously exploited in order to obtain additional information on the nature of the underlying interaction forces.

In section 4.2., the interaction forces determining the conformation of polymethacrylates were discussed. Besides, Coulombic interaction between the carboxyl groups, van der Waals attraction and hydrophobic bonding between the methyl groups in the main chain were taken into account.

Firstly, a further characterization of free and adsorbed PMA-pe was obtained by potentiometric titration. Data for adsorbed PMA-pe were found by titrating polyelectrolyte covered emulsion droplets. The main conclusion was that the conformational transition from the hyper-coiled or a-conformation towards the extended or b-conformation occurs also in adsorbed PMA-pe. As compared with free PMA-pe, the transition is somewhat broadened and moved to a lower degree of ionization (between $\alpha' = 0.10$ and $\alpha' = 0.55$). In the presence of Ca^{++} ions, the transition region is moved to higher α' (between $\alpha' = 0.35$ and $\alpha' = 0.80$).

Rheological measurements of emulsions stabilized by Na-PMA-pe and Ca-PMA-pe were reported in section 4.4. Both from the viscosity and dynamic data, it was found that strong attraction between the emulsion droplets occurs only if a substantial part of the adsorbed PMA-pe is in the a-conformation. The conclusion was that the high values of the viscosity and the dynamic moduli of PMA-pe stabilized emulsions at low α are due to interactions between extending loops and/or tails, anchored onto different droplets.

Both from the titration data and the rheological measurements it was concluded that the intramolecular interaction in free polymethacrylates and the intermolecular interaction between adsorbed polyelectrolytes were very similar.

As a further check on this conclusion, the influence of methanol on Na-PMA-pe stabilized emulsions and the effect of temperature were investigated. The main conclusion was that, probably, the conformational transition occurring in polymethacrylates at low α is to a large extent due to hydrophobic bonding.

A short discussion concerning the importance of Ca^{++} ions in stabilizing the compact conformation concludes this chapter.

5. POLYMER STABILIZED THIN FREE LIQUID FILMS

5.1. INTRODUCTION

The same factors that govern the stability of hydrophobic colloidal systems, including emulsions, influence the behaviour of free liquid films. Thus soap films are used as a tool for studying double layer-repulsion and VAN DER WAALS attraction (LYKLEMA and MYSELS, 1965b; SHELUDKO, 1967). In the same way, polymer stabilized thin free liquid films (henceforth abbreviated as polymer films) can be used to study the interaction between two adsorbed polymer layers and hence be looked upon as a tool for investigating the stabilization of dispersions by adsorbed macromolecules. A review of the effect of adsorbed polymers on the stabilization of dispersions has been given for instance by VINCENT (1974) and, emphasizing non-aqueous systems, by LYKLEMA (1968). The stabilization of emulsions by polymers has been described by KITCHENER and MUSSELWHITE (1968). They stated that the very good stability against coalescence for these systems, correlates with the viscoelastic properties of the adsorbed interfacial polymer films. BISWAS and HAYDON (1962) suggested that the shear properties are very important. However, KANNER and GLASS (1969) mentioned examples, at variance with these conclusions. According to GRAHAM and PHILLIPS (1976a) the disjoining pressure and the thickness of the aqueous lamellae are critical in determining the emulsion stability. However, in a subsequent paper GRAHAM and PHILLIPS (1976b) concluded, that the rheological properties (resistance to shear and dilatational moduli) of the protein film are of dominating importance in determining the stability of foams.

The general conclusion is, that at present there is no theory satisfactorily explaining all factors, involved in the stabilization of emulsions and foams. In order to gain more insight into these problems, we have studied polymer films. As far as we are aware hitherto, only very few papers have been published on free polymer films. MUSSELWHITE et al. (1967; 1968) reported measurements of bovine serum albumin (BSA) and casein stabilized free liquid films. The casein films were irregular in thickness. Their stability depended on the casein fraction used and on the salt concentration. The reported thicknesses of BSA films varied between 3.5 and 10.5 nm, depending on pH and salt concentration. GRAHAM and PHILLIPS (1976a) reported thicknesses of BSA films amounting to 16–19 nm and for casein films to 8–9 nm. No explanation was offered for the difference in the reported thicknesses. Maybe time effects (ageing of the adsorbed layers at the surfaces before forming a film) play a part.

The process of the formation of a thin liquid lamella between foam bubbles or emulsion droplets and its eventual rupture, can be subdivided schematically into a few stadia.

a. The droplets (or air bubbles) approach each other, stay near each other long enough for the next processes to occur.

b. The forming of an aqueous lamella between the droplets and its thinning. The rate of thinning depends on, for instance the viscosity of the continuous phase and on the rheological properties of the adsorbed polymer layers. In the case of metastable systems the film thins to an equilibrium thickness. The thicknesses and other properties of those films are determined mainly by interactions between the two adsorbed polymer layers, across the film.

c. The film ruptures either or not at a certain thickness and either or not due to a critical disturbance. This causes the coalescence of the adjoining liquid emulsion droplets or air bubbles. In this step forces in the plane of the interface will play the main part.

The results of processes a. and b. are closely correlated with flocculation of the systems. They are of great importance in determining the rheological properties of concentrated emulsions. We will return to this last subject in chapter 6. The rate of thinning will play a role in establishing time required to attain the equilibrium thickness or a thickness, at which rupture occurs. As both the amount of polymer adsorbed and its conformation at the interface are determined by the history of the formation of the layer, one can imagine that the factor time influences the equilibrium thickness and the change on rupture in an indirect way. Measurements on polymer films give information on process b. mainly. In favourable cases, the equilibrium thickness and the rate of thinning of the films can be measured. By determining the equilibrium thickness at various hydrostatic suctions (see for the experimental procedure section 3.6.2.) information can be obtained on the interaction forces in the film. Extrapolation of the measured rate of thinning to the case of an aqueous lamella between emulsion droplets or foam bubbles requires considerable prudence, because of the large discrepancy in magnitude of the film areas.

The factors determining the equilibrium thickness of polymer films are discussed in section 5.2. The properties of films stabilized by PVA and PMA-pe are described in sections 5.3. and 5.4. respectively. In section 5.5. some factors concerning the stability of polymer films against rupture will be briefly discussed.

5.2. Interaction forces in polymer stabilized thin free liquid films

In this section we shall discuss the interaction forces, determining the equilibrium thickness of the films. In mechanical equilibrium, the sum of the forces across the film, promoting the films to thin further and those, opposing this trend, is zero. This is the fundamental difference with a film still draining, or in a metastabile mechanical equilibrium. In the latter case not the equilibrium thickness is measured, but a kind of frozen non equilibrium situation (Prins and van den Tempel, 1970), for instance following evaporation of water.

In contrast with the previous chapter, now 'long range' interaction forces determine the relevant properties. 'Short range' forces influence the conformation of the adsorbed polymer and hence, indirectly the 'long range' forces.

Two groups of forces can be distinguished:

a. attractive forces, including VAN DER WAALS and hydrostatic or capillary forces.
b. repulsive forces, including steric interaction and electrical double-layer repulsion.

Steric interaction can also be attractive. Because PVA is uncharged (FLEER, 1971) electrostatic repulsion does not play a part in the case of films stabilized by this polymer. The PMA-pe stabilized films contained 0.05 M NaCl. The thickness of the electrical double-layer κ^{-1} (κ reciprocal DEBYE length) around individual carboxyl groups is then of the order of 2 nm. It is supposed that the electric double-layer repulsion between the carboxyl groups is reflected in the excluded volume term. Thus it influences the steric interaction between two adsorbed PMA-pe layers in two ways:

a. directly through the interactions between the tails and/or loops in the overlap region. It is assumed that this contribution is relatively small and can be neglected in comparison with the other contribution for not too large overlap.
b. indirectly in that it determines to a large extent the conformation of the adsorbed polyelectrolyte layer (section 4.3.).

In the next sections firstly the attractive VAN DER WAALS and capillary forces will be discussed. In section 5.2.3. the steric interaction is dealt with.

5.2.1. VAN DER WAALS *attraction*

DE VRIES (1958) pointed out, that the VAN DER WAALS attraction per unit area compressing a liquid film of thickness h in air, is equal to the VAN DER WAALS attraction between two semi-infinite liquid layers of the same composition as the film, separated by an air gap of thickness h. According to the macroscopic theory (LIFSHITS, 1955; DZYALOSHINSKII et al., 1959) it is not entirely correct. However, in this study the classical microscopic theory is used for practical reasons:

a. often the macroscopic theory is not workable because insufficient optical data are available.
b. anticipating the discussion in section 5.3.5. it may be stated already that V_A plays only a minor role in the total interaction energy. Therefore a small error does not alter the final conclusions.

The attraction energy V_A between two flat semi-infinite plates at distance h, ignoring retardation, can be calculated by integrating equation (4.1.), assuming simple additivity (DE BOER, 1936; VERWEY and OVERBEEK, 1948). It leads to:

$$V_A = -\frac{A_{11}}{12\pi h^2} \tag{5.1.}$$

where A_{11} is the HAMAKER constant, which in the case of two bodies of material 1 in vacuum is given by:

$$A_{11} = \pi^2 q_1^2 \beta_{11} \tag{5.2.}$$

where q_1 is the number of atoms per m^3 and β_{11} is defined by equation 4.1. The attraction force over a film can be obtained, by differentiating equation (5.1.).

$$F_A = -\frac{A_{11}}{6\pi h^3} \tag{5.3.}$$

The value of A can also be calculated by way of the macroscopic theory. The agreement between the microscopic and the theoretically better macroscopic theory is rather good (VISSER, 1972).

As the distance h becomes comparable with the principal wavelength λ of the LONDON theory, the attraction energy decreases more strongly than by the h^{-2} power law. The interaction then becomes retarded (VERWEY and OVERBEEK, 1948). A quantitative description of the effect has been given by CASIMIR and POLDER (1948); OVERBEEK (1952) and LYKLEMA and MYSELS (1965a). The calculations predict a gradual change with increasing h of the h^{-2} power law to a h^{-3} power law. The modified formula for the LONDON attraction energy between two flat semi-infinite plates, in order to account for retardation, takes the form

$$V_A' = -\frac{A_{11}}{12\pi h^2} \times \text{correction factor} = f' V_A \tag{5.4.}$$

where f' is the correction factor and V_A is the short-range form of the attraction energy. The values of f' are listed and shown as a function of the parameter $p = 2\pi h/\lambda$ by OVERBEEK (1952), where λ is the wavelength of maximum absorption of the material considered. For water λ is about 100 nm. The variation of f' with distance is shown in fig. 5–1. The corresponding correction factor f'' for the attractive forces between two flat semi-infinite plates has been shown by LYKLEMA and MYSELS (1965a). This factor can be obtained from:

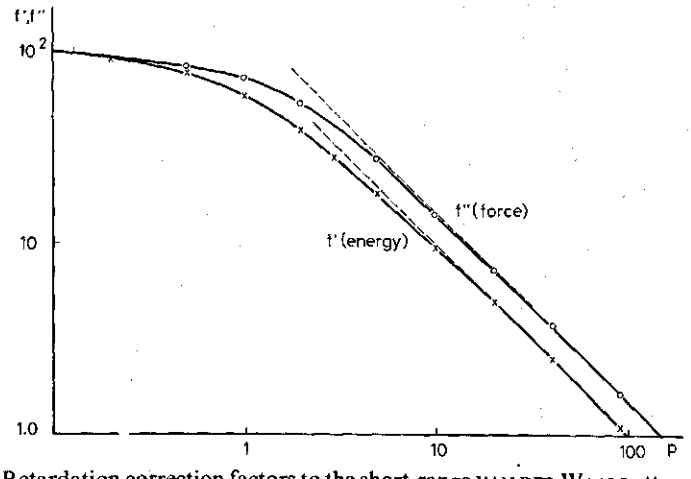

FIG. 5-1. Retardation correction factors to the short-range VAN DER WAALS attraction energy f' and attraction force f'' as a function of the parameter $p = 2\pi h/\lambda$.

$$f'' = f' - \tfrac{1}{2}\frac{\delta f'}{\delta \ln h} \tag{5.5.}$$

The variation of f'' with distance is also shown in fig. 5–1. Then equation (5.3.) takes the form:

$$F_A' = -f'' \frac{A}{6\pi h^3} \tag{5.6.}$$

In the macroscopic theory retardation is automatically built in. Then no special correction is necessary.

With polymer films a complicating factor arises, because they are not homogeneous. They consist of two polymer layers, which might influence the VAN DER WAALS attraction (OSMOND et al., 1973). However, the polymer segment concentration is mostly only a few per cent and the polymers are strongly hydrated. Then to a good approximation, the HAMAKER constant of the adsorbed layer may be made equal to that of water. The same assumption has been made previously for adsorbed layers on colloids (SONNTAG, 1968; FLEER, 1971). Anticipating the discussion which follows in section 5.3.5. it may be stated, that F_A is rather small in comparison with the other contributions to the interaction energy. Hence neglecting the influence of the polymer on the VAN DER WAALS attraction term over the film cannot lead to serious errors.

5.2.2. *Hydrostatic pressure*

This force originates from the height difference between the horizontal film and the surface of the bulk solution. The hydrostatic pressure F_h is determined by the relation:

$$F_h = -\Delta\rho\, g\, l \tag{5.7.}$$

where $\Delta\rho$ is the density difference between the film phase and the outer phase, g is the gravitational constant and l is the height difference between the film and the level of the bulk solution. The PLATEAU-border suction is included in F_h.

5.2.3. *Steric interaction*

Various theories on steric interaction have been published over the last 25 years. Reviews are given by for instance: VINCENT (1974) and especially for non-aqueous systems by LYKLEMA (1968). Steric interaction between adsorbed macromolecules may cause both attraction and repulsion, depending on the properties of the system.

Obviously, some knowledge of the mode of adsorption of the polymer at an interface is one of the prerequisites for understanding steric interaction. Many theories, mainly on non-ionic polymers, have been published on the subject. Of them, only a few will be mentioned. Reviews have been published by for instance: PATAT et al. (1964); STROMBERG (1967) and VINCENT (1974). FRISCH and SIMHA (1954; 1955 and 1957) developed the earliest theory of any consequence. They regarded the segment distribution as due to a random walk

reflecting against a surface. Their approach was shown to be too simple (SILBERBERG, 1962a). More modern theories make use of the concept, that part of the segments is adsorbed at the interface (trains), whereas other segments extend into the bulk solution (loops and/or tails) (SILBERBERG, 1962a, b; 1967 and 1968). HOEVE et al. (1965) introduced the concept of loop size distribution. Lateral interactions between the adsorbed polymer molecules have been incorporated in the theory by SILBERBERG (1968) and HOEVE (1970; 1971). HOEVE (1966) and SILBERBERG (1968) found, that in a Θ solvent the adsorbed layer thickness is roughly proportional to the square root of the molecular weight. In a better (athermal) solvent the dependence on the molecular weight is much weaker.

For the theory of steric interaction it is important to know the segment density distribution normal to the interface. HOEVE (1965) and later HESSELINK (1971a) calculated this quantity for an adsorbed homopolymer. HESSELINK (1969; 1971a and 1975) gave also the segment distribution for adsorbed tails, single loops and random copolymers. An extension of the theory to incorporate also the adsorption of polyelectrolytes has been given by HESSELINK (1972).

The main mechanisms by which adsorbed polymers play a role in steric interaction are (MEIER, 1967):

I Volume restriction. A macromolecule, adsorbed at an interface loses conformational entropy on the approach of a second impermeable interface.

MACKOR and VAN DER WAALS (1951; 1952) were the first to attempt to calculate the repulsive free energy of steric interaction. Their model was based on terminally adsorbed inflexible rods, freely jointing with the adsorbent. Then the loss of conformation entropy on the approach of a second flat interface can be calculated, using the BOLTZMANN relationship:

$$S = k \ln \Omega \qquad (5.8.)$$

where S is the entropy per molecule and Ω was taken proportional to the area, swept out by the free end of the rod. Next the entropic repulsion between two plates was found by multiplying by the number of rods m^{-2}. Lateral interactions were neglected. By using essentially the same approach, CLAYFIELD and LUMB (1966; 1968) calculated by Monto Carlo computations the steric repulsion for flexible, terminally adsorbed polymers and random copolymers. MEIER (1967) calculated the volume restriction effect for terminally adsorbed polymers on flat plates, using random flight statistics. Later the segment density distribution used by MEIER has been corrected by HESSELINK (1969). HESSELINK et al. (1971a, b) also gave calculations of the repulsion for equal loops, homopolymers, random copolymers and also for equal tails. Their results will be discussed further in section 5.2.3.2.

II Free energy of mixing term, or osmotic pressure term. When macromolecules which are adsorbed on two interfaces interpenetrate each other, the density of segments in the space between the interfaces increases. This will lead to an increased number of segment-segment interactions, and decreased number of segment-solvent interactions. The free energy of mixing, being the sum

effect of these can be positive or negative, depending on the quality of the solvent.

FISHER (1958) was the first to point out, that this term should be taken in to account. He assumed that the FLORY-KRIGBAUM theory (FLORY, 1953) of diluted polymer solutions is applicable. MEIER (1967) combined this term with the volume restriction effect. It was assumed that the calculated free energy of mixing and the free energy of volume restriction are additive. Essentially the same approach was followed by HESSELINK et al. (1971b). The volume restriction effect increases linearly with the amount of polymer adsorbed, whereas the mixing effect increases with the square. EVANS and NAPPER (1973a, b) criticized this approach. They claimed that if the mixing term is properly calculated by using the FLORY-KRIGBAUM theory the volume restriction term is already automatically incorporated. Their theory predicts that the Θ-point corresponds to a limit of stability of sterically stabilized dispersions. OSMOND et al. (1975) argued that the EVANS and NAPPER theory does not contain the correct conformational term for the molecules in the overlap volume. Moreover, DOROSZKOWSKI and LAMBOURNE (1973) showed the existence of a steric repulsion term at small particle distances, even under worse than Θ-conditions. Besides, we have found that polymer stabilized emulsions are stable against coalescence under worse than Θ-conditions. Maybe the EVANS and NAPPER approach can be improved by incorporating higher than second virial coefficients. However, even the best theory of polymer solutions cannot incorporate volume restriction by a second interface. Perhaps the contribution of it is less important than calculated by HESSELINK et al. (1971b). Compression by the second adsorbed polymer layer occurs long before compression by the second interface, depending on the segment concentration of polymer in the overlap region. Moreover, a possible change in the conformation, due to the interaction is a second factor which had to be incorporated in any exact theory. Also OSMOND et al. (1975) criticized the HESSELINK et al. (1971a, b) approach. They argued that the basic models used to calculate the volume restriction and the mixing effect, differ too much to justify simple additivity.

In the next sections we shall use the HESSELINK theory in the calculation of the steric repulsion, because it is the most complete one available at the moment.

5.2.3.1. The density distribution of polymer segments in an adsorbed layer

An adsorbed polymer consists of trains on the interface and loops and tails protruding into the solution. The polymer segment density distribution beyond the first layer results from the loops and tails. The normalized density distribution $\rho_l(x)$ for a single loop has been derived by HESSELINK (1971a):

$$\rho_l(x) = 12 \frac{x}{i\, l_s^2} \mathrm{e}^{-6x^2/i\, l_s^2} \tag{5.9.}$$

where x is the distance from the interface and i the number of statistical chain elements (s.c.e.) of length l_s in the loop.

If end effects are neglected (no tails), the number of loops of size i s.c.e. per unit area n_i for a homopolymer is given by (HOEVE et al., 1965; ROE, 1965; HESSELINK, 1971a):

$$n_i = \frac{na}{\bar{i}\sqrt{\pi}} i^{-3/2} \, e^{-i(a/\bar{i})^2} \tag{5.10.}$$

where n is the total number of s.c.e. in the loops per unit area, $\bar{i}$ is the average number of s.c.e. per loop and a is a numerical constant, approximately equal to 0.7 (HESSELINK, 1971a). According to HESSELINK (1971a), the normalized loop size distribution for an adsorbed homopolymer can be calculated by integration of equation (5.9.), together with (5.10.), resulting in the next exponential distribution:

$$\rho_h(x) = \frac{2a\sqrt{6}}{\bar{i}\, l_s} e^{-2ax\sqrt{6}/\bar{i}\, l_s} \tag{5.11.}$$

As mentioned before, equation (5.11.) is only valid if end effects can be neglected. However, ROE (1965; 1966) and MOTOMURA et al. (1969) concluded on theoretical grounds, that a considerable fraction of the adsorbed polymer can be present in one or two tails per macromolecule. This is especially the case for not too long macromolecules. The statistical weight for a loop of i segments is proportional to $i^{-3/2}$ (equation 5.10.), whereas for a tail it is only proportional to $i^{-1/2}$ (HESSELINK, 1975).

The distribution function $\rho_t(x)$ for a single isolated tail has been given by HESSELINK (1969):

$$\rho_t(x) = \frac{6}{i\, l_s} \int_x^{2x} e^{3t^2/2i\, l_s^2} \, dt \tag{5.12.}$$

For a combination of equal tails this equation must be modified to read (HESSELINK, 1975):

$$\rho_t(x) = 2\left(\frac{3}{\bar{i}\, l_s^2}\right)^{1/2} e^{-\left(\frac{3}{\bar{i}\, l_s^2}\right)^{1/2} x} \; e^{-2\left(\frac{3}{\bar{i}\, l_s^2}\right)^{1/2} x} \tag{5.13.}$$

In several cases a combination of equations (5.11.) with (5.12.) or (5.13.) has to be used. All equations given apply under Θ-conditions, i.e. when the linear expansion factor $\alpha = 1$. If α is different from unity the quantity il_s^2 ($= \overline{r_0^2}$) in these equations should be replaced by $\alpha^2 il_s^2$ ($= \overline{r^2}$).

The density distributions mentioned in this section can be used in calculating the steric interaction.

5.2.3.2. The free energy of steric interaction between two adsorbed polymer layers

In the theory of steric interaction (MEIER, 1967 and HESSELINK et al., 1971a, b) a few basic assumptions are made:

1. The adsorption of the polymer is irreversible. No redistribution occurs between the loops, tails and trains during the interaction. Moreover lateral rearrangement of the polymer is not allowed. This assumption will be better for solid/liquid interfaces than for liquid/liquid interfaces. Notwithstanding the long contact times usually encountered with polymer stabilized films (at least a few hours) before measuring the equilibrium thickness, rearrangements are neglected as a second order effect, although their absence cannot be confirmed.
2. Each molecule is adsorbed on one interface only. For polymer films, this assumption seems to be realistic, because the formation of the polymer films was completely reversible: the two PVA monolayers forming a film could easily be separated again, even if the film was a few days old.
3. The adsorbed polymer layers are interpenetrable, while the interfaces are thought to be impenetrable. This assumption is valid, if the segment concentration is low and if the time of contact is long. The time of contact is long (a few hours or more) for polymer films. Initially the concentration of PVA in the overlap region is very low (KOOPAL et al.,1975; section 5.3.5.). Therefore we also reject a denting mechanism as proposed by for instance BAGCHI (1974) in the case of PVA stabilized films for not too large overlap of the adsorbed polymer films. Of course, upon strong thinning of the films mutual volume restriction (compression) of the adsorbed layers can occur.

As mentioned before, we shall use the HESSELINK et al. (1971b) theory for calculating the steric repulsion. If the premisses hold the two main mechanisms by which adsorbed polymers contribute to interaction can be calculated. In view of the nature of these assumptions and those made furhter on the results are only semiquantitative.

The increase in free energy ΔV_{VR} per unit area due to volume restriction by the second interface at the approach to each other of two plane interfaces both covered by v ($= n/\bar{\imath}$) tails or loops per unit area is given by (HESSELINK et al., 1971[b]):

$$\Delta V_{VR} = -2kT \sum_i n_i \ln R(i, h) \tag{5.14.}$$

where i is the number of segments per tail or loop, h the distance between the interfaces and $R(i,h)$ the relative loss of configurational entropy for a single tail or for a single loop. HESSELINK (1971a) derives an expression for $R(i,h)$ in the case of a single tail or loop. For equal tails and loops $n_i = v$, whereas for a homopolymer n_i is given by equation (5.10.). Replacement of the summation over i in equation (5.14.) by integration gives:

$$\Delta V_{VR} = 2v\,kT\,W(\bar{\imath},h) \tag{5.15.}$$

with $W(\bar{\imath},h) = -\bar{\imath}\, n^{-1} \int_0^\infty n_i \ln R(i,h)\, di$. It gives the rise in free energy per averaged loop or tail in units of kT. Values for $W(\bar{\imath},h)$ as a function of $h/\sqrt{\bar{\imath}\, l_s^2}$

are tabulated by HESSELINK et al. (1971b) for equal tails, equal loops and for copolymers.

The increase in free energy ΔV_M, per unit area due to the overlap of the polymeric regions at the approach of two interfaces, covered with adsorbed polymer gives also rise to a local osmotic repulsion. MEIER (1967) has described ΔV_M, modifying the method used by FLORY and KRIGBAUM. Next the polymer-solvent interaction parameter is expressed in terms of α, by means of the FLORY equation (FLORY, 1953, p. 600). Combination of these theories results in:

$$\Delta V_M = 2(2\pi/9)^{3/2} (\alpha^2 - 1)\, kT\, v^2\, (\overline{r^2})\, M(\bar{\imath},h) \qquad (5.16.)$$

where

$$M(\bar{\imath},h) = (\overline{r^2})^{1/2} \left[\int_0^h (\rho_a)_h^2\, dx + \int_0^h (\rho_a \rho_b)_h\, dx - \int_0^\infty (\rho_a)_\infty^2\, dx\right] \qquad (5.17.)$$

Here $(\rho_a)_h$ and $(\rho_a)_\infty$ are the normalized density distributions of the segments of the polymer molecules adsorbed on the interface a per unit area in the presence of an interface b at a distance h and in the absence of a second layer respectively. HESSELINK et al. (1971b) have tabulated the values of $M(\bar{\imath},h)$ as a function of $h/\sqrt{\bar{\imath}}\, l_s^2$ for interfaces covered by equal tails, equal loops and copolymers. By homopolymers the value of $M(\bar{\imath},h)$ and of $W(\bar{\imath},h)$ depends on the particular choice of $\bar{\imath}$. An analytical expression for $M(\bar{\imath},h)$ is given for homopolymers by HESSELINK et al. (1971b).

5.3. PVA STABILIZED THIN FREE LIQUID FILMS

Equilibrium thicknesses and rates of thinning of PVA stabilized films were measured as a function of the hydrostatic suction over the film. The thicknesses of the films extrapolated to obtain the values at zero attraction force over them, are compared with the ellipsometric thickness of adsorbed layers. It is tried to get some information on the segment distribution by comparing these thicknesses with theoretical predictions (section 5.3.4.). The free energy of steric repulsion between two adsorbed polymer layers as a function of the distance between them, is calculated from the equilibrium thickness as a function of hydrostatic suction. The results are compared with theoretical predictions (section 5.3.5.). The stability of the films is discussed in section 5.5.

In the course of this study we became aware that Dr. H. SONNTAG in Berlin was doing the same kind of measurements on PVA films. Some preliminary results of his (SONNTAG, 1976) are also mentioned.

The experimental procedure has been described in section 3.6.

5.3.1. *Drainage behaviour*

The drainage time of the films stabilized by PVA 205 and 217 samples (KURARAY) varied between 4 and 6 hours, depending slightly on the radius of the film. For PVA R-2 films the drainage time was only 1 to 3 hours. The drainage pattern of all films looked like that of mobile soap films although there was a specific influence of the properties of the PVA used. It is imaginable that the

relative motion of patches of film is to a large extent influenced by the rheological properties of the adsorbed polymer layers. Thus the specific properties of the polymer determine to a large extent the drainage behaviour of the films.

Initially all PVA films drained with a dimple. This feature is usually observed for circular horizontal free films, with a thickness > 100 nm (SHELUDKO, 1967). Usually after some time (5 minutes to a few hours) the dimple disappeared. After that, films were obtained which were visually plane parallel and homogeneous. However, in the case of PVA 217 films, which had an equilibrium thickness of ~ 90 nm, the dimple disappeared only very slowly (up to 18 hours). With most films after some time a small dimple was situated near the border (diameter of the films ~ 2 mm). Both the diameter and the thickness of this dimple decreased slowly. The remaining (larger) part of the film was at this stage already visually plane parallel. In the finally attained equilibrium, all films were plane parallel by visible inspection. By scanning the film, no irregularities could be detected. However, the estimated accuracy of this procedure is only ± 5 nm.

Usually the thinning of the films proceeded fast till h amounted to ca. 1.5–2 times the equilibrium thickness. The duration of this part of the drainage process corresponded roughly with the time necessary for the dimple to disappear except with PVA 217 films. After that stage the thinning of the films slowed down upon approach of the equilibrium thickness. SHELUDKO and coworkers (SHELUDKO, 1967) derived that the rate of thinning of a plane circular film with zero velocity at the two surfaces obeyed the relationship:

$$\frac{d(i/h^2)}{dt} = \frac{4}{3\eta r_0^2} \Delta P \qquad (5.18.)$$

where r_0 is the radius of the film and ΔP the capillary suction operating on the film. Inserting reasonable values ($\Delta P = 50$ Nm^{-2}, $r_0 = 1.5$ mm and $\eta = 0.3$ Nsm^{-2}) showed that in order to explain the observed rates of thinning, some mobility of the surfaces had to be accepted.

The effect of the radius on the rate of drainage is counteracted by the fact that in the case of larger films the hydrostatic suction is also higher. The radius effect is in qualitative agreement with theoretical predictions (SHELUDKO, 1967; CLUNIE et al., 1971).

5.3.2. *Equilibrium thicknesses*

The results of the equilibrium thickness measurements on films stabilized by PVA at varying hydrostatic pressure are shown in fig. 5–2. The hydrostatic pressure was calculated with equation 5.6. (for $\Delta\rho$ was taken 1020 kg m^{-3} and $g = 9.8$ m s^{-2}). As can be seen the films are remarkably thinner at higher hydrostatic pressures. A second feature is, that there is a strong influence of the molecular weight and/or nature of the sample on the equilibrium thickness.

The influence of a tenfold change in the PVA concentration is only small in the region studied. The adsorbed amount at a 1 M aqueous glycerol solution-air surface was also almost the same for the two concentrations used (section 5.3.3.).

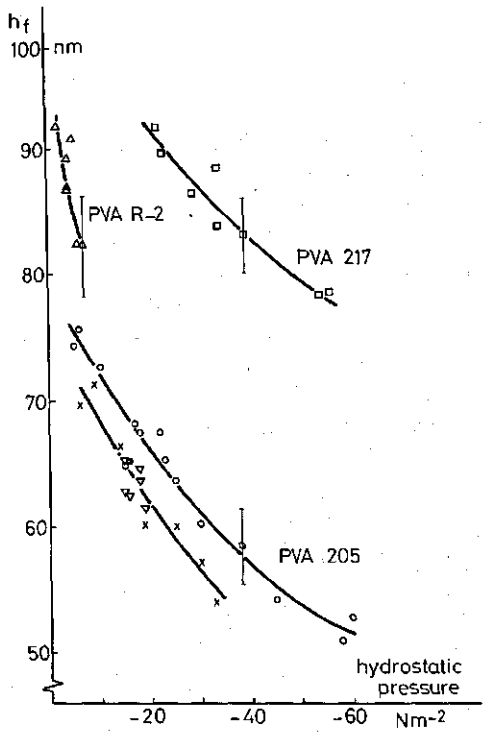

FIG. 5-2. Equivalent aqueous solution thickness of PVA stabilized films as a function of the hydrostatic pressure.
× PVA 205 400 ppm.
○ PVA 205 4000 ppm.
▽ PVA 205 400 ppm, time experiments.
□ PVA 217 4000 ppm.
△ PVA R-2 4000 ppm.

Reduction of the waiting time before bringing the two surfaces together (see section 3.6.2.) from 1 hour till 15 or 2 minutes did not influence the equilibrium thickness. It appears that the adsorption of PVA proceeds so fast, that it has been completed within such short periods. However, LANKVELD and LYKLEMA (1972b) observed time effects of about 10 hours in the interfacial tension of solutions of various PVA samples. Therefore a more reasonable explanation appears to be that during the thinning of the film adsorption and reconformation of the polymer at the surface proceeds. If the influence of thinning , which takes several hours, on these processes is only relatively small or always the same, one can imagine that the equilibrium thickness does not depend on the waiting time. Besides, it is possible that the reconformation of the adsorbed PVA leads to a measurable change in the interfacial tension but not to a measurable change in the steric repulsion.

The measured equivalent solution thickness h_f has to be corrected for the different optical properties of the surfaces. The correction h^* to be applied to

TABLE 5-1. Correction h^* to be applied to the equivalent solvent thickness h_f.

PVA sample	solution concentration/ppm	adsorbed amount at one surface/mg m^{-2}	h^* nm	h_0 nm
205	400	3.1	−3.1	76
205	4000	3.2	−3.2	77
217	4000	3.7	−3.7	100
R-2	4000	2.0	−2.0	

h_f is calculated by means of equation (3.11.). The change in the refractive index in the equivalent polymer surface layer (see fig. 3–6) was calculated taking $(dn/dc)_T$ = constant. The constant measured for PVA was 0.15 cm^3/g. This result is in good agreement with the values, reported by KLENIN et al. (1974) and collected by HUGLIN (1975). The concentration in the equivalent polymer surface layer was estimated from ellipsometric measurements on adsorbed PVA layers (section 5.3.3.). The calculated corrections are listed in table 5–1.

The VAN DER WAALS attraction over a film with a thickness h was calculated by equation (5.6.). Then the total compressive forces over the film have been calculated by summing F_A and F_H. Because of the balance $F_A + F_H + F_S = 0$, in this way F_S is found. The results are represented in fig. 5–3.

As expected the steric repulsion becomes stronger, when the two adsorbed polymer layers approach each other. There is a pronounced influence of the

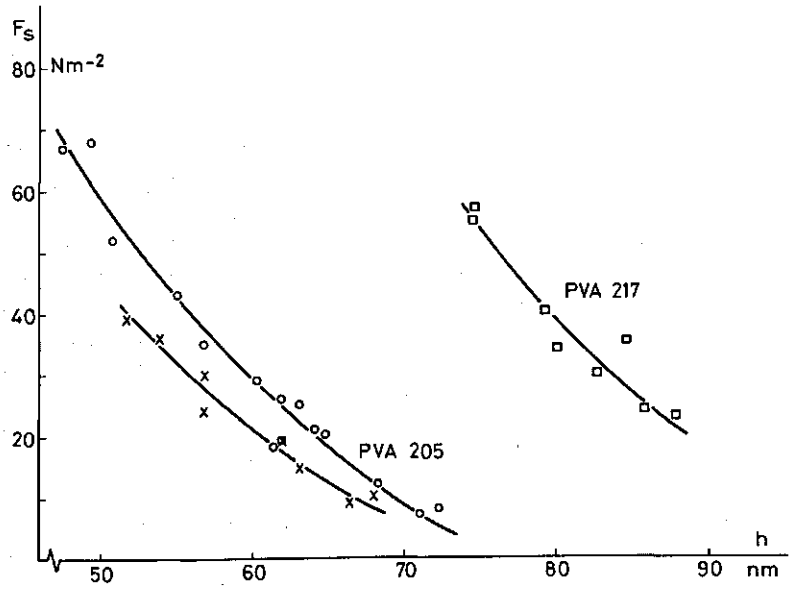

FIG. 5-3. Steric repulsion of PVA stabilized films as a function of the thickness.
× PVA 205 400 ppm.
○ PVA 205 4000 ppm.
□ PVA 217 4000 ppm.

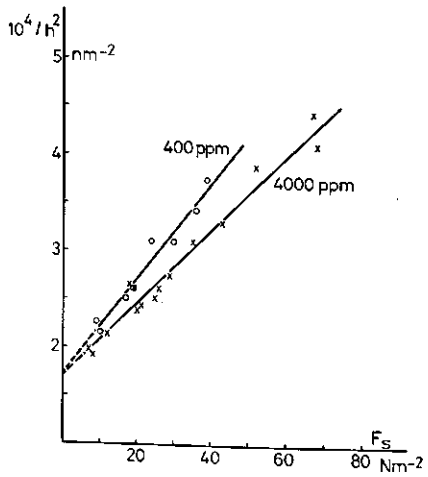

FIG. 5-4. Extrapolation of $1/h^2$ to $F_S \rightarrow 0$ for films stabilized by PVA 205. Solution concentration PVA is given.

molecular weight on the distance, at which the adsorbed polymer layers start to interact. The shapes of the curves (the first and second derivatives) depend hardly on the molecular weight. At given F_s the slopes are almost identical. Apparently, the shape is much more determined by the properties of the adsorbed PVA. Some indication for it can be found by comparing the results of PVA 205 and 217 with those of PVA R-2 in fig. 5–2.

The dependence of h at given F_S on M_v is for PVA 205 and 217 of the order of

$$h \sim M_v^{0.3}$$

A rough indication of the thickness h_0 at which the two adsorbed layers start to interact can be obtained by extrapolating the curves of fig. 5–3 to $F_S \rightarrow 0$. It appeared to be more suitable to extrapolate F_S against h^{-2} because then a linear dependency is obtained over a large region of h (fig. 5–4). (It should be noted, that extrapolation against h^{-3} also gives a straight line within the experimental accuracy though over a smaller region of h. The resulting h_0's were nearly the same for the two ways of extrapolation.) The values found for h_0 are listed in table 5–1. It is noteworthy that the h_0's for films made of a 400 and 4000 ppm PVA 205 solution are almost identical. This means that the maximum extension of the adsorbed polymer layers is equal. However, the different slopes in fig. 5–4 imply that the F_S (h) relations are not the same. The rise of F_S with decreasing h is lower in the case of the 400 ppm solution, than for the 4000 ppm solution. It implies that, if other factors being equal, in films made of a 400 ppm solution the segment concentration is somewhat more spread in the overlap region than in those made from 4000 ppm solutions.

SONNTAG (1976)[2] found for different PVA samples h_0 values of the same order.

[2] The author thanks prof. SONNTAG for making available his unpublished results.

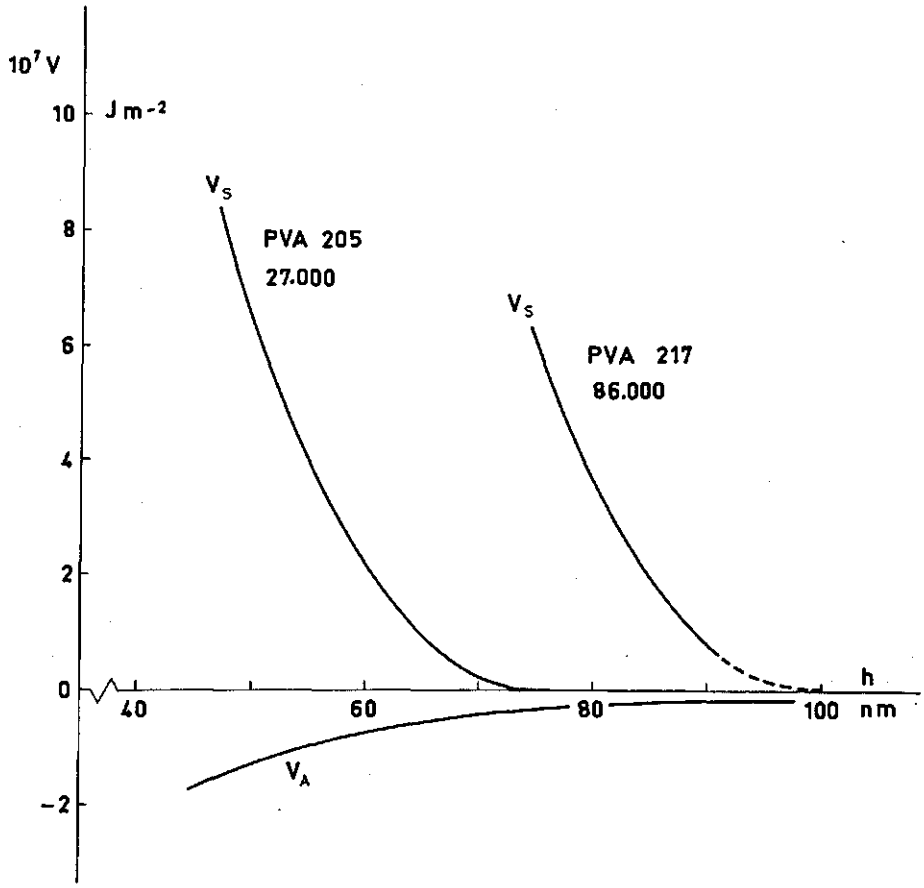

FIG. 5-5. Steric repulsion energy and VAN DER WAALS attraction energy over PVA stabilized thin free liquid films. The molecular weight of the PVA is indicated. HAMAKER constant used $4.38\ 10^{-20}$ J.

as found by us. His results depend somewhat on the added KCl concentration. For a KCl concentration of 10^{-2} M he found for PVA samples with 12% acetate groups and M = 35000, h_0 = 50.5 nm and for M = 55000, h_0 = 66 nm. The values depend somewhat on the manufacture of the PVA samples. However, SONNTAG observed a much smaller dependence of the thickness on the hydrostatic pressure. So in his case the found steric repulsion increases much faster (till 10 times) with a decrease in thickness than in fig. 5–3. We do not have an explanation for this difference. Maybe it is a consequence of our using different PVA samples.

The free energy of steric repulsion V_S between two adsorbed PVA layers was calculated by graphical integration of the F_s (h) curves in fig. 5–3. As zero point h_0 was chosen. The results are represented in fig. 5–5.

In section 5.3.4. the value of h_0 is compared with the ellipsometric thickness of an adsorbed layer. The found V_S (h) curves are discussed in section 5.3.5.

TABLE 5-2. Survey of ellipsometric measurements on PVA monolayers at a 1 M aqueous glycerol solution-air surface.

PVA sample	concentration PVA solution c_p/ppm	ellipsometric thickness t_{el} nm	$2\,t_{el}/h_0$	adsorption mg m^{-2}	t_{rms} for an exponential distribution nm
205	400	17	0.45	3.1	11.5
205	4000	21	0.55	3.2	14.3
217	4000	29	0.58	3.7	19.7
R-2	4000	18	~0.4	2.0	

5.3.3. *Ellipsometric thickness of adsorbed PVA layers*

Some ellipsometric measurements on the adsorption of PVA at a 1 M aqueous glycerol solution-air surface were done by J. BENJAMINS[3], of the Unilever Research Laboratory, Vlaardingen. The surface concentrations and adsorbed film thicknesses were determined, by using an ellipsometric arrangement with a monochromatic laser (λ = 632.8 nm.) as light source and a photomultiplier as detector, as described by for instance BOOTSMA and MEYER (1969). The results are listed in table 5–2.

As was to be expected twice the ellipsometric thickness t_{el} is lower than h_0 (nm). It illustrates that t_{el} is a kind of average thickness and not a maximum thickness.

As pointed out by MCCRACKIN and COLSON (1963), the ellipsometric thickness is correlated with the root mean square thickness t_{rms} of inhomogeneous films. For an exponential distribution they found $t_{rms} = (1/1.47)t_{el}$. The values of t_{rms} are also listed in table 5–2. These values are used in the next sections, in order to get more information on the segment distribution.

5.3.4. *Conformation of adsorbed PVA*

In this section it is tried to obtain some information on the conformation, particularly on the density distribution of the segments of the adsorbed PVA. The discussion will be limited to PVA 205 and 217 and a concentration of the PVA solution of 4000 ppm. The approximations which have to be made are too large to justify discrimination between the 400 and 4000 ppm PVA 205 solutions.

The average number i of s.c.e. can be calculated from h_0 for the different theoretical density distributions mentioned in section 5.2.3.1., if a reasonable estimation of the segment concentration at $x = \frac{1}{2}h_0$ can be made. However, no definite information on $\rho(\frac{1}{2}h_0)$ is available. Therefore we chose arbitrarily for $\rho(\frac{1}{2}h_0)$ a value equal to the segment concentration in the bulk solution.

Next the adsorbed amount of segments per unit area must be known. HOEVE (1965, 1970) pointed out that due to the different conditions between the first segment layer near an interface and those further away, a discontinuity occurs at a distance δ from the interface. In the first layer the segment concentration is

[3] The author thanks mr. BENJAMINS for making available his unpublished results.

ρ_0 ($0 \leqslant x \leqslant \delta$). The equations which have been mentioned in section 5.2.3.1., apply to $x \geqslant \delta$. Integration of mentioned distribution functions between $\delta < x < \infty$ (taking into account that they are normalized) yields the total adsorbed amount of segments minus those, adsorbed in the first layer. The number of adsorbed segments in the first layer can be found by taking 0.30 nm^2 for the surface area per segment and the surface completely occupied by PVA (LANKVELD and LYKLEMA, 1972b). It results in 3.3 segments nm^{-2}. The total number of segments N_t, adsorbed per unit area is related to Γ by the molecular weight per segment (49 for PVA with 12% acetate groups) resulting in $N_t = 12.3\,\Gamma$, if N_t is expressed in nm^{-2} and Γ in mg m^{-2}.

Now $\bar{\imath}$ can be calculated for the different theoretical density distributions. As was to be expected for the case of isolated loops or tails, equations (5.9.) and (5.12.), no realistic values for $\bar{\imath}$ were found. The results for the two other functions (equation (5.11.) and equation (5.13.)) are listed in table 5–3. The values found had to be compared with a mean number of s.c.e. per molecule of 75 for PVA 205 and 238 for PVA 217. It can be concluded that the values found for $\bar{\imath}$ are not unrealistic for both distribution functions. Additional information can be obtained from the ellipsometric thickness. If it is assumed that an exponential density distribution applies $\bar{\imath}$ can also be calculated from t_{rms} listed in table 5–2 with (HESSELINK, 1971a):

$$t_{rms}^2 = \frac{\bar{\imath}^2\, l_s^2}{12a^2} \qquad (5.19.)$$

This results for PVA 205 in a value of $\bar{\imath} = 22$ and for PVA 217 in $\bar{\imath} = 29$. Using these two values for the calculation of ρ_h ($\frac{1}{2}h_0$) (equation 5.11.) results in 0.15 segments nm^{-3} in both cases. This is about three times higher than the segment concentration in the bulk solution. It indicates that probably the real segment concentration at large distances is lower than predicted by equation (5.11.). Of course, the same tentative conclusion follows from a comparison of the found $\bar{\imath}$ values. Comparison of equations (5.11.) and (5.13.) shows that, except for small values of $\bar{\imath}$, the segment concentration at large distances from the interface is lower in the case of a set of tails than for an exponential distribution for a certain value of $\bar{\imath}$. Therefore, perhaps it is even allowed to conclude that the obtained data are in favour of a substantial contribution of the tails to the density distribution of the segments of adsorbed PVA 205 and 217. The ratio of the listed values of $\bar{\imath}$ in table 5–3 to the mean number of s.c.e. per molecule of 75 for PVA 205 and 238 for PVA 217 also points in this direction. This

TABLE 5-3. Average number of s.c.e. $\bar{\imath}$ per loop or tail calculated with $\rho(\frac{1}{2}\,h_0) = 4000$ ppm.

	$\bar{\imath}$ PVA 205	$\bar{\imath}$ PVA 217
combination of tails of equal length (equation (5.13.))	38	60
exponential (equation (5.11.))	15	19

tentative conclusion agrees with theoretical predictions (ROE, 1965; 1966; MOTOMURA et al., 1969; HESSELINK, 1975).

Finally, it has to be noted that in this section the polymer is taken as being monodisperse. In fact, the molecular weight distribution is rather broad and probably of the FLORY-type (PRITCHARD, 1970; SCHOLTENS, 1977). Consequently the analysis given above requires some modification. A wide distribution of tail lengths is probable. It cannot even be excluded that some relatively long tails dominate the properties of an adsorbed layer at a long distance from the interface. This possibility is examined in the next section.

5.3.5. *Steric interaction between two adsorbed PVA layers*

In this section it will be tried to analyse the steric repulsion energy curves, shown in fig. 5–5. This graph includes the curve for the VAN DER WAALS attraction energy, in order to show its relatively small contribution.

In the previous section no definite conclusion was obtained with respect to the density distribution of the segments of adsorbed PVA 205 and 217. Indications were obtained that tails play an important part. In this section we shall calculate the steric repulsion energy between two adsorbed PVA layers for a density distribution estimated, with the HESSELINK et al. (1971b) theory (section 5.2.3.2.). By comparing the results with the measured ones, information is obtained on the correctness of this distribution. In doing so, it is implicitly assumed, that the HESSELINK theory is correct, which is certainly not entirely warranted. However, if the described procedure leads to a reasonable density distribution, one can at least conclude that apparently the HESSELINK theory and our experimental facts are consistent.

HESSELINK et al. (1971b) have tabulated the dimensionless volume restriction function $W(\bar{\imath},h)$ and the osmotic function $M(\bar{\imath},h)$, for the case of equal loops and tails. For an exponential density distribution of the segments of the adsorbed polymer an analytical expression for $M(\bar{\imath},h)$ is given. For a combination of tails of equal lengths no easily workable equation is available.

As already indicated in the previous section, the assumption that the density distribution is a combination of tails of equal lengths is not valid. This is in the first place caused by the fact that the molecular weight distribution of the PVA's used is wide. Probably the molecular weight distribution is of the 'most probable', or FLORY type (PRITCHARD, 1970; SCHOLTENS, 1977). Using this fact it is easy to calculate the number of molecules in a certain molecular weight fraction f (M_v) (table 5–4). By calculating the number of adsorbed molecules it is assumed that their molecular weight distribution is the same as that of the dissolved ones. In fact short molecules adsorb faster owing to their higher diffusion coefficient. However, in the later stages of the adsorption process longer molecules start to dominate on account of their higher free energy of adsorption. In view of the semiquantitative character of the calculations to be given, the above assumption will not lead to serious errors. Next we used the rather crude approximation that on the average a certain fixed percentage of the segments, independent of the length of the polymer molecule, is adsorbed in the one or two

TABLE 5-4. Number of adsorbed polymer molecules as a function of the molecular weight M_v.

$f(M_v)$	percentage of total	number of adsorbed polymer molecules in $f(M_v)$ m^{-2}	
		PVA 205	PVA 217
$0 < < M_v$	63.2	$45\ 10^{15}$	$16.3\ 10^{15}$
$M_v < < 2M_v$	23.3	$16.5\ 10^{15}$	$6.0\ 10^{15}$
$2M_v < < 3M_v$	8.55	$6.1\ 10^{15}$	$2.2\ 10^{15}$
$3M_v < < 4M_v$	3.15	$2.2\ 10^{15}$	$0.8\ 10^{15}$
$4M_v < < 5M_v$	1.16	$0.8\ 10^{15}$	$0.3\ 10^{15}$
$5M_v < < \infty M_v$	0.67	$0.5\ 10^{15}$	$0.17\ 10^{15}$

tails per molecule. This assumption, together with the accepted molecular weight distribution of the polymer results in a density distribution of the segments of the adsorbed PVA, that at the outer part of the adsorbed layer is completely determined by relatively few long tails, provided the fraction of segments adsorbed as tails is not too small. Because of their large mutual distances they can be considered as nearly isolated (see fig. 5–6).

If it is supposed that such a density distribution applies, one can calculate the steric interaction between two adsorbed PVA layers. The only additional assumption that is needed is that the steric interaction between the long tails may be dealt with as if the tails were entirely isolated ones. For the outer parts of the adsorbed layer this assumption is probably correct, but it does not hold for the parts of the tails near the interface, because of lateral crowding by loops, a feature that we shall neglect. A consequence of this assumption is, that our calculations apply only to a small overlap of the two adsorbed PVA layers. In the calculations, the percentage of the polymer segments X_t adsorbed in tails, and the number of tails per polymer molecule can be used as variables. The dimensionless volume restriction function $W(i,h)$ and osmotic function $M(i,h)$ are shown in fig. 5–7. The volume restriction effect and the mixing term can

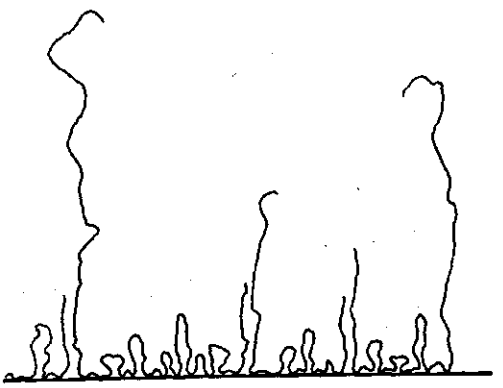

FIG. 5-6. Possible model of a PVA layer adsorbed at an aqueous solution-air interface.

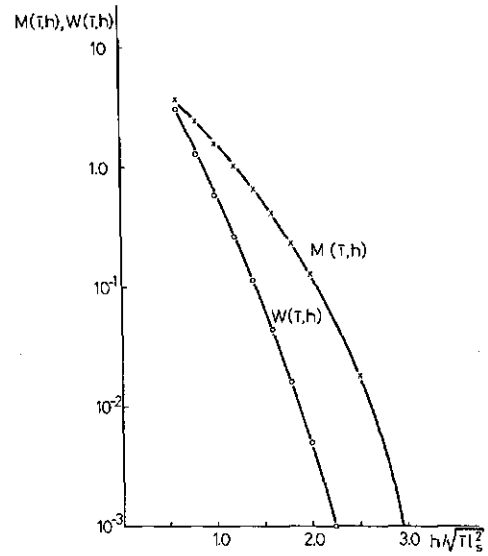

FIG. 5-7. Values for the dimensionless volume restriction function $W(\bar{\imath}, h)$ and osmotic function $M(\bar{\imath}, h)$ for single tails according to HESSELINK et al. (1971b).

now be calculated with equations (5.15.) and (5.16) respectively. The values of α and l_s are taken from table 2–4 and 2–5.

The calculated steric interaction between two adsorbed PVA 205 or PVA 217 layers is shown in fig. 5–8, for a few percentages of the segments, adsorbed as tails. The agreement between the theoretically calculated curves and the experimental ones is good. It endorses the view that in the investigated cases, the properties of the adsorbed layer far away from the interface and the interaction between two of such layers is dominated by a few tails only.

Prior to further discussing this conclusion a few remarks can be made.

a. In the considered overlap region the volume restriction term amounted to maximally 50% of the total (i.e. mixed) term. Therefore the conclusions cannot be influenced seriously by adding both the mixing and the volume restriction term. Anyway, addition of these terms is not justified in every respect.
b. The experimentally found steric repulsion cannot be explained, by assuming interaction to occur between identical isolated tails for any reasonable value of $\bar{\imath}$.
c. An exponential distribution, taking for $\bar{\imath}$ the values listed in table 5–3, would result in a much too strong steric repulsion at the investigated distances between the interfaces. This supports the conclusion of section 5.3.4., that this density distribution function is not in agreement with our experimental results.
d. In view of all the assumptions made, the values for X_t have only a qualitative meaning. Anyway the obtained percentages are reasonable. The fact that

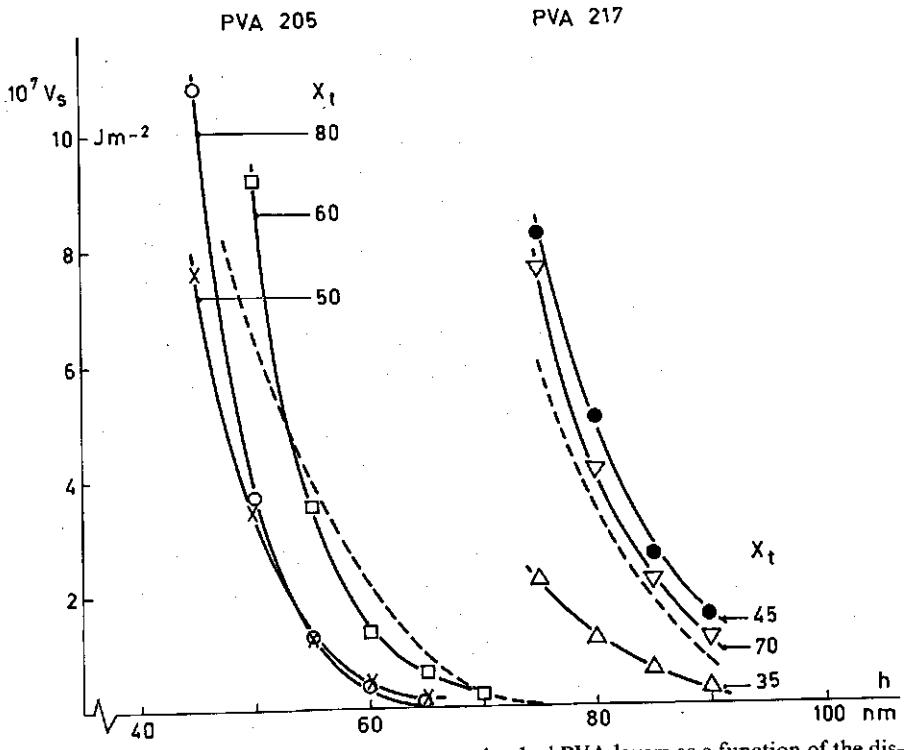

FIG. 5-8. Steric repulsion energy between two adsorbed PVA layers as a function of the distance.
Full curves calculated according to the theory of HESSELINK et al. (1971b).
Dashed curves experiments.
The percentage of polymer segments X_t adsorbed in tails per molecule is indicated.
× □ △ ● one tail per molecule.
○ ▽ two tails per molecule.

for PVA 217 the percentages are lower than for PVA 205, agrees with theoretical considerations.

e. In our calculations it was explicitly assumed, that the tail lengths of polymer molecules in a certain molecular weight fraction are the same. Actually, their lengths will vary. This variation would result in a slower increase of the steric interaction with decreasing separation of the interfaces than considered.

The conclusion that a few long tails dominate the properties of the outer part of an adsorbed polymer layer in the described system, is of considerable practical interest. For instance, it can be used in the further development of a flocculation theory. On the other hand, it can be invoked to explain the relatively large thicknesses, which have been found by viscometry, using capillaries coated with polymer (see for instance ROWLAND and EIRICH, 1966). In that respect, it must be expected, that just a few long tails dominantly influence the hydrodynamics of the flowing solvent, whereas their contribution to the change in refractive index as measured by ellipsometry, is only small, so that

their presence is easily overlooked in establishing the adsorbed amount and the ellipsometric thickness. The repulsive energy curves found by DOROSZKOWSKI and LAMBOURNE (1973) at not too small separations can also be explained by the proposed density distribution model of the segments of adsorbed polymers. These authors found that the steric repulsion between two adsorbed polymer layers starts already at large distances of the interface and increases relatively slowly with decreasing separation. The molecular weight distribution of the polystyrene used as stabilizer was wide ($M_w/M_n = 2$). Their calculations with the theory of MEIER and of HESSELINK et al., using the concept of isolated tails of equal length, resulted in a steric repulsion starting at too small separations (see fig. 5–9). The calculated repulsion was too low at a small overlap of the adsorbed polymer layers, whereas it was much too high at shorter distances, i.e. in the region of strong overlap.

5.4. PMA-PE STABILIZED THIN FREE LIQUID FILMS

Equilibrium thicknesses and the drainage behaviour of PMA-pe stabilized films have been measured. The degree of neutralization of the PMA-pe was an important variable. The equilibrium thicknesses were compared with ellipsometric thicknesses of an adsorbed PMA-pe layer and the drainage behaviour was correlated with surface rheological measurements. The stability of the films will be discussed in section 5.5.

The experimental procedure has already been described in section 3.6. In all measurements the electrolyte was 0.05 M NaCl.

5.4.1. *Drainage behaviour*

The drainage behaviour of the PMA-pe films depends strongly on the degree of neutralization α. At $\alpha = 1.0$ the films drain rapidly (ca. 1 hour) till a thickness of about 120 nm. After that the thinning of the film continues much more slowly, till after 16–24 hours an equilibrium thickness was obtained. The drainage pattern resembles that of mobile soap films. These films drained with an

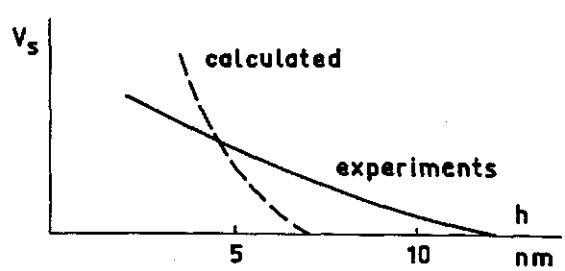

FIG. 5-9. Schematic representation of some results obtained by DOROSZKOWSKI and LAMBOURNE (1973).

initial dimple. The same behaviour is found with films at $\alpha = 0.7$. Films stabilized by PMA-pe with $\alpha = 0.5$ also drained fast in the early stages, but at a thickness of about a few hundred nm (visible inspection) the thinning became extremely slow. The formation of a visually plane parallel film with no detectable thinning over 1 day required more than one week. At $\alpha = 0.1$ the films were rigid and even thick films drained extremely slowly. Usually, film irregularities were visible. These films are very stable. Films made without the addition of glycerol were also rigid, but drained a little faster. Only twice did we succeed in obtaining an equilibrium film with parallel faces on visual inspection. Their formation required more than a week. Usually the films were not plane parallel, because of film irregularities.

An interesting feature is, that the transition between rigid and mobile behaviour correlates well with the conformational transition of PMA-pe adsorbed at a paraffin-water interface and with the change in the rheological properties of emulsions, stabilized by PMA-pe (section 4.3. and 4.4.).

5.4.2. *Equilibrium thicknesses*

The exploratory results obtained are listed in table 5–5. The correction h^* has been calculated by using the adsorbed amounts, which were measured by ellipsometry. The adsorbed amount was not known for films stabilized by PMA-pe with $\alpha = 0.7$. For the constant $(dn/dc)_T$ 0.15 $cm^3\ g^{-1}$ was taken. In view of the substantial uncertainty in the measured thicknesses at the lower α's, the correction was not applied there. The high estimated inaccuracy is due to the extremely long drainage times and in the case of $\alpha = 0.1$, also to possible surface irregularities and perhaps to the increased evaporation, if glycerol was omitted.

A reduction of the waiting time to a few minutes (see section 3.6.2.) does not influence the observed properties of the films.

TABLE 5-5. Equilibrium thicknesses of PMA-pe stabilized thin free liquid films. Electrolyte 0.05 M NaCl. PMA-pe concentration 1000 ppm.

α	glycerol	hydrostatic pressure/Nm^{-2}	$h\dagger$ nm	h^* nm	h nm
0.1	–	ca. 10	45 ± 20	−2	45 ± 20
0.5	+	ca. 13	50 ± 10	−1	50 ± 10
0.7	+	ca. 15	60 ± 6		60 ± 6
1.0	+	10	32 ± 3	−1	31 ± 3
		13	34 ± 3	−1	33 ± 3

5.4.3. *Ellipsometric thickness of adsorbed PMA-pe layers*

Ellipsometric measurements at an air-water interface were done by BENJAMINS of the Unilever Research Laboratory, Vlaardingen. The experimental procedure is described in section 5.3.3. The results are collected in table 5–6.

The values found at $\alpha = 0.1$ or 0.5 or at $\alpha = 1.0$ after one day correspond reasonably well with half the corresponding film thicknesses (see table 5–5).

TABLE 5-6. Survey of ellipsometric measurements on PMA-pe monolayers adsorbed at a water-air surface. Electrolyte 0.05 M NaCl. PMA-pe concentration 100 ppm.

degree of neutralisation	ellipsometric thickness/nm	adsorption mg m^{-2}
0.1	12	2.4
0.5	25	1.5
1.0	70 after 1 hour	1.0
	15 after 1 day	1.0

The reason of the decrease in thickness of the layer adsorbed at $\alpha = 1.0$ is not well known. Possibly it is a reconformation effect. In connection with this, BÖHM (1974) reported at pH $\geqslant 7$ a large time dependence of the interfacial tension of PMA-pe at a paraffin-aqueous solution interface during more than 7 hours. He ascribed this effect to a diffusion of the PMA-pe to the interface followed by a slow reconformation. Our data indicate that the diffusion process must be completed after one hour. No large time effects were found at the other α's.

5.4.4. *Surface dilatational modulus*

Some exploratory measurements on the surface dilatational modulus of an adsorbed PMA-pe layer have been done by BENJAMINS of the Unilever Research Laboratory, Vlaardingen. The dynamic modulus $|\varepsilon|$ was measured with the longitudinal wave method as described by LUCASSEN-REYNDERS et al. (1969) and LUCASSEN et al. (1972). The experimental procedure has been described by BENJAMINS et al. (1975). As a barrier, a square of rubber bands (15 × 15 cm) placed in the surface, was used. At the corners the bands were connected to metal bars, which could move synchronously along the diagonals of the surface. A sinusoidal movement was applied. The change in surface tension γ produced by the change of the surface area A, was measured in the centre of the square, using a Wilhelmy plate. The absolute value of ε was obtained from the maximum change in γ during an expansion/contraction cycle upon a maximum change in A:

$$|\varepsilon| = A \frac{\Delta \gamma}{\Delta A} = \frac{\Delta \gamma}{\Delta \ln A} \tag{5.20.}$$

The results are listed in table 5–7. Only at $\alpha = 0.1$ was a nonzero phase angle found (around 10°, depending on frequency). It points to a small viscous component. In the other cases, the phase angle was negligibly small indicating that the dilatational modulus is purely elastic. The dilatational modulus decreases with increasing degree of neutralization, pointing to a raise in compressibility and a decrease in cohesion. Again the time effects at $\alpha = 1.0$ are relatively large.

Because both surface rheology and drainage behaviour of films reflect the complex interactions in PMA-pe surface layers, some correlation between these phenomena would not seem unexpected. Indeed a correlation is found

TABLE 5-7. Dilatational modulus of PMA-pe monolayers adsorbed at a water-air surface. Electrolyte 0.05 M NaCl. PMA-pe concentration 100 ppm.

α	age of interface (in hours)	frequency range/s^{-1}	$\lvert\varepsilon\rvert$/mN m^{-1}
0.1	2	0.033–0.84	30–50
	24	0.033–0.84	36–63
0.5	2	0.033–0.84	12–18
	24	0.033–0.84	21–29
1.0	2	0.17–0.84	3–3
	24	0.17–0.84	11–12

between a more rigid behaviour of the films and a higher dilatational modulus. Both the increased film rigidity and the higher dilatational modulus are observed with the compact or a-conformation of the adsorbed PMA-pe (see sections 4.3. and 4.4.). It indicates that there probably is some relation between the mentioned phenomena, the interaction forces responsible for the occurrence of the a-conformation in the PMA-pe molecule and the ensuing considerable changes in the rheological properties of paraffin in water emulsions stabilized by this polyelectrolyte observed at low α. Because of the observed correlation, this work deserves further experimental investigation. Perhaps the shear properties should also be considered.

5.5. STABILITY OF POLYMER FILMS AGAINST RUPTURE

In this section only a few remarks will be made, concerning the stability of polymer films and its connection with the stability of emulsions and foams.

The stabilization of polymer films is less understood, than that of soap films. All films are inherently unstable, because they possess a higher free energy level than the bulk liquid. Therefore the stability problem really centers around the question, which factors determine the activation energy for rupture. Upon thinning some films became metastable whereas others drained till collapse (often called transient films). Metastability is reached, when the attractive and repulsive forces over the film equilibrate.

The stability of the PVA films was generally good. Equilibrium films were stable for several days. There was no difference between the two KURARAY samples. At high hydrostatic pressure the stability was impaired, but in that case the stability can be improved by using a porous plug in the opening of the needle (see fig. 3–3), used for injection (SONNTAG, 1976). It indicates that it is not a property of the polymer, but that it is connected with the inner radius of the needle (0.25 mm). In the case of PVA R-2 only small films at low hydrostatic pressure were stable.

With PMA-pe films the stability depends on α. At $\alpha = 1.0$ the films were re-

latively unstable. We succeeded only a few times to obtain a stable equilibrium film at low hydrostatic pressure ($< -15\ Nm^{-2}$). However, at low α the films were very stable. At that α, films could be made, that were stable for more than two weeks (including a draining time of around $1\frac{1}{2}$ week).

The fact that in all cases investigated films could be prepared, which drained to an equilibrium thickness, indicates that in principle PVA and PMA-pe films are metastable. The found equilibrium thicknesses were of the order of a few tens of nm or more. DE VRIES (1958) showed already that rupturing of a film through the formation of a hole, if the film is thicker than a few nm, required such a high activation energy that such a process is highly improbable. SHELUDKO (1962) pointed out that at and below a certain critical thickness h_{cr}, films become unstable with respect to small surface corrugations. This is caused by the fact that then upon further thinning (growing of the deformation) the gain in VAN DER WAALS energy exceeds the increase in surface energy, due to the enlargement of the surface area. It would occur for films with a thickness of around 30 nm depending on γ and A (HAMAKER constant). The theory was further developed by VRIJ (1966). He showed that a surface ripple will grow, if its wavelength is larger than λ_{cr} where:

$$\lambda_{cr} = \left(\frac{-2\pi^2 \gamma^f}{d^2 V_T / dh^2} \right)^{1/2} \tag{5.21.}$$

Here, V_T is the free energy of interaction per unit area and γ^f the surface tension of the film. The equation can only be solved for $d^2 V_T/dh^2 < 0$. Through $d^2 V_T/dh^2$ λ_{cr} is related to h. The wavelength λ_{cr} must be smaller than the diameter of the film. For that reason, there can be a difference in λ_{cr} (and hence in h_{cr}) between large and small liquid films or, for that matter, between microscopic films and the thin lamella remaining between two oil drops in a creamed oil in water emulsion (VRIJ and OVERBEEK, 1968). VRIJ et al. (1970) calculated, that the growth of corrugations is independent of the surface dilatational modulus ε if $\varepsilon \geqslant 10^{-4}\ mNm^{-1}$. In the case of transient films, the deformation grows until the film breaks, whereas with metastable films a black film is formed. However, in the measured polymer films $d^2 V_T/dh^2$ is already positive at large thicknesses which results in a counteracting of the growth of surface ripples.

It has often been suggested, that the rheological properties of the adsorbed layer of macromolecules correlate with the stability of liquid films (for instance KITCHENER and MUSSELWHITE, 1968). GRAHAM and PHILIPS (1976b) stated that the strength of the gel-like adsorbed protein layer is crucial in determining the stability of foams. MACRITCHIE (1976) suggested that the energy of activation for the coalescence of foam bubbles and emulsion droplets corresponds with the energy, necessary for the compression of the adsorbed monolayers, in order to clean a small part of the interfaces at the contact place. With the investigated PMA-pe films it was found, that they were more stable at low pH, which correlates with a higher dilatational modulus and more rigid films. However, the PVA films were also very stable, although the films were mobile. This

indicates that in addition to the observed correlation certainly more factors are involved. Other exceptions to the rule that the stability of liquid films correlates directly with the rheological properties, have been mentioned by NIELSEN et al. (1958) and KANNER and GLASS (1969).

In addition to the discussion above, it may be noted that the stability against rupture of the polymer films correlates also with the shelf stability of paraffin in water emulsions, stabilized by the used polymers. However, it should be pointed out, that in this respect only a few exploratory experiments have been done. Therefore, no definite conclusion can be drawn. In the case of PMA-pe emulsions the stability against centrifugation of the emulsions did not correlate with the mentioned phenomena.

5.6. SUMMARY

In this chapter the stabilization of thin free liquid films by polymer was described, with special emphasis on the steric interaction forces between the adsorbed polymer layers in such a film. Measurements on films stabilized by PVA and PMA-pe, were reported. For the measured PVA films the free energy of steric interaction between the two adsorbed polymer layers was compared with theoretical predictions.

In section 5.2. the interaction forces in polymer stabilized thin free liquid films (polymer films) were discussed. For uncharged polymers VAN DER WAALS attraction, hydrostatic pressure and steric interaction had to be taken into account. Possible theoretical density distribution functions of the segments of the adsorbed polymer molecules were described in section 5.2.3.1. Knowledge of these distribution functions is a prerequisite for the calculation of steric interaction. The steric interaction can be divided into two main mechanisms: the volume restriction effect and the osmotic pressure, or mixing term.

Measurements on PVA films were reported in section 5.3. The drainage behaviour and equilibrium film thicknesses were discussed. The latter quantity was determined, at varying hydrostatic pressures. The VAN DER WAALS attraction over the films can be calculated. Then the steric repulsion force F_S between the two adsorbed PVA layers was found by equalizing $-F_S$ with the VAN DER WAALS attraction and the hydrostatic pressure. In that way the steric repulsion force could be calculated for different equilibrium thicknesses. Next the free energy of steric repulsion was obtained by graphical integration of the force-distance curve. Information on the density distribution function of the segments of the adsorbed polymer molecules was obtained by comparing the extrapolated film thichness at $F_S \rightarrow 0$, with the ellipsometric thickness. Indications were found that tails play a much more important role than is usually assumed. In section 5.3.5. a semiquantitative model for the density distribution of the segments of adsorbed PVA molecules was developed, valid for the outer part of the adsorbed layer. It is based on the consideration, that the molecular weight distribution of the used PVA's is wide and the assumption that a large fraction

of the segments is adsorbed as tails. It results in the fact that the properties of the outer part of the adsorbed layers are determined by a few tails only, which can be dealt with as if they were essentially isolated tails. The steric repulsion, calculated between the two adsorbed PVA layers by making use of this model, agrees well with the experimentally found ones for reasonable lengths of the tails.

In section 5.4. the drainage behaviour and the equilibrium thicknesses of PMA-pe stabilized films were discussed. Films were made at different values of the degree of neutralization α. The measured equilibrium thicknesses correlate well with ellipsometric measurements on an adsorbed layer. The drainage pattern changes if α is varied. At high α the films are mobile, whereas at low α they are rigid. Also the dilatational modulus increases from $\alpha = 1.0$ to $\alpha = 0.1$. Perhaps the same interaction forces between the polyelectrolyte segments are responsible for the phenomena mentioned as those which stabilize the a-conformation in the molecule, or which are responsible for the substantial changes in rheological properties of emulsions, stabilized by PMA-pe if α is reduced.

A few remarks concerning the stability of polymer films and its connection with the stability of emulsions and foams conclude this chapter.

6. RHEOLOGICAL BEHAVIOUR OF EMULSIONS STABILIZED BY PMA-PE

6.1. INTRODUCTION

As already mentioned in section 4.4., the interaction between polyelectrolyte-covered paraffin droplets is reflected in the rheological properties of emulsions. If among the forces, acting between the droplets, the repulsive ones dominate, a fluid system is obtained, provided the volume fraction of paraffin is not too high. In the case where the net force is attractive, a three dimensional network structure can be built up (VAN DEN TEMPEL, 1958; PAPENHUIZEN, 1972). Rheological measurements on emulsions and other dispersions can broadly be classified into two different types.

1. Measurements during which the network structure is not disturbed. Both static measurements (e.g. creep measurements) and dynamic ones are usable.

The behaviour of emulsions at very small deformations was investigated by e.g. VAN DEN TEMPEL (1961) and STRENGE and SONNTAG (1974; 1975) in creep measurements. DAVIS (1971) and ECCLESTON et al. (1973) studied oil in water emulsions both by creep and by dynamic measurements. The agreement between the results of both types of measurements was generally good.

2. Measurements during which the network structure is broken down. The rheological properties at very large deformations can be studied by steady state shear (VAN DEN TEMPEL, 1963; FRIEND and HUNTER, 1971; NEVILLE and HUNTER, 1974). VAN DEN TEMPEL explained the results by assuming that the network structure was destroyed to such an extent, that only non-interacting aggregates of particles remained. This assumption seems a little conflicting, but is justified owing to the difference in mean distance between the aggregates and that between the droplets in it. The only effect on η of the aggregates is immobilization of a part of the continuous phase. The size of the aggregates depends on the value of the net interaction forces. HUNTER et al. measured the shear stress of latices as a function of the shear rate D till such high rates that the suspension behaved newtonian. For rapidly coagulating colloidal suspensions energy in excess of the normal viscous energy is required to sustain flow. This excess energy is correlated with the interaction energy between the particles. It can be calculated from the yield value which is found by a rather long extrapolation of the linear part of the shear stress-shear rate curve to zero shear rate.

PAPENHUIZEN (1972) discussed the behaviour of dispersions, subjected to deformations between the extreme cases of very small and very large ones. In these cases, most deformations occur in restricted regions, rather than uniformly through the sample (VAN DEN TEMPEL, 1958).

In this chapter measurements will be reported, in which the network structure is not disturbed or only to a very small extent. In general the interpretation of rheological measurements on viscoelastic systems is described in section 6.2.

There are two different methods of analyzing the obtained data.

a. Phenomenological representation of the obtained data by mechanical analogues (e.g. SHERMAN, 1968; BARRY, 1975).
b. Interpretation of the rheological properties of the emulsions in terms of particle interactions (e.g. VAN DEN TEMPEL, 1961; STRENGE and SONNTAG, 1974; 1975).

Because at the moment in contrast to the second method the phenomenological approach does not result in a deeper understanding of the physical background of the structure of the emulsions, we will follow the second way. Especially the role of adsorbed polyelectrolytes at the emulsion droplets surfaces will be investigated. In order to be able to relate the rheological properties of emulsions with the interactions between the droplets, a model of the emulsion structure has to be accepted. In section 6.3. the interaction forces between the emulsion droplets and possible models of network structures will be discussed. An attempt to interpret the rheological properties of emulsions in terms of particle interactions will be made in the sections 6.5. and 6.6.

6.2. INTERPRETATION OF RHEOLOGICAL MEASUREMENTS ON VISCOELASTIC SYSTEMS

A system is viscoelastic when its reaction on a stress or strain consists partly of a viscous contribution and partly of an elastic one. It reacts both elastic and viscous. In a more negative way it can be stated that a system is viscoelastic when it cannot be described with NEWTON's law or HOOKE's law alone. The rheological properties of the system partly resemble those of a liquid and partly those of a solid. A system is mentioned linear viscoelastic, when the elastic effects obey HOOKE's law and the viscous deformations are NEWTONIAN. The stress to strain ratio depends on the time only and not on the magnitude of the strain. Therefore for the rheological characterization of a viscoelastic system it is necessary and sufficient to measure the strain or stress as a function of time, after applying a stress or strain respectively. Methods of measurements of viscoelastic bodies are:

I Static measurements:

A. Stress relaxation. A constant strain γ is applied to the sample and the stress σ is measured as a function of time.

$$\sigma(t) = G(t)\gamma \tag{6.1.}$$

where $G(t)$ is the relaxation modulus (Nm^{-2}).

B. Creep measurements. The strain $\gamma(t)$ is measured as a function of time, after applying a constant stress σ.

$$\gamma(t) = J(t)\sigma \tag{6.2.}$$

where $J(t)$ is the creep compliance ($N^{-1}m^2$).

An idealized creep curve for a viscoelastic body is shown in fig. 6–1. It can be subdivided into three characteristic regions.

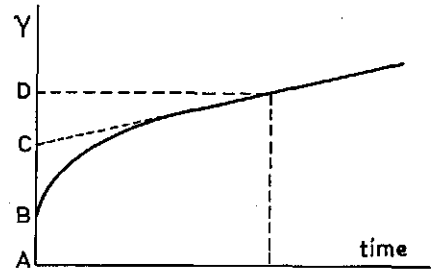

FIG. 6-1. A creep curve for a viscoelastic material. Explanation in text.

a. A region of instantaneous elastic deformation (A-B) resulting in an instantaneous elastic compliance J_0 or an instantaneous shear modulus $G_0 = \sigma/\gamma_0 = 1/J_0$.
b. A 'mixed elastic-viscous' deformation region (B-C). In this region bonds are broken and reformed. Because all bonds do not break and reform at the same rate, a spectrum of i retarded elastic compliances are obtained.
c. A region of viscous deformation. Individual droplets or aggregates of droplets flow past each other, when the time required to restore broken bonds is longer than the test period.

Creep measurements on emulsions stabilized by Na-PMA-pe will be reported in section 6.6. Then the theoretical interpretation of such measurements will also be discussed further.

II Dynamic measurements:

In this case an oscillating deformation (or stress) with an angular frequency ω (rad s^{-1}) is applied to the system. It is convenient to vary the strain sinusoidally. For a linear viscoelastic sample, the stress amplitude is proportional to the strain amplitude and oscillates at the same frequency, but out of phase with the strain (see fig. 6–2). The strain and stress can be described by complex variables. The complex shear strain γ^* is defined as:

$$\gamma^* = \gamma_0 \exp(i\omega t) \qquad (6.3.)$$

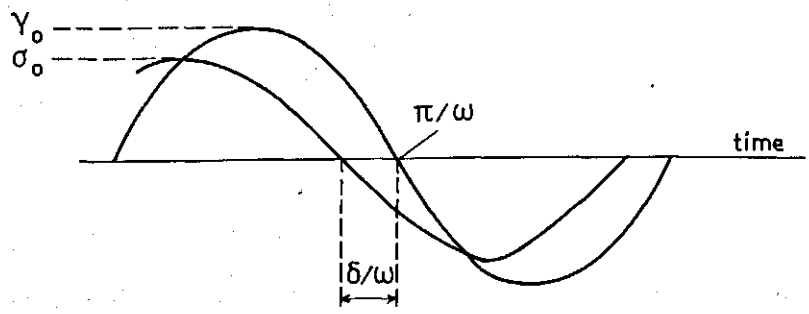

FIG. 6-2. Sinusoidal variation of strain and stress in a dynamic rheological study of a viscoelastic material. Explanation of symbols in text.

in which γ_0 is the maximum shear strain and i is $\sqrt{-1}$. Then the complex stress σ^* varies also sinusoidally, but with a phase angle δ before the strain.

$$\sigma^* = \sigma_0 \exp \{i(\omega t + \delta)\} \tag{6.4.}$$

where σ_0 is the maximum shear stress. The complex shear modulus G^* is defined as:

$$G^* \equiv \sigma^*/\gamma^* \tag{6.5.}$$

Combination of equations (6.3.), (6.4.) and (6.5.) gives:

$$G^* = \sigma_0/\gamma_0 \exp (i\delta) = \sigma_0/\gamma_0 (\cos \delta + i \sin \delta) \tag{6.6.}$$

The first or real part of the right hand side of equation (6.6.) is the part of the stress in phase with the strain. It is called the storage shear modulus G'. The out of phase (imaginary) component is mentioned the loss shear modulus G''. G' is associated with the storage and release of energy, during the periodic application of strain and G'' is associated with the dissipation of energy into heat. In formulae,

$$G' = (\sigma_0/\gamma_0) \cos \delta \tag{6.7.}$$

$$G'' = (\sigma_0/\gamma_0) \sin \delta \tag{6.8.}$$

$$\text{Then } G^* = G' + iG'' \tag{6.9.}$$

The ratio of the maximum shear stress to the maximum shear strain is the absolute shear modulus $|G^*|$

$$|G^*| = (G'^2 + G''^2)^{1/2} = \sigma_0/\gamma_0 \tag{6.10.}$$

Furthermore

$$\text{tg}\delta = G''/G' \tag{6.11.}$$

In order to obtain the time dependencies $G'(\omega)$ and $G''(\omega)$ dynamic measurements at various frequencies ω are required. The courses of the storage shear modulus and the loss shear modulus (further abbreviated as storage modulus and loss modulus respectively) as a function of ω for viscoelastic polymers and gels are discussed by e.g. FERRY (1970). In the next sections we hope to show, that it is possible to describe the viscoelastic properties of polymer stabilized emulsions largely in the same way as those of gels.

The dynamic and the static moduli can be transformed into each other to a certain extent (FERRY, 1970).

6.3. INTERPRETATION IN TERMS OF A NETWORK STRUCTURE

In many emulsions the net interparticle force is attractive over at least part of the interparticle distance. These forces cause the particles to aggregate into a three dimensional network structure. In the next sections first the interaction

forces between emulsion droplets will be discussed shortly, after which models of the network structure will be given.

6.3.1. *Interaction forces between emulsion droplets*

a. Interaction between polyelectrolyte molecules adsorbed on different emulsion droplets.

In the case of PMA-pe stabilized emulsions, the interaction between the adsorbed polyelectrolyte molecules largely determines the rheological properties of the emulsions (BÖHM and LYKLEMA, 1976). The nature of these interaction forces between the polyelectrolyte segments is treated in section 4.2. and 4.5. At a low degree of neutralization ($\alpha \leqslant 0.15$) the attractive forces (propably to a large extent hydrophobic bonding) dominate, whereas at $\alpha \geqslant 0.3$ electrostatic forces induce a net repulsion between the segments. Of course, steric interaction forces of entropic origin (see section 5.2.) also play a role.

b. VAN DER WAALS attraction between the emulsion droplets.

HAMAKER (1937) calculated the LONDON-VAN DER WAALS attraction energy between two spherical particles embedded in medium 2

$$V_{A112} = -\frac{A_{112}}{6}\left[\frac{2}{s^2-4} + \frac{2}{s^2} + \ln\left(\frac{s^2-4}{s}\right)\right] \qquad (6.12.)$$

where $s = 2 + 2H_0/d$, in which H_0 is the shortest distance between the two spherical surfaces and d the diameter of the spheres. In the case of $H_0 \ll d$, V_A can be approximated by:

$$V_{A112} = -\frac{A_{112}\, d}{24\, H_0} \qquad (6.13.)$$

For the interaction between two bodies of material 1 embedded in a medium 2 the HAMAKER constant reads to a good approximation in the microscopic theory (HAMAKER, 1937):

$$A_{112} = A_{11} + A_{22} - 2A_{12} \approx (\sqrt{A_{11}} - \sqrt{A_{22}})^2 \qquad (6.14.)$$

where A_{11}, HAMAKER constant of the disperse phase

A_{22}, HAMAKER constant of the dispersion medium

A_{12}, mixed HAMAKER constant, approximately equal to $\sqrt{A_{11}.A_{22}}$.

For large distances of H_0 one has to account for retardation. Because of the large radii of the emulsion droplets one can use in this case to a good approximation the same correction factors as for flat plates. The correction factor has been given in section 5.2.1., fig. 5–1.

The attractive force between the droplets can be obtained by differentiating equation 6.12. For $H_0 \ll d$:

$$F_{A112} = -\frac{A_{112}\, d}{24\, H_0^2} \qquad (6.15.)$$

The HAMAKER constant of the adsorbed polyelectrolyte layer has been assumed to be equal to that of water (see section 5.2.1.).

We will return to the importance of the mentioned interaction forces in the next sections by giving a more quantitative description of their influence on the rheological properties.

6.3.2. *Network models*

Various models can be used to represent the three dimensional structure, which can be built up as a result of the attractive forces between emulsion droplets. We will consider only the most simple models, taking all the particles having the same size. The diameter d assigned to the particles in the model is determined by the condition, where the volume fraction ϕ and the number of dispersed particles N in the model should be the same as in the real system. The following models can be considered:

a. All droplets are arranged in a statistical network of chains (ideal network model) (fig. 6–3a). They all contribute to the same extent to the rigidity of this network.

b. The droplets are aggregated in clusters or agglomerates (fig. 6–3b), which are connected by chains of particles. The mechanical strength of the network is mainly determined by the relatively few particles, which link the agglomerates together. It is possible to consider an agglomerate of droplets as a rheological unit. These units are arranged statistically.

The degree of cluster forming depends on ϕ and on the particle size. The particle concentration appears to be an important parameter (VAN DEN TEMPEL, 1976). It is rather difficult to discriminate between the two models by means of rheological measurements. The best way of discrimination is to test the ϕ and d dependency.

Still a third model can be considered, only valid for concentrated emulsions. In this picture, the assumption is made that the droplets are surrounded by a thick rigid layer in such a way, that a dense packing of these 'effective' particles

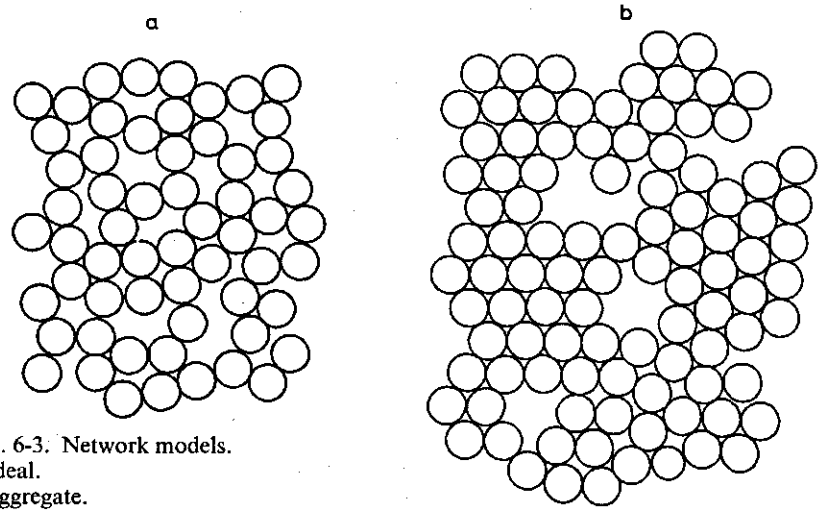

FIG. 6-3. Network models.
a ideal.
b aggregate.

fills the complete volume. The volume fraction of dispersed phase was 0.5 in the experiments reported in this chapter. Taking a reasonable value of d (5×10^3 nm), one would require a layer of 700 nm around the droplets. That is much more than can be expected for such a layer, so this model is not further considered.

With the definition of the diameter given above, it is possible to derive an expression for the number of chains carrying a potential tensile stress across one m² for the two models. In the aggregate model (VAN DEN TEMPEL, 1976) we assume that N droplets form N_A aggregates, each containing $n = N/N_A$ particles. Then the volume of an aggregate (which contains also continuous phase) is $nf\pi d^3/6$, where $f = 1.6$. The effective diameter d_A of an aggregate is $d(fn)^{1/3}$. The two network structure models can then be compared (see table 6–1). We shall use these results later in making the decision which model is the most appropriate for PMA-pe stabilized emulsions (at $\alpha = 0.1$; $\phi = 0.5$) (section 6.5.).

6.4. EMULSIONS AS A GEL

When attractive forces between emulsions droplets dominate, at least over a range of values for the interparticle distance, a three dimensional network structure will be built up. As mentioned in section 6.3.1., these forces can stem from attraction between the adsorbed polyelectrolyte sheets and VAN DER WAALS attraction between the emulsion droplets. For the latter case a few authors (VAN DEN TEMPEL, 1961; NEDERVEEN, 1963; STRENGE and SONNTAG, 1974) derived a relation between the shear modulus G of a dispersion and the VAN DER WAALS attraction between the particles. Likewise it is possible to derive a relation between the shear modulus G of a dispersed system and the modulus G_g of a micro-gel formed by two interacting polymer sheets, adsorbed onto different particles (VAN DEN TEMPEL, 1974). In the next sections we shall first discuss the possibility of the formation of a gel by the adsorbed PMA-pe between two emulsion droplets. After that the relation between the moduli of the emulsions and the interaction forces between the dispersed droplets will be discussed for the two network models.

TABLE 6-1. Comparison of the ideal network model and the aggregate model.

	ideal network model	aggregate model
Number of rheological units, m^{-3}	N	N_A
Effective volume fraction dispersed	$\phi = N\pi d^3/6$	$\phi_A = N_A nf\pi d^3/6 = f\phi$
Total length of stresscarrying chains, m^{-2}	Nd	$N_A d_A$
Number of chains carrying a tensile stress across one m^2	$\frac{1}{3} Nd = 2\phi/\pi d^2$	$\frac{m}{3} N_A d_A = 2mf^{1/3}\phi/\pi d^2 n^{2/3}$*

* m is the number of chains connecting two aggregates.

6.4.1. *Gelation of PMA-pe in bulk and at an interface*

The gelation of aqueous solutions of polymethacrylic acid (PMA) has been studied by a number of authors (e.g. KATCHALSKY, 1951; LIPATOV et al., 1959; ELIASSAF and SILBERBERG, 1962; SILBERBERG and MIJNLIEFF, 1970). The gel formation is reversible. No permanent crosslinks (i.e. bonds of infinite lifetime) are formed. The concentration of PMA-pe at which gelation starts, depends on the degree of neutralization and the temperature. PMA-pe solutions which are sufficiently concentrated form thermoreversible gels on heating.

In this paper only some exploratory experiments on bulk gelation will be reported. Next the possibility of forming a gel between two adjacent emulsion droplets by the interacting adsorbed PMA-pe sheets will be discussed.

Gels were prepared by evaporation of the solvent at 30 °C, starting from a 2% solution of PMA-pe with a degree of neutralization of 0.1. The electrolyte concentration was 0.136 M NaCl, resulting from the way of preparing the polyelectrolyte solution (section 2.4.1.). The concentrations of PMA-pe in the gels were determined by weighing.

6.4.1.1. Results and discussion

It was very difficult to establish exactly, at which concentration a gel was formed. Gelation started at a concentration between 7–8%, whereas at 9–10% rigid gels were formed. The storage modulus of a solution with a PMA-pe concentration of 8–8.5% (NaCl concentration ca. 0.55 M) varied between 100–500 Nm^{-2} ($\omega = 5.28$ rad s^{-1}) and for a 10% solution (NaCl concentration 0.68 M) amounted to ca. $5 - 10 \times 10^3$ Nm^{-2}. SILBERBERG and MIJNLIEFF (1970) chose a value of G of 50 Nm^{-2}, as division between a sol and a gel. As a criterion this value is rather arbitrary. However, the actual choice of G has only a minor influence on the resulting gel point concentration. Accepting this criterion and neglecting the difference between G and G', we find as gel point concentration for PMA-pe with $\alpha = 0.1$ in a salt solution; ca. 8%. The gel point concentrations found by SILBERBERG and MIJNLIEFF are tabulated in table 6–2. The conclusion is, that the agreement with our measurements is reasonable. The somewhat lower value found by us for PMA-pe at the same equivalent degree of neutralization may be attributed to the presence of salt. The sodium ions screen the negative charges of the carboxyl groups.

Next we turn to the problem of gel formation by PMA-pe, adsorbed at an

TABLE 6-2. Gel point concentrations (g.p.c.) for PMA ($M = 3.35 \times 10^3$) at 25 °C. Data of SILBERBERG and MIJNLIEFF (1970). α^* is the equivalent degree of neutralization for PMA-pe resulting in the same percentage of dissociated carboxyl groups based on the total number of segments as for PMA.

α	α^*	g.p.c. (g cm^{-3})
0	0	0.082
0.04	0.06	0.10
0.08	0.12	0.12

interface. The amount of PMA-pe ($\alpha = 0.1$, electrolyte concentration 0.05 M NaCl) adsorbed at the emulsion droplets surfaces is 2.2 mg m^{-2}, of which ca. 0.5 mg m^{-2} is adsorbed as trains (BÖHM, 1974). Then the amount adsorbed in loops and tails is ca. 1.7 mg m^{-2}. The thickness of a PMA-pe stabilized thin liquid film (consisting of two adsorbed layers) is ca. 45 nm (section 5.4.2.). From creep measurements (section 6.6.2.) we found for the distance between the paraffin-aqueous solution interfaces of two emulsion droplets ca. 30 nm. The ellipsometric thickness of an adsorbed layer is 12 nm (section 5.4.3.). Accepting 35 nm as a reasonable but arbitrary value for the thickness of the liquid film between two emulsion droplets, the mean concentration of PMA-pe in the film can be calculated. The result is ca. 0.1 g cm^{-3}, which exceeds the gel point concentration. Considering the fact that the occurrence of micro gelation is more likely than that of macro gelation, it seems not unrealistic to conclude that a kind of gel can be built up between two emulsion droplets. A definite conclusion cannot be drawn, because it must be taken into account that the segment concentration is probably lower in the overlap region than near the interface. Therefore theoretically the possibility exists that indeed a gel is formed near the interface but not in the overlap region. Anticipating the discussion in section 6.5.1., it is perhaps even allowed to involve the results of the measurements presented in figs. 6–7, 6–8, 6–10 and 6–11, as an indication that a kind of gel is formed.

The connection of the formation of a gel between two emulsion droplets with the rheological properties of the emulsion is discussed in the next section.

6.4.2. *Interpretation of the shear modulus in terms of interaction forces between emulsion droplets*

In this section the relation between the shear modulus and the interaction forces between the dispersed emulsion droplets is discussed. Firstly the VAN DER WAALS attraction between the droplets is regarded and secondly the interaction between the adsorbed polyelectrolyte sheets. The last term includes all sorts of interaction forces between the polyelectrolyte molecules (see section 4.2. and 5.2.). Only the net results of these forces is taken into account as far as these interactions are reflected in a certain distance between the emulsion droplets and lead to a number of interaction points (cross-links) between the adsorbed polyelectrolyte sheets. The assumption is made, that in the case of strong viscoelastic emulsions a gel is formed between the emulsion droplets.

When a shear stress is applied to an emulsion, the deformation of it is determined by the elongation of the chains of particles. It is assumed that this elongation may be interpreted in terms of an extension of the interparticle distances (fig. 6–4). By deformation, the initial length L of a chain of particles is extended to $L + \Delta L$,

where $L = x\,(d + H_0)$

$L + \Delta L = x\,(d + H_0 + \Delta H)$

x = number of droplets in the chain

ΔH = extention of the distance between two droplets.

Then the relative extension $\varepsilon = x\Delta H/x(d + H_0) \approx \Delta H/d$ for $H_0 \ll d$. When we

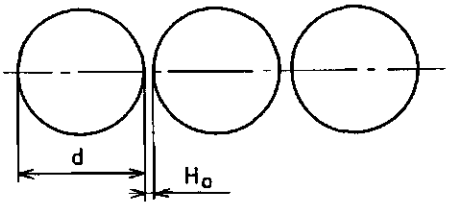

FIG. 6-4. Elongation of a chain of emulsion droplets.
d = droplet diameter.
H_0 = shortest distance between two droplets.

regard the elongation along one of the principal axis (fig. 6–5). (For a definition of the principal axis is referred to LODGE, 1964, p. 32.) The elongation ratio along the principal axis λ' is:

$$\lambda' = \frac{L + \Delta L}{L} = 1 + \frac{\Delta L}{L} = 1 + \varepsilon$$

It can be proved (LODGE, 1964; VAN DEN TEMPEL, 1976) that:

$$\gamma = \lambda' - 1/\lambda'$$

Then for small shear strain holds:

$$\gamma \backsimeq 2\varepsilon = 2\Delta H/d \qquad (6.16.)$$

It can be shown geometrically for the diagonal AC'. In a square:

$$AC = AB\sqrt{2} \qquad AC' \backsimeq AB\sqrt{2}\,(1 + \tfrac{1}{2}\gamma)$$

$$\varepsilon = \frac{AC' - AC}{AC} = \tfrac{1}{2}\gamma$$

The tensile stress along the principal axis is the same as the shear stress σ. So we obtain the expression:

$$G = \frac{\sigma}{\gamma} = \frac{\sigma}{2\varepsilon} = \tfrac{1}{2}E \qquad (6.17.)$$

where E is the YOUNG modulus of the considered chain of particles.

In order to derive a relation between the shear modulus G of an emulsion and the VAN DER WAALS attraction between the droplets, it is assumed that either the ideal network model or the aggregate model holds. Firstly we give the derivation for the ideal network structure and after that we will correct the results according to the aggregate model. The derivation is founded and to a certain extent similar to the one that has been given by VAN DEN TEMPEL (1961) and NEDERVEEN (1963). An essentially similar derivation has been given by STRENGE and SONNTAG (1974). They use a somewhat different model for calculating the number of stress carrying points. The assumption is made that all the bonds between emulsion droplets in a stress carrying chain contribute to the response of the chain to it. This can be the case if all the droplets are crosslinked with the

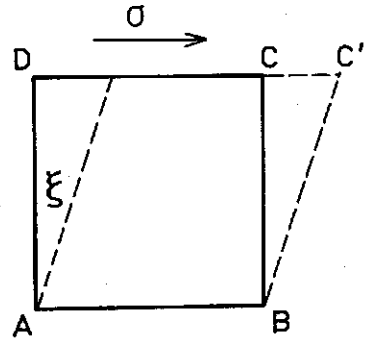

FIG. 6-5. Relation between shear and extension in a chain of particles.
ζ angle of deformation.
Shear strain $\gamma = \text{tg}\,\zeta$.

droplets of the neighbouring chains. This model is appropriate only at a very dense packing of the particles. VAN DEN TEMPEL and NEDERVEEN neglected crosslinking between adjacent chains. At high ϕ this leads to underestimation of the stress carrying points. However, this is compensated for to a certain ex-extent by loose ends of chains of particles. In addition to this objection we believe that STRENGE and SONNTAG introduced the energy per bond between two emulsion droplets in a not completely correct way.

In the derivation of a relation it must be realized, that repulsive forces are also operative. The assumption is made, that in the considered case of PMA-pe (with $\alpha = 0.1$) stabilized emulsions, repulsion other than that of steric origin can be neglected. Unfortunately, we were not able to measure the steric repulsion between two PMA-pe layers as a function of the distance. For a PVA stabilized thin liquid film the repulsion is as a first approximation proportional to $1/d^2$ or $1/d^3$. In the case of PMA-pe ($\alpha = 0.1$) stabilized films the distribution of segments normal to the interface is more like a step function (section 5.4.). Therefore we assumed, that the steric repulsion will show a larger dependence on the distance than in the case of PVA stabilized films. We chose the to a large amount arbitrary dependence on $1/d^3$.

If for this moment retardation is neglected, one can write for the total force between two droplets:

$$F = -\frac{Ad}{24\,H^2}\left\{1 - a'\left(\frac{H_0}{H}\right)^3\right\} \qquad (6.18.)$$

where H_0 is the shortest distance between the droplets in equilibrium and a' is a constant. Following HESSELINK et al. (1971b) and EVANS et al. (1973b) it is assumed that the DERYAGIN approximation (DERYAGIN, 1934) can be used to calculate the steric repulsion for spheres from the results for plates. It results in that the steric repulsion force F_S is proportional to d, so that the total interaction force $F = F_{A121} + F_S$ is proportional to d. In equilibrium $F = 0$ and $H = H_0$, from which it follows that $a' = 1$. Upon elongation of a chain of particles from

H_0 to $H = H_0 + \Delta H$, equation (6.18.) changes into:

$$F = -\frac{Ad}{24\,H_0^2\left(1+\frac{\Delta H}{H_0}\right)^2}\left[1-\frac{1}{\left(1+\frac{\Delta H}{H_0}\right)^3}\right]$$

After series expansion and neglecting terms higher than $(\Delta H/H_0)^2$ is found:

$$F = -\frac{Ad\,\Delta H}{8\,H_0^3}\left[1-4\frac{\Delta H}{H_0}\right] \tag{6.19.}$$

The numerical factor 8 depends somewhat on the exponent, used in the repulsive term. From (6.19.) the stress σ per m^2 is obtained by multiplying the force F in each chain by the number of chains per m^2.

$$\sigma = F \times \frac{2\phi}{\pi d^2} = -\frac{A\,\phi\,\Delta H}{4\pi\,d\,H_0^3}\left[1-4\frac{\Delta H}{H_0}\right] \tag{6.20.}$$

The shear modulus of the emulsion then is:

$$G_{v.d.W.} = \frac{\sigma}{\gamma} = \frac{A\,\phi}{8\pi\,H_0^3}\left[1-4\frac{\Delta H}{H_0}\right] \tag{6.21.}$$

The subscript *v.d.W.* means that G is determined by VAN DER WAALS attraction and steric repulsion between the emulsion droplets.

In the case of retardation ($H_0 > 10$ nm) F must be corrected by a factor f'' and so must G. The correction factor has been given in section 5.2.1., fig. 5–1. Equation (6.21.) then becomes:

$$G_{v.d.W.} = f''\frac{A\,\phi}{8\pi\,H_0^3}\left[1-4\frac{\Delta H}{H_0}\right] \tag{6.22.}$$

It can easily be seen that there is a limit of linearity if a chain of particles attracting each other by VAN DER WAALS forces and repelling each other sterically, is extended. In practice, if for instance the inaccuracy in the $G_{v.d.W.}$ measurement is 30%, a drop in $G_{v.d.W.}$ would be measured if $\sim 4\,\Delta H/H_0 > 0.3$. With equation (6.16.) this would result in an upper limit of γ of $0.15\,H_0/d$. Because H_0/d is of the order of 0.01, γ must be smaller than 0.0015 in order to stay within the limits of linear behaviour.

In the aggregate model the number of chains carrying a tensile stress across one m^2 is different from that for the ideal network model (tabel 6–1). Then equation (6.20.) must be modified to read:

$$\sigma = f''\frac{A\,\phi\,\Delta H}{4\pi\,d\,H_0^3}\left(\frac{m^3 f}{n^2}\right)^{1/3}\left[1-4\frac{\Delta H}{H_0}\right] \tag{6.23.}$$

which results in:

$$G_{v.d.W.} = f'' \frac{A\,\phi}{8\pi\,H_0^3} \left(\frac{m^3 f}{n^2}\right)^{1/3} \left[1 - 4\frac{\Delta H}{H_0}\right] \qquad (6.24.)$$

VAN DEN TEMPEL (1974)[4] derived a relation between the storage modulus G' of a dispersed system and the number of polymer bonds between two dispersed particles. We shall follow a similar way of reasoning.

It is assumed, that the gel which is formed between two emulsion droplets can be described as a purely elastic rubber-like gel (FLORY, 1953). In fact this is a very crude approximation. We will return to it in the discussion of section 6.5.1.2. We need this approximation in order to be able to calculate the number of polymer bonds between two emulsion droplets. It is not necessary to make this assumption for the derivation of the relation between G' of the emulsion and the storage modulus G'_g of the micro-gel between two droplets. A second assumption is, that no desorption of trains occur during the measurements. In view of the irreversible character of polymer adsorption, this assumption is justified, normally.

The concentration of elastically effective chains ν between two adjacent emulsion droplets is (fig. 6–6):

$$\nu = \frac{c'\,b}{A_{eff}\,H_0} \qquad (6.25.)$$

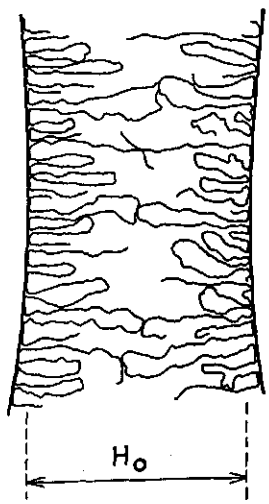

FIG. 6-6. Interactions between polyelectrolyte molecules adsorbed on different emulsion droplets.

[4] We are much indebted to Dr. M. VAN DEN TEMPEL of Unilever Research Laboratory, Vlaardingen, for allowing us to use his unpublished derivation.

where A_{eff} is the effective contact region between two emulsion droplets, b the number of bonds between the droplets and c' the number of elastically effective chains per bond (crosslink). This factor is 2, when two loops are cross-linked, but it is 1 if two tails are cross-linked. Using the assumption that a purely elastic rubber-like gel is formed, the storage modulus G'_g of it can be written as:

$$G'_g = \nu\, k\, T \tag{6.26.}$$

Elongation of the polymer bridges between the droplets from H_0 to $(H_0 + \Delta H)$ gives a force F in the polymer chains. If the difference between G and G' is neglected:

$$F = 3G'_g \frac{\Delta H}{H_0} A_{eff} = 3c'\, b\, k\, T \frac{\Delta H}{H_0^2} \tag{6.27.}$$

The stress σ per m^2 is obtained, by multiplying the force F between two droplets by the number of chains carrying a tensile stress per m^2.

$$\sigma = F \times \frac{2\phi}{\pi\, d^2} = 6\, c'\, b\, k\, T \frac{\Delta H}{H_0^2} \frac{\phi}{\pi\, d^2} \tag{6.28.}$$

The modulus G of the emulsion then is:

$$G_{pol} = \frac{\sigma}{\gamma} = \frac{\sigma}{\Delta H} \frac{\Delta H}{\gamma} = \frac{3\, c'\, b\, k\, T\, \phi}{\pi\, d\, H_0^2} \tag{6.29.}$$

The subscript *pol* means that G is the result of interactions between polyelectrolyte molecules adsorbed on different emulsion droplets.

If the aggregate model holds equation (6.29.) must be modified in the same way as equation (6.22.) which results in:

$$G_{pol} = \frac{3\, c'\, b\, k\, T\, \phi}{\pi\, d\, H_0^2} \left(\frac{m^3 f}{n^2}\right)^{1/3} \tag{6.30.}$$

Now a set of equations are available describing the relationship between G of emulsions and the forces between the droplets for the ideal network model and the aggregate model. One of the most striking results is that in the case of the ideal network model G is proportional to the volume fraction of the disperse phase, whereas in the aggregate model it is normally more than proportional. If it is assumed that a variation of ϕ does not influence H_0 to a large extent, one can conclude that a more than linear dependence of G on ϕ points to the aggregate model. If VAN DER WAALS attraction between the emulsion droplets is the driving force for structure building, in the ideal network model G would be independent of d. In the literature often en ideal network model is used, although a large dependence of G or G' (ignoring the difference) on ϕ and/or d is found. For instance NEDERVEEN (1963) found an eighth power dependence of the YOUNG modulus on ϕ for glyceryl tristearate particles in oil in the concentration region of 20%–30% solid material. STRENGE and SONNTAG (1974; 1975) observed for Aerosil 200 in water dispersions that G was proportional to $1/d^3$ and showed a

TABLE 6-3. Dynamic and static moduli. A brief survey.

symbol	meaning	equation
G	shear modulus, σ/γ	
G_0	instantaneous shear modulus (creep measurements), σ/γ_0	
$G_{(t)}$	relaxation modulus $\sigma(t)/\gamma$ (γ constant)	(6.1.)
G'	storage shear modulus $\sigma_0 \cos \delta/\gamma_0$	(6.7.)
G''	loss shear modulus $\sigma_0 \sin \delta/\gamma_0$	(6.8.)
$\|G^*\|$	absolute shear modulus $\sigma_0/\gamma_0 = (G'^2 + G''^2)^{1/2}$	(6.10.)
G^*	complex shear modulus $\sigma^*/\gamma^* = \sigma_0 \exp(i\delta)/\gamma_0 = G' + iG''$	(6.5.) and (6.9.)
G'_g	storage shear modulus of the micro-gel formed between two emulsion droplets	(6.26.)
G_{vdW}	shear modulus of an emulsion due to VAN DER WAALS attraction and steric repulsion between the droplets	(6.22.)
G_{pol}	shear modulus of an emulsion as the result of the interaction between polyelectrolyte molecules adsorbed on different emulsion droplets	(6.29.)

strong dependence on ϕ (concentration 2–6%). If the reasonable assumption is made, that the degree of cluster forming depends on ϕ and d, these results are in favour of the aggregate model. In connection with this PAPENHUIZEN (1972) showed that the rheological behaviour of a 8% triglyceryl stearate dispersion in oil could be explained only by assuming a kind of aggregate model.

For easy reference the different moduli mentioned thus far in this chapter are listed in table 6–3.

6.5. DYNAMIC MEASUREMENTS

Dynamic moduli have been measured of emulsions stabilized by PMA-pe. The volume fraction of paraffin was 0.5. The frequency was varied between 2.7×10^{-2} and 10 rad. s^{-1}. At a higher frequency the results were not accurate enough. Measurements (creep measurements) at a lower frequency will be reported in section 6.6. The amplitudes used depend on the properties of the emulsions. For viscous emulsions ($G' \geqslant 1$ Nm^{-2}) the applied deformation γ was < 0.03. The meaning of this range of γ, in relation to the discussion after equation (6.22.), is treated in the next section. It was checked that they were low enough to ensure linear viscoelasticity.

The apparatus has been described in section 3.5.2. After bringing the viscoelastic emulsions into the rheometer, a waiting time of ca. 3 hours was observed before the measurements were started. The structure of the emulsions is largely destroyed by bringing them into the rheometer. It was verified that this breakdown of the emulsion structure is reversible (BÖHM, 1974). After 3 hours the measured moduli became independent of the waiting time. Too long waiting times were avoided, because after one night sometimes syneresis effects were visible. Reported data are the mean of at least two independent measurements.

The reproducibility can be as poor as 40–50%. Around half of it can be attributed to inaccuracy in the dynamic measurements. The other part follows from the irreproducibility in the emulsification process and the filling up of the rheometer. For example, small bubbles of air sometimes stay between the inner and outer cylinder. As this 40–50% uncertainty limit covers both instrumental and material irreproducibilities, it is a good measure of the overall absolute accuracy.

6.5.1. *Emulsions stabilized by Na-PMA-pe*

The first results of the dynamic measurements are represented in fig. 6–7. There is a drastic influence on the results of the degree of neutralization α. In addition to the discussion in section 4.4. about the relationship of the rheological properties of polyelectrolyte stabilized emulsions with the intra- and intermolecular interaction forces between the PMA-pe segments, the following remarks can be made:

At $\alpha > 0.2$ the loss modulus G'' exceeds the storage modulus G'. This means, that during a deformation cycle the dissipation of energy as heat is stronger than the storage and release of energy. This phenomenon is characteristic of systems which are fluid over the frequency range studied. The moduli are also relatively strongly dependent on the frequency ω in this range of α.

At $\alpha \leqslant 0.15$ the reverse can be seen. Now G' exceeds G'', both being relatively independent of the frequency. These features reflect a strong viscoelastic gel-like behaviour. The results at $\alpha = 0.2$ take up an intermediate position. A second striking feature is that the value of G'' is higher in comparison with G' than is usually found for gels and polymer melts in frequency ranges where G' is nearly independent of ω. We shall return to this phenomenon in section 6.5.1.2.

The influence of the polyelectrolyte supply on the storage modulus is represented in figs. 6–8 and 6–9. The loss modulus is related to the polyelectrolyte supply in the same way as G'. This indicates that the relatively high dissipation of energy to heat, leading to the high values of G'' must be of the same origin as that which makes the values of G' high, namely the forming of micro-gels between the emulsion droplets. At a low supply, the value of G' depends to a large extent on the polyelectrolyte supply. At higher supplies a levelling off is observed. For comparison in fig. 6–9 the steady state viscosity is also shown. It is impossible to correlate the rise in G' with just one parameter. With higher polyelectrolyte supplies the resulting droplet diameter decreases whereas the adsorbed amount Γ increases. This last factor can influence H_0. Both H_0 and d influence G' (section 6.4.2.).

The close relationship between the rheological properties of PMA-pe stabilized emulsions and the intermolecular interactions between polyelectrolyte molecules, adsorbed onto different droplets is also apparent from fig. 6–10. In this graph the influence is shown of the addition of salt on the dynamic moduli of Na-PMA-pe stabilized emulsions, manufactured with an electrolyte concentration of 0.025 M NaCl. The dependence of the dynamic moduli on the salt concentration at this particular α (= 0.25) shows a close similarity with the

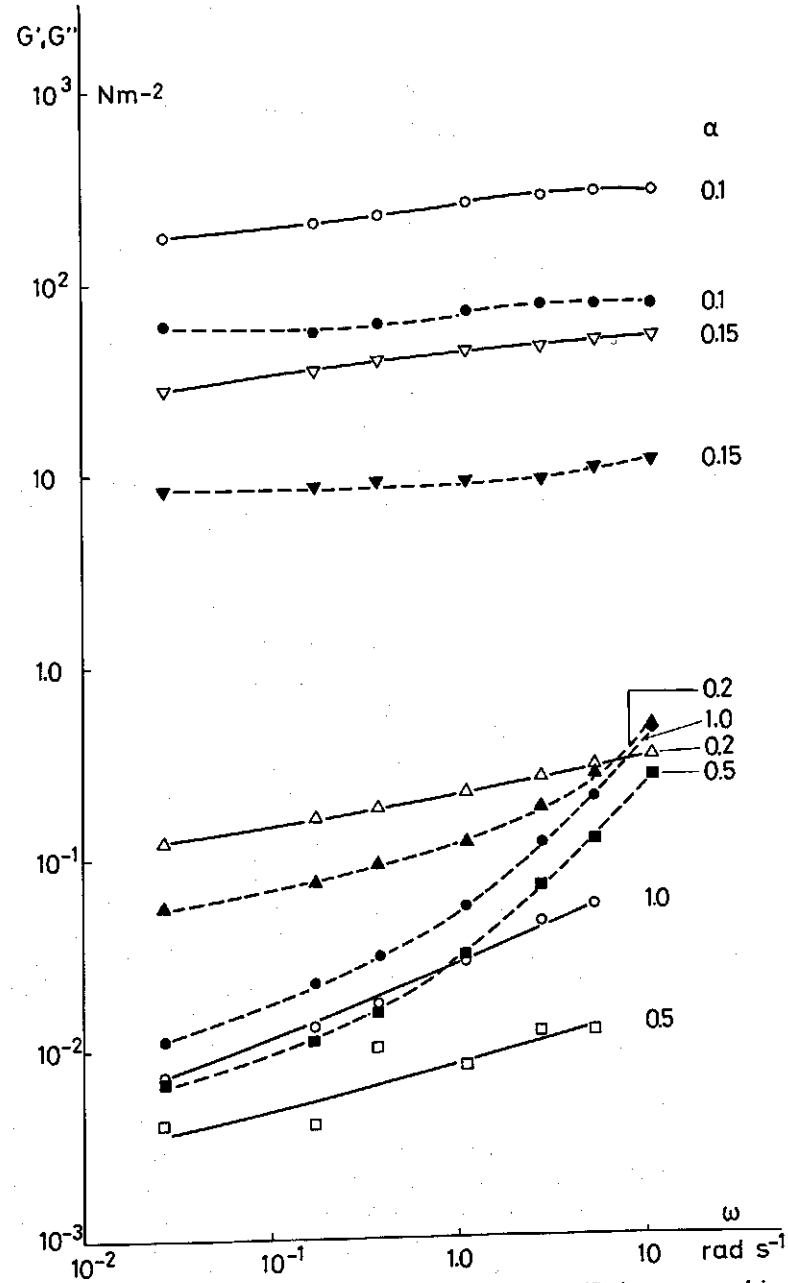

FIG. 6-7. The storage and loss moduli of PMA-pe stabilized paraffin in water emulsions as a function of the frequency. The degree of neutralization is given. Electrolyte 0.05 M NaCl. $\phi = 0.5$. Polyelectrolyte supply 2 mg per cm^3 of paraffin.
Storage moduli G' open symbols.
Loss moduli G'' filled symbols, dashed curves.

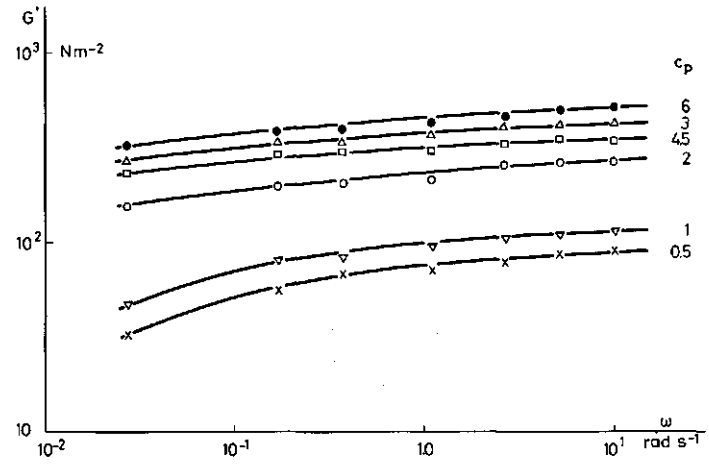

FIG. 6-8. The storage modulus of PMA-pe stabilized emulsions as a function of the frequency. $\alpha = 0.10$. Electrolyte 0.05 M NaCl. $\phi = 0.5$. The polyelectrolyte supply c_p in mg per cm^3 of paraffin is given.

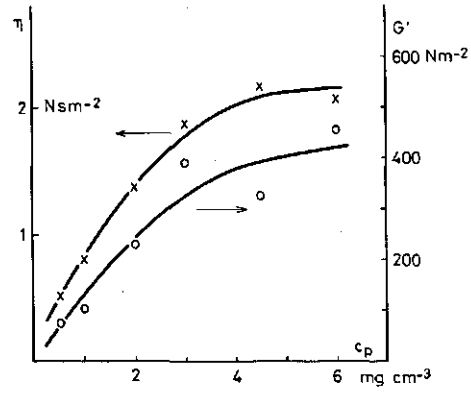

FIG. 6-9. Storage modulus G' and viscosity of emulsions stabilized by PMA-pe as a function of the polyelectrolyte supply c_p in mg per cm^3 of paraffin. $\alpha = 0.10$. Electrolyte 0.05 M NaCl. $\phi = 0.5$.
O Storage moduli (ω 2.75 rad s^{-1}).
× Viscosities ($D = 7.05$ s^{-1}).

dependence on α (fig. 6–7). As already discussed in section 4.4., the two phenomena largely depend on the balance between the repulsion (COULOMBIC) forces and the attractive (hydrophobic bonding and VAN DER WAALS attraction) forces between the PMA-pe segments.

The main conclusion is that the emulsions are viscoelastic, when the attractive forces between the polyelectrolyte molecules (and hence the attractive forces between the emulsion droplets) dominate. Then a three dimensional network structure is built up.

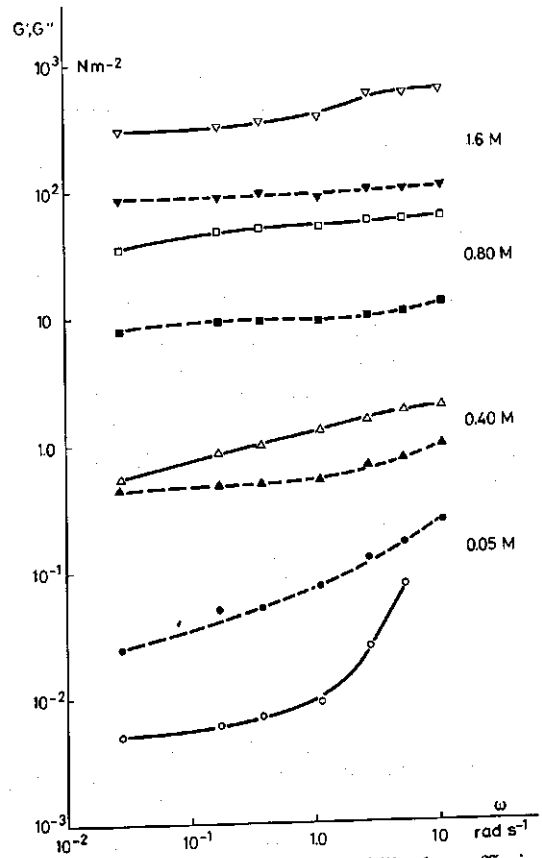

FIG. 6-10. The storage and loss moduli of PMA-pe stabilized paraffin in water emulsions as a function of the frequency. $\alpha = 0.25$. NaCl concentration is given. $\phi = 0.5$. Polyelectrolyte supply 2 mg per cm³ of paraffin.
Storage moduli G' open symbols.
Loss moduli G'' filled symbols, dashed curves.

A second conclusion can be that VAN DER WAALS attraction between the emulsion droplets does not play an important part in building up the network structure. This conclusion is also supported by a further consideration of equation (6.22.). In the discussion of this equation it was found that there is a limit in the linearity above a certain $\Delta H/H_0$. However, in the experimental accuracy of G' (error in $G' < 30\%$, corresponding to $4\ \Delta H/H_0 < 0.3$ which gives $\gamma < 0.0015$) no deviation from linearity could be detected till $\gamma \sim 0.04$.

6.5.1.1. The order of magnitude of the factors contributing to the storage shear modulus, in terms of an ideal network model

The shear modulus G' can be calculated with one of the equations derived in section 6.4.2. Most factors contributing to it can be calculated and other ones

estimated. By comparing the calculated values for the modulus with the experimental ones, information is obtained on the correctness of the used equations and on the values substituted for the various parameters.

Unfortunately, it was not possible to decide unambiguously which of the two emulsion structure models on which the mentioned set of equations is based, is the best. An indication about it can be obtained by varying ϕ and/or d. In our case the possibility to vary ϕ was very limited because at low ϕ the emulsions were no longer homogeneous. In that case separation occurred in a creamed layer and a layer containing mainly continuous phase. A substantially higher ϕ gave emulsification problems. Neither was it possible to vary d as the sole factor. Therefore we have to use a less rigorous way namely we will try to explain the measurements with the simplest model, the ideal network model. If this gives an acceptable result, one would conclude that for the moment the ideal network model serves us well enough to assess at least the orders of magnitudes of the various parameters. Therefore first calculations will be done with the next two equations:

$$6.22. \qquad G_{vdW} = f'' \frac{A\,\phi}{8\,\pi\,H_0^3}$$

$$6.29. \qquad G_{pol} = \frac{3\,c'\,b\,k\,T\,\phi}{\pi\,d\,H_0^2}$$

The analysis will be limited to emulsions, stabilized by Na-PMA-pe with a degree of neutralization of 0.1. The properties of these emulsions are tabulated in table 6–4. The volume averaged droplet diameter has been determined by Coulter Counter (model A) measurements. The experimental technique which was used, has been described by WALSTRA and OORTWIJN (1969) and LANKVELD (1970). Differences between G and G' will be neglected.

The most critical parameter for which an estimation had to be made, is H_0. Unfortunately, no good thickness measurements could be done on Na-PMA-pe ($\alpha = 0.1$) stabilized films, because of the irregularities in the surface of the film and the long drainage times. Only indications were obtained that H_0 is ca. 45 nm. From creep measurements (section 6.6.2.) a value of ca. 30 nm is found for H_0. Ellipsometric thickness measurements on one adsorbed layer support these thicknesses. Since we are not quite sure of the value to be assigned to H_0,

TABLE 6-4. Properties of the Na-PMA-pe stabilized emulsions on which the calculations leading to tables 6-5 and 6-6 have been done.

Volume fraction of paraffin	0.5
Supply of PMA-pe	2 mg/ml paraffin
Degree of neutralization	0.1
Adsorbed amount Γ (BÖHM, 1974)	ca. 2.2 mg m^{-2}
Electrolyte content continuous phase	0.05 M NaCl
Volume averaged particle diameter	$5\ 10^{-6}$ m
HAMAKER constant A (VISSER, 1972)	$1.7\ 10^{-20}$ J
Storage modulus G' (ω 5.28 rad s^{-1})	300 Nm^{-2}

calculations were done for a few thicknesses. Next a value for c' had to be accepted; it lies between 1 and 2 Because only the order of magnitude of the following calculations is right, the exact value of c' is not important. Arbitrarily we chose 1.5.

The storage modulus G'_g of the micro-gel between two emulsions can be calcalculated by combining equation (6.25.), (6.26.) and (6.29.), resulting in:

$$G'_g = G_{pol} \frac{\pi d H_0}{3 \phi A_{eff}} \tag{6.31.}$$

The effective contact region between two emulsion droplets A_{eff} was estimated, using the following two assumptions: a. The emulsion droplets are not disturbed in the contact region. b. Interaction occurs maximally over a distance of 2 H_0. Below that distance the interaction is independent of it. The influence of varying the choice of A_{eff} is also shown in table 6–5. It is assumed that for the calculations reported in table 6–5 G_{pol} may be made equal to the measured quantity G' of the emulsions.

The strong influence of H_0 on the calculated factors is clearly apparent in table 6–5. The resulting values for the number of polyelectrolyte bonds b between two neighbouring droplets are reasonable. The values of b/w indicate that about 10–20% of the polyelectrolyte molecules, present in the contact region between two emulsion droplets, are directly involved in the formation of these bonds. The storage modulus G'_g of the micro-gel between two droplets is of the same order of magnitude as G' of the emulsions. The contribution of the VAN DER WAALS attraction forces to the structure building of the emulsions is of minor importance.

Moreover the data of table 6–5 indicate that the measured rheological properties of the emulsions can be described semiquantitatively with the ideal network model within the experimental accuracy. Then the characteristics of an emulsion, mentioned in table 6–1 can be calculated (table 6–6).

In the aggregate model, the number of chains carrying a tensile stress across one m^2 will be lower. For a given G_{pol} (assumed to be equal to the measured

TABLE 6-5. Calculated order of magnitude of the factors, contributing to the built up of an ideal network structure for emulsions with the properties mentioned in table 6-4.

H_0 nm	maximum interaction distance nm	A_{eff} 10^{-12} m^2	number of polymer molecules w adsorbed on A_{eff}	b	b/w	G'_g Nm^{-2}	G_{vdw} Nm^{-2}
25	50	0.21	2800	300	0.1_2	560	13
30	60	0.25	3300	450	0.1_4	380	7
30	50	0.17	2200	450	0.2_0	550	7
30	80	0.41	5300	450	0.0_8	230	7
40	80	0.32	4200	800	0.2_0	390	2
50	100	0.41	5300	1300	0.2_4	380	1

TABLE 6-6. Characteristics of the emulsion described in table 6-4 for an ideal network model.

Number of rheological units, m^{-3}	$7.6\ 10^{15}$
Total length of stress-carrying chains, m^{-2}	$3.8\ 10^{10}$
Number of chains carrying a tensile stress across one m^2	$1.3\ 10^{10}$
Density of cross-links, $1.5\ (2\phi/\pi d^2)^{3/2}$, m^{-3}	$2\ 10^{15}$
Number of cross-links/number of emulsion droplets, $0.4\ \sqrt{\phi}$	0.28

quantity G') of the emulsion, it will result in higher values for b, b/w and G'_g, if it is assumed that the other factors (e.g. H_0) are not dependent on the choice of the model.

6.5.1.2. The loss shear modulus

The following analysis will also be limited to emulsions, stabilized by Na-PMA-pe with a degree of neutralization of 0.1.

Over the entire range of ω $G'' < G'$ (see fig. 6–7). However, the value of G'' is higher than usually observed for elastic systems (tg $\delta = G''/G'$ is large). PAPENHUIZEN (1971) observed the same feature for glyceryl tristearate crystals in paraffin oil dispersions. It was also found by DAVIS (1971) and ECCLESTON et al. (1973) for oil in water emulsions stabilized by a mixed emulsifier of a surfactant and a long chain alcohol. In the case of covalently linked gels G'' is around a few per cent of G' in the frequency regions where this last one is independent of ω.

The loss modulus is a measure of the energy, dissipated per cycle of sinusoidal deformation. The dynamic viscosity η_ω can be calculated from G'' with:

$$\eta_\omega = G''/\omega \tag{6.32.}$$

For the emulsions described in table 6–4 at $\omega = 5.28$ rad s^{-1} $G'' = 80$ Nm^{-2} which results in $\eta_\omega = 15.2$ Ns m^{-2}.

Qualitatively the relatively high tg δ values can be accounted for by the following mechanisms:

a. Liquid must move in and out of the small gel region between adjacent emulsion droplets by the expansion and compression of it during a deformation cycle Liquid motion through a gel dissipates much energy and so a large G'' would result. It is very difficult to calculate the importance of this effect quantitatively.

b. Relaxation during a deformation of cycle of the cross-links between the polyelectrolyte molecules and of the VAN DER WAALS interaction energy between the emulsion droplets. The density of interactions between adjacent emulsion droplets can be calculated from the number of droplets and the number of cross-links between chains of emulsion droplets resulting in ca. 1.2×10^{16} m^{-3}. The energy of a VAN DER WAALS interaction is for $H_0 = 35$ nm: 3.7×10^{-20} J. It is assumed that the energy content of a polyelectrolyte-polyelectrolyte cross-link is $6\ kT \approx 2.4 \times 10^{-20}$ J (section 6.6.2.). If during a deformation cycle the VAN DER WAALS interaction and b' polyelectrolyte cross-links per droplet-droplet bond would relax, the total energy dissipation per second is then for $\omega = 5.28$ rad s^{-1}: $(0.8 + 0.5b')\ 10^{-3}$ J m^{-3} s^{-1}. In that case the dynamic viscos-

ity η_ω corresponds with an energy dissipation of $\eta_\omega \dot{\gamma}^2$ ($\dot{\gamma} = d\gamma/dt$) $\sim 3\,10^{-2}$ J $m^{-3}\,s^{-1}$. This would require the relaxation of $\sim$ 60 polyelectrolyte cross-links per deformation cycle, which is a fraction of $\sim$ 10–20% (see table 6–5) of the total number of cross-links. Of course, the above estimation is only semiquantitative. However, the result does not seem unrealistic. Relaxation of part of the polyelectrolyte cross-links is in agreement with the small dependence of G' on ω. A logical conclusion of this relaxation is that the conditions for applying $G' = \nu\, kT$ (equation (6.26.)) are not satisfied completely. The relaxation of the cross-links also results in an energetic contribution to the reaction of the gel on a deformation. The quantitatieve importance of this contribution is not known but it indicates that the values calculated in table 6–5 are at best semiquantitative.

Recapitulating, the expectation is that the large value of tg δ follows from the fact that liquid must move in and out of the micro-gels between adjacent emulsion droplets or from the relaxation of the polyelectrolyte cross-links, during a deformation cycle. The relative inportance of the two contributions is not known. The latter has consequences for the application of equation (6.26.).

6.5.2. *Emulsions stabilized by Ca-PMA-pe*

The storage and the dynamic moduli of Ca-PMA-pe stabilized emulsions as a function of the frequency at different α's are shown in fig. 6–11. Again there is a strong influence of α on the values of the moduli, but the relation is much more complex than in the case of Na-PMA-pe. There is a maximum in the moduli at $\alpha \sim 0.4$. The values of G' and G'' are then about the same as those for emulsions stabilized by Na-PMA-pe at $\alpha = 0.1$. However, for $\alpha = 0.1$ the values of the moduli are lower than in the corresponding case of Na-PMA-pe emulsions. All emulsions have a more or less viscoelastic character in contrast with Na-PMA-pe stabilized emulsions. In all cases $G' > G''$. Both are relatively independent of the frequency. These features demonstrate once again the strong influence of bivalent cations on the properties of negatively charged polyelectrolytes. For an extensive discussion of this influence we refer to sections 4.3. and 4.5.3.

For a discussion of the general aspects of the emulsion network structure reference is made to section 6.5.1. No special discussion will be given for Ca-PMA-pe stabilized emulsions because: a. the model is not detailed enough to consider specific effects caused by the presence of Ca^{++}; b. moreover the necessary parameters such as H_0 are not known.

6.6. Creep measurements

Creep measurements can be used for the study of the network structure of an emulsion in the almost undisturbed state. The data obtained by creep measurements can be transformed into dynamic parameters (Ferry, 1970; Barry,1975). An idealized creep curve has been described in section 6.2. A few methods are known for the analysis of creep measurements.

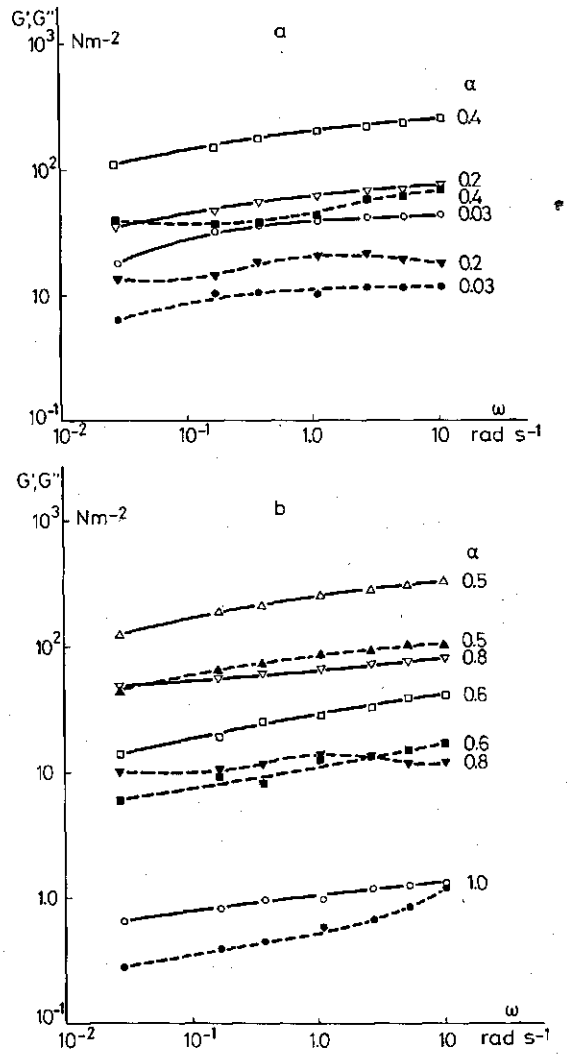

FIG. 6-11. The storage and loss moduli of Ca-PMA-pe stabilized paraffin in water emulsions as a function of the frequency. The degree of neutralization is given. Cation 0.0076 M Ca^{++}. $\phi = 0.5$. Polyelectrolyte supply 2 mg per cm^3 of paraffin. Storage moduli open symbols. Loss moduli filled symbols, dashed curves.

1. Phenomenological representation of the creep curves by mechanical analogues. This method has been described by for instance: INOKUCHI (1955), SHERMAN (1968) and BARRY (1975). We shall not follow this method because, as already mentioned, it does not result in a better understanding of the physical background of the structure of the emulsion.
2. Analysis of the obtained instantaneous shear modulus in the same way as described in section 6.4.2. (STRENGE and SONNTAG, 1974; 1975).

3. A same analysis as mentioned under 2, but with using additional information obtained from the non linearity of the deformation, just outside the linear region (VAN DEN TEMPEL, 1961). This method will be described extensively below in section 6.6.1.

Creep measurements have been done on emulsions, stabilized by Na-PMA-pe with a degree of neutralization of 0.11. The electrolyte concentration was 0.05 M NaCl and the polyelectrolyte supply 2 mg cm^{-3} paraffin. The volume fraction of paraffin was 0.5.

The apparatus has been described in section 3.5.3. Emulsions were brought into the viscometer after preparation and cooling down to 20°C. A waiting time of one night was observed, before measurements were started. At a certain σ the difference in the measured $\gamma(t)$ between two independent measurements was 20% at most, primarily due to the irreproducibility in the emulsification process.

6.6.1. *Creep curves, correlation with the ideal network model*

The theory described in this section is based on and to a large extent identical to an analysis, given by VAN DEN TEMPEL (1961 and 1976). The same nomenclature will be used, with a few exceptions. It is assumed, that the emulsions can be described by a network model. An essential prerequisite for employing this analysis is, that during the creep experiments the coherence of the material is maintained.

It is assumed that in the network structure one can distinguish two kinds of interparticle bonds, viz. *primary* bonds and *secondary* bonds. Bonds which remain intact during an experiment are called 'primary' bonds. The so called 'secondary' bonds could be broken and re-formed, during the time of the measurement (relaxation of bonds). The essential feature of the primary bonds is that the restoration of a broken bond takes much more time, than the time scale of the experiment. Principally they can be the same sort of bonds, but only differing in bond-strength. Alternatively, they can be two different types of bonds e.g. VAN DER WAALS attraction between adjacent emulsion droplets and interaction between adsorbed polymer sheets. The energy content of primary bonds and the resilience against stretching are larger, than those of secondary bonds. The contribution of the secondary bonds to the network structure can be calculated, if irreversible breakdown of the primary bonds during the measurement is prevented. The method to determine this contribution is essentially based on measuring the strain before and after relaxation of the secondary bonds.

As early as 1943 TOBOLSKY and EYRING discussed the rheological behaviour of materials, containing both primary and secondary bonds. It was assumed, that the total number of bonds per unit area consists of N_1 primary bonds and N_2 secondary bonds. The stress σ, normal to the cross section considered, is distributed over the chains in such a way, that:

$$\sigma = f_1 N_1 + f_2 N_2 \qquad (6.32.)$$

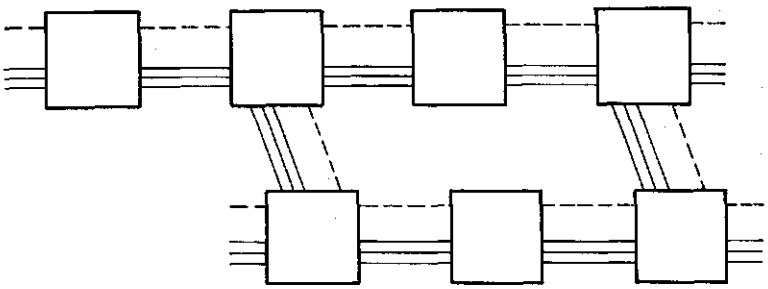

FIG. 6-12. Schematic representation of an emulsion with primary and secondary bonds.
Squares rheological units.
≡ ≡ ≡ primary bonds.
– – – – – secondary bonds.

where f_1 is the average force in the primary bonds and f_2 the one in the secondary bonds. A schematic representation of a possible model is given in fig. 6–12. The squares represent rheological units. They could be emulsion droplets, agglomerates of droplets or mutually cross-linked parallel chains of droplets. The rate of breaking the secondary bonds under the influence of a force, follows from the reaction rate theory as:

$$\frac{1}{N_2}\frac{dN_2}{dt} = \frac{1}{\theta}\exp\left(-\frac{\Delta U_2}{kT}\right)\exp\left(\frac{f_2\lambda_2}{kT}\right) \tag{6.33.}$$

where ΔU_2 is the mean energy of activation of breaking a secondary bond and λ_2 the distance across which two droplets must be moved apart to break the bond. The parameter θ is a characteristic time connected with this process. TOBOLSKY and EYRING (1943) found that with such a type of equation the viscoelastic properties of rubber-like substances can be interpreted.

The rate of strain of the chains is then determined firstly by the rate of stretching of the primary and unbroken secondary bonds and secondly by the rate at which secondary bonds are broken. The first contribution depends on the average resiliences g_i $(i = 1,2)$ of the bonds and the average forces f_i on the bonds. As long as coherence in the sample is maintained the rate of strain $d\gamma_i/dt$ is the same for primary and secondary bonds. Together with equation (6.33.) this gives:

$$\frac{d\gamma}{dt} = \frac{n_1}{g_1}\frac{df_1}{dt} = \frac{n_2}{g_2}\frac{df_2}{dt} + n_2\lambda_2\frac{1}{\theta}\exp\left(-\frac{\Delta U_2}{kT}\right)\exp\left(\frac{f_2\lambda_2}{kT}\right) \tag{6.34.}$$

where n_1, n_2 are the numbers of primary and secondary bonds per unit length (m) of the chain respectively. It is assumed, that the strain increases by an amount λ_2, upon breaking of a secondary bond.

In a creep experiment the stress is constant in time. Together with equation (6.32.) this results in:

$$\frac{df_1}{dt} = -\frac{N_2}{N_1}\frac{df_2}{dt} \tag{6.35.}$$

Combining equation (6.34.) with (6.35.) and integration gives:

$$\frac{f_2\lambda_2}{kT} = \frac{\Delta U_2}{kT} \ln \frac{\theta kT}{g n_2 \lambda_2^2 t} = -\ln \frac{t}{\tau} \tag{6.36.}$$

where

$$1/g = \left(\frac{n_1}{g_1 N_1} + \frac{n_2}{g_2 N_2} \right) N_2 \tag{6.37.}$$

and the relaxation time

$$\tau = \frac{\theta kT}{g\lambda_2^2 n} \exp\left(\Delta U_2/kT\right) \tag{6.38.}$$

The relaxation time τ is the time, required to make a secondary bond stress-free, if the relaxation process of this type of bonds can proceed undisturbed for a sufficiently long time.

With $\gamma_1 = \gamma = n_1 f_1/g_1$ and equation (6.32.) it is found that:

$$\gamma = \frac{n_1}{g_1} \left(\frac{\sigma}{N_1} - f_2 \frac{N_2}{N_1} \right) \tag{6.39.}$$

The force f_2 can be eliminated with equation (6.36.), which results in:

$$\gamma = \left(\frac{\sigma}{M_1} - \frac{N_2 kT}{M_1 \lambda_2} \ln \tau \right) + \frac{N_2 kT}{M_1 \lambda_2} \ln t \tag{6.40.}$$

where

$$M_1 = \frac{g_1 N_1}{n_1} \tag{6.41.}$$

Equation (6.40.) shows that if the theory holds, creep curves in a semi-logarithmic plot are straight lines with a slope $N_2 kT/M_1\lambda_2$. The first term of the right hand side of equation (6.40.) represents the elastic deformation γ_0. The second term is due to the breakdown of secondary bonds. The slope is independent of the stress, as long as primary bonds are not broken. This can be verified experimentally. Breakdown of primary bonds results in a reduction of M_1 and thus in an increase of the slope.

The meaning of M_1 can be found by considering the instantaneous shear modulus $G_0 = \sigma/\gamma_0$. The instantaneous shear strain is the deformation of the sample immediately after loading, but before relaxation has occurred. Then the next equation holds:

$$G_0 = \frac{\sigma}{\gamma_0} = \frac{g_1 N_1}{n_1} + \frac{g_2 N_2}{n_2} = M_1 + M_2 \tag{6.42.}$$

where M_1 represents the contribution of the primary bonds and M_2 the contribution of the secondary bonds. M_1 can be calculated from two semi-logarithmic creep curves with equation (6.40.).

$$M_1 = \frac{\sigma - \sigma'}{\gamma - \gamma'} \tag{6.43.}$$

If M_1 and G_0 are known M_2 can be calculated. Experimental determination of G_0 is not so simple because of slowness in the apparatus. The slowness is estimated to be < 2 seconds, so only a rough estimate of G_0 was obtained. The term N_2/λ_2 can be calculated from the slopes of the curves, after which ln τ can be found. Further calculations require a value for N_2 and so a further specification of the network model, which is used.

It has already been concluded in the section before, that the ideal network model applies. Then equations (6.22.) and (6.29.) represent the two types of interaction between the emulsion droplets. In section 6.5. it has been found that the VAN DER WAALS attraction between adjacent emulsion droplets is much weaker than the interactions between the adsorbed polyelectrolyte sheets. In the following treatment it will be assumed, that the polyelectrolyte-polyelectrolyte interactions correspond to the primary bonds and the VAN DER WAALS interaction to the secondary bonds. Both types of interaction occur between all adjacent emulsion droplets. Then the number of bonds of type 2 in a cross section, normal to the direction of stress is (table 6–1):

$$N_2 = 2\phi/\pi d^2 \tag{6.44.}$$

and

$$n = 1/d$$

If d is known, ΔU_2 can be calculated.

6.6.2. *Results and discussion*

Creep curves at different stresses are represented in fig. 6–13. The instantaneous shear strain γ_0 is shown in fig. 6–14. Above $\gamma_0 > 0.025$ the network

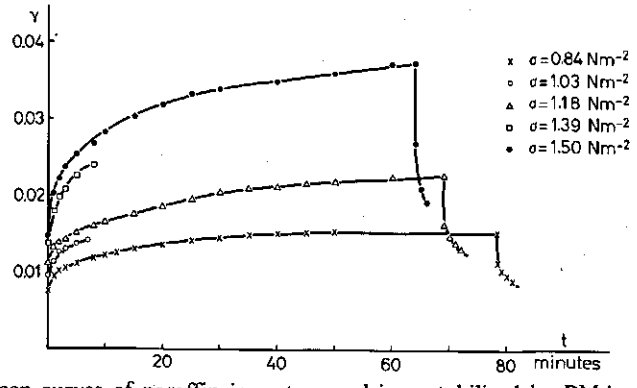

FIG. 6-13. Creep curves of paraffin in water emulsions stabilized by PMA-pe. $\alpha = 0.11$. Electrolyte 0.05 M NaCl. $\phi = 0.5$. Polyelectrolyte supply 2 mg per cm^3 of paraffin. The shear stress σ is given.

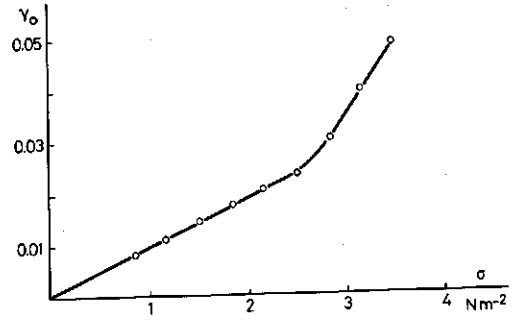

FIG. 6-14. The instantaneous shear strain γ_0 as a function of the applied stress σ for paraffin in water emulsions stabilized by PMA-pe. $\alpha = 0.11$. Electrolyte 0.05 M NaCl. $\phi = 0.5$. Polyelectrolyte supply 2 mg per cm^3 of paraffin.

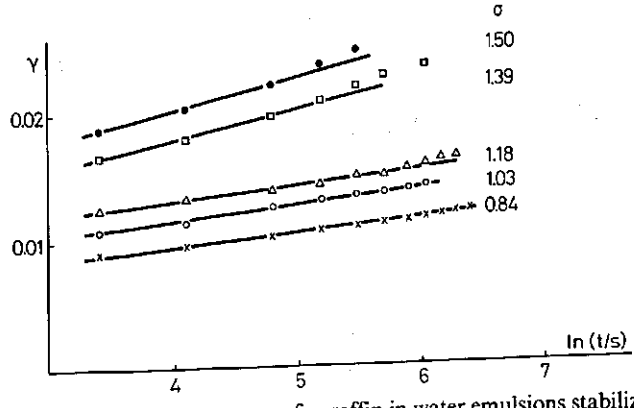

FIG. 6-15. Semi-logarithmic creep curves of paraffin in water emulsions stabilized by PMA-pe. $\alpha = 0.11$. Electrolyte 0.05 M NaCl. $\phi = 0.5$. Polyelectrolyte supply 2 mg per cm^3 of paraffin. The shear stress σ in Nm^{-2} is given.

structure is broken down. Semi-logarithmic creep curves are represented in fig. 6–15. At stresses exceeding 1.39 Nm^{-2} a clear rise of the slope is observed, indicating a loss of coherence of the sample. For lower stresses the slopes are independent of σ. It is in this region that the results may be interpreted in terms of the theory, described in section 6.6.1.

The properties of the emulsions investigated are mentioned in table 6–4 except for the degree of neutralization which was 0.11. The instantaneous shear modulus G_0 can be found in fig. 6–14. The slope of the semi-logarithmic creep curves (fig. 6–15) is 0.0011 s^{-1}. Then a variety of parameters can be calculated if a value for θ is accepted (table 6–7). For a molecular process the frequency of the vibration in the energy minimum would be used as the value to substitute for θ (TOBOLSKY et al., 1943). Likewise the longest relaxation time can be used for macromolecules. VAN DEN TEMPEL (1976) suggested to use $\theta = (d\gamma/dt)^{-1}$ for a particle suspension. It means that θ is the time, necessary to enlarge the distance between two emulsion droplets by $d/2$. However, $(d\gamma/dt)^{-1}$ itself depends on t,

TABLE 6-7. Results of creep measurements.

G_0	106 Nm^{-2}	n_2	2.0 10^5 m^{-1}
M_1	93.4 Mm^{-2}	λ_2	4.9 10^{-10} m
M_2	12.6 Nm^{-2}	g_1	1.5 10^{-3} Nm^{-1}
τ	34 s	g_2	2.0 10^{-4} Nm^{-1}
N_2	1.25 10^{10} m^{-2}	g	8.9 10^{-10}
		ΔU_2	$-11.2\,kT$ at $t = 30$ s to $-13.5\,kT$ at $t = 300$ s

$d\gamma/d\ln t$ being constant in the investigated region. From equation (6.38.) follows for ΔU_2:

$$\Delta U_2 = -kT \ln \frac{\theta\, kT}{n_2 \lambda_2^2 g \tau} \tag{6.45.}$$

Inserting the values recorded in table 6–7 and $\theta = (d\gamma/dt)^{-1}$ in equation (6.46.) results in:

$$\Delta U_2 = -kT \ln \left[2.8 \left(\frac{d\gamma}{dt} \right)^{-1} \right]$$

$$= -kT \left\{ \ln \left[2.8 \left(\frac{d\gamma}{d \ln t} \right)^{-1} \right] + \ln t \right\} \tag{6.46.}$$

For $d\gamma/d \ln t = 0.0011$

$$\Delta U_2 = -[7.8 + \ln t]\, kT.$$

The value of λ_2 (defined as the distance across which two droplets must be moved to break the bond) which has been found, is strongly dependent on d ($\lambda = c/d^2$) and therefore it is influenced, to a large extent by the way of averaging in determining d. A second remark can be, that stretching of VAN DER WAALS bonds is linear for $\gamma < 0.001$ (PAPENHUIZEN, 1971). This implies that for $H_0 \sim$ 35 nm ΔH must be lower that 1.7 nm, which is of the same order as λ.

Implicitly it is assumed in the theory that there is only one relaxation time τ. The value found would mean that it takes some tens of a second to make a secondary bond stress free. A more exact physical meaning cannot be given.

Next one can interpret M_2 further by equalization of M_2 with G_{vdW} resulting in:

$$M_2 = \frac{A\,\phi}{8\pi H_0^3} f'' \tag{6.47.}$$

Because in equation (6.47.) all parameters except H_0 are known, this one can be calculated. A value of 25 nm was found. Regarding the very crude approximations which we have made and the high inaccuracy in the determination of M_2, this value correlates satisfactorily with the found film thickness and the ellipsometric thickness of one adsorbed layer (45 and 12 nm respectively).

Still another way of calculating H_0 is by equalization the found value of ΔU_2 to:

$$\Delta U_2 = -\frac{Ad}{24\,H_0} f' \qquad (6.48.)$$

where f' is the correction factor for retardation (fig. 5–1). Actually in equation (6.48.) the VAN DER WAALS attraction energy is equalized to the activation energy for breaking a secondary bond. This energy ΔU_2 is less sensitive to experimental inaccuracy than M_2, but the value which has been adopted for θ is open to discussion. Accepting the value for $\Delta U_2 = -12\,kT$ (4.8×10^{-20} J.), given in table 6–7 one obtains $H_0 \sim 30$ nm. This value is of the same order as those found before.

Summarizing the discussion hitherto, it seems possible to determine the contribution of the VAN DER WAALS attraction to the droplet-droplet interaction for viscoelastic paraffin in water emulsions, stabilized by Na-PMA-pe. Values found for ΔU_2 and G_{vdW} correspond satisfactorily with theoretical predictions, based on an ideal network model for reasonable values of H_0. A point in the theory which deserves further attention is the meaning of θ and which value to assign to it. Moreover, the results obtained for λ and τ are not clear in every respect.

All VAN DER WAALS bonds between adjacent emulsion droplets are secondary in our picture. In addition to them there are also primary bonds. It is assumed (section 6.6.1.) that these latter bonds correspond with the interaction between polyelectrolyte molecules, adsorbed onto different droplets. Then M_1 can be identified with G_{pol}. Next the number of polymer bonds between two droplets can be calculated, resulting for $H_0 = 30$ nm and $c' = 1.5$ in $b = 150$.

By means of equation (6.28.) the stretching force in the polymer chains can be calculated. Next the energy can be found, required to extend the polymer chains over a distance ΔH from

$$U_{pol} = \frac{3\,c'\,b\,kT\,(\Delta H)^2}{2\,H_0^2} \qquad (6.49.)$$

If ΔH at which the primary bonds break is known, the order of magnitude of the interaction energy between the polyelectrolyte sheets can be calculated. It can be seen from figs. 6–13 and 6–14 that primary bonds start to break at $\gamma =$ 0.020 – 0.025. For $\gamma = 0.02$, ΔH is 50 nm, which results in $U_{pol} = 3.7 \times 10^{-18}$ J or 920 kT. Then the energy of activation for breaking one polyelectrolyte-polyelectrolyte bond is ca. 6 kT. Of course, this is only an order of magnitude. In order to get some idea of the quality of such a calculation, we have calculated the shear stress σ with equation (6.28.). For ΔH is 50 nm. is found $\sigma = 1.9\,\mathrm{Nm}^{-2}$, which is in good agreement with the shear stress, one has to apply in order to get a deformation $\gamma = 0.02$ (fig. 6–14). In other words the value obtained has at least internal consistency.

The value of 6 kT found for the energy of activation for breaking one poly-

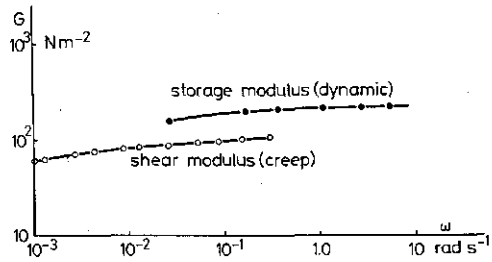

FIG. 6-16. Rheological properties of paraffin in water emulsions stabilized by PMA-pe. α = 0.11. Electrolyte 0.05 M NaCl. ϕ = 0.5. Polyelectrolyte supply 2 mg per cm^3 of paraffin.

electrolyte-polyelectrolyte bond is in reasonable agreement with hydrophobic interaction between 5–10 pairs of methyl groups per bond.

6.6.3. *Comparison of the shear modulus obtained by creep measurements with the dynamic storage modulus*

A creep measurement after a time t is equivalent to a dynamic one with a frequency $2\pi/t$ rad s^{-1}. In fig. 6–16 are compared the shear modulus G, obtained by creep measurements and the storage modulus G', found by dynamic measurements. The distinction between G and G' is neglected.

It can be seen clearly, that the shapes of the curves as a function of the frequency are identical. In the overlap region G' is ca. twice as high as G. Such a disparity is normal. At long times no strong descent of the G' (ω) curve was observed, indicating that the cross-links between polyelectrolyte molecules adsorbed onto different droplets are semi-permanent over a not too extreme time scale. This indicates, that the assumption about the permanence of the cross-links, made in the derivation of equation (6.29.) is not too bad.

6.7. SUMMARY

The rheological behaviour of paraffin in water emulsions stabilized by PMA-pe, has been studied by dynamic and creep measurements.

In the dynamic experiments the storage modulus G' and the loss modulus G'' have been measured as a function of the frequency ω. The degree of neutralization, the polyelectrolyte supply and the salt concentration were varied. It has been found, that when the attraction forces between the polyelectrolyte segments dominate, free PMA-pe can form a gel. By comparison of the gel point concentration with the concentration in the layer between two adjacent emulsion droplets, it was concluded that there also a gel could be formed. This conclusion is supported by analysis of the G' (ω) curves. Then it is possible, to derive an equation relating G' of an emulsion with the number of polyelectrolyte cross-links between two droplets both for an ideal network model and for an aggregate model of the emulsion structure. Equations were also derived relating

G' and the VAN DER WAALS attraction between the emulsion droplets. Calculations were done for emulsions with a volume fraction of paraffin of 0.5, stabilized by Na-PMA-pe with a degree of neutralization = 0.1. The polyelectrolyte supply was 2 mg cm^{-3} paraffin. Electrolyte concentration 0.05 M. NaCl. The ideal network model appeared to be good enough to interpret semiquantitatively the results obtained for the viscoelastic emulsions. The interparticle distance H_0 was assumed to be ca. 30 nm. It was calculated, that 400–1000 polyelectrolyte bonds were formed between two emulsion droplets. The VAN DER WAALS attraction between the emulsion droplets proved to be much less important than the interactions between the two polyelectrolyte sheets.

It was found for the emulsions described above that over the entire range of ω $G'' < G'$. However, the value of G'' is higher than as usually observed for elastic systems (tg $\delta = G''/G'$ is large). The expectation is that this high value of tg δ follows from the fact that liquid must move in and out of micro-gels between adjacent emulsion droplets or from the relaxation of the polyelectrolyte cross-links, during a deformation cycle.

The creep curves were analysed by means of a model developed by VAN DEN TEMPEL (1961). It is based on the ideal network model. The creep curves were interpreted by assuming the existence of strong and weak bonds between the droplets. If measured under the proper conditions the weak (secondary) bonds are broken, but not the stronger (primary) bonds. As long as the coherence of the sample is maintained, semi-logarithmically creep curves give a straight line with a slope independent of the applied stress. In these cases it is possible to calculate from a non-linearity in γ as a function of the shear stress, if any, the contribution of secondary bonds to the interaction between two adjacent emulsion droplets. The secondary bonds were identified with the VAN DER WAALS attraction between two adjacent emulsion droplets and the primary bonds with the interaction between the polyelectrolyte molecules, adsorbed onto different droplets. Again it was found, that the VAN DER WAALS attraction is relatively unimportant, but not negligible. From the found G_{vdW} and the VAN DER WAALS interaction energy between two droplets the interparticle distance H_0 was calculated to be 25–30 nm. This value is of the right order of magnitude, compared with the results of the film thickness measurements. An order of magnitude calculation, made for the activation energy necessary to break a primary bond resulted in: $U_{pol} = 3.7 \times 10^{-18}$ J $\gtrsim$ 900 kT. This value correlates with an energy effect per polyelectrolyte-polyelectrolyte bond of 4–8 kT.

It was found that the results of creep and dynamic measurements are in good accordance with each other. At long times no strong decline of the $G'(\omega)$ curve was found indicating that the cross-links between the polyelectrolytes adsorbed onto different droplets are semi-permanent over a not too extreme time scale.

SUMMARY

The aim of this study was to gain more insight into the factors, determining the inter- and intramolecular interactions between adsorbed macromolecules. To that end several experimental and theoretical approaches were followed, using well-defined systems. It was shown that these interactions could conveniently be studied by measurements on emulsions and thin free liquid films. Two different macromolecules were used: a nonionic one: polyvinyl alcohol (PVA) and an ionic one: a copolymer of methacrylic acid and the methyl ester of methacrylic acid (PMA-pe) in the molar ratio 2:1.

The characterization of the used materials has been described in chapter 2. The conformational transition, occurring in dissolved polymethacrylates was briefly discussed. At low pH, the molecules occur in a compact form, the hypercoiled form, or a-conformation. At pH above ~ 6 the molecules occur in the common, more extended b-conformation. From viscometry on PVA solutions conformational parameters, such as the root mean square end-to-end distance, the length of a statistical chain element and the linear expansion factor were determined. These conformational parameters were determined in a 1 M aqueous glycerol solution because in the film experiments 1 M glycerol was present in the PVA solutions in order to lower the water vapour pressure.

In chapter 3 the experimental methods have been described. In the first part attention was paid to the preparation of the emulsions and to the determination of basic properties, such as specific area and adsorbed amount. A variety of rheological measurements were described in the second part. A more detailed description was given of the apparatus for the dynamic measurements (the rheometer) and of that for creep measurements.

The end of chapter 3 deals with the thickness measurements of polymer-stabilized free liquid films. First, a description of the apparatus and the experimental procedure was given. Subsequently, a discussion followed of the calculation of thicknesses from the intensity of the reflected light. It was shown that, for the calculation of the correction to be applied to the equivalent aqueous solution thickness, the smeared out adsorbed polymer segment layers may be formally replaced by a block distribution.

The inter- and intramolecular interactions between the PMA-pe segments and the effect of these interactions on the conformation of the polyelectrolyte molecule and on the rheological properties of emulsions stabilized by this polyelectrolyte, have been discussed in chapter 4. As possible attractive forces responsible for the compact conformation at low pH, VAN DER WAALS attraction and hydrophobic bonding between the methyl groups in the main chain were considered. In addition, the strength of the COULOMBIC interaction between the carboxyl groups also plays a role in the conformational transition.

The conformational transition from the a- to the b-conformation in free and adsorbed PMA-pe, was studied by potentiometric titration. Data for adsorbed

PMA-pe were obtained by titrating polyelectrolyte-covered emulsion droplets. It was found that the conformational transition also occurs in adsorbed PMA-pe. This conformational transition is reflected in the rheological properties of paraffin in water emulsions, stabilized by PMA-pe. It could be concluded both from viscosity and dynamic data, that strong attraction between the emulsion droplets occurs only at a low degree of neutralization α, that is, if a substantial part of the adsorbed PMA-pe is in the a-conformation. Then both the dynamic moduli and the viscosities are very high. On the contrary at high α the emulsions were very fluid with little or no indication of attraction between the adsorbed polyelectrolyte sheets.

The main conclusions from the potentiometric titration data and the rheological measurements are:

a. the attraction between the polyelectrolyte segments, observed at low α in solution occurs also between loops and/or tails, adsorbed on *one* emulsion droplet;
b. the high values of the dynamic moduli and of the viscosities at low α are due to attraction between extending loops and/or tails, adsorbed on *different* droplets;
c. the two types of interaction are very similar.

This conclusion was confirmed by the influence of methanol on Na-PMA-pe stabilized emulsions and the effect of temperature. Moreover, from these experiments it could also be concluded, that probably the hyper-coiled conformation at low α is to a large extent due to hydrophobic bonding.

The influence of Ca^{++} ions on the properties of the polyelectrolyte was also investigated. Potentiometric titration showed that, in the presence of Ca^{++} ions, the conformational transition is moved to higher α. Again the transition is reflected in the rheological properties of emulsions, stabilized by Ca-PMA-pe. The balance between the inter- and intramolecular interaction forces and the interactions themselves are more complicated than in the case of Na-PMA-pe. This complex character is reflected in the more complex rheological functionalities ($\eta(\alpha)$, $G'(\alpha)$ curves) of emulsions stabilized by Ca-PMA-pe.

The interactions between adsorbed macromolecules were further investigated by studying the properties of polymer stabilized thin free liquid films. Measurements on films, stabilized by PVA or PMA-pe, were reported in chapter 5.

The interaction forces which must be taken into account in a PVA film are VAN DER WAALS attraction, hydrostatic pressure and steric interaction. The VAN DER WAALS attraction over a film can be calculated. The equilibrium film thicknesses of the films were determined at varying hydrostatic pressure. Then the steric repulsion force Fs between the two adsorbed PVA layers was obtained by equalizing $-Fs$ with the hydrostatic pressure and the VAN DER WAALS attraction. So the steric repulsion force could be calculated for different equilibrium thicknesses. Next the free energy of steric interaction was found by graphic integration of the force-distance curve. These values can be compared with theoretical predictions.

In order to calculate the free energy of steric interaction theoretically, a model

of the segment density distribution had to be developed. The proposed semi-quantitative model was based on the consideration that the molecular weight distribution of the used PVA samples is wide and the presumption that a large fraction of the segments is adsorbed as tails. Indications for this presumption were found by comparing the extrapolated ($F_S \rightarrow 0$) film thickness with the ellipsometric thickness of an adsorbed layer. This model leads to the conclusion, that the properties of the outer part of the adsorbed layers are dominated by a few extending tails. The free energy of steric repulsion, thus calculated with the HESSELINK et al. (1971b) theory of steric repulsion, between two adsorbed PVA (M_v = 27,000 or 86,000) layers, agrees well with the experimentally determined values for reasonable lengths of the tails.

In chapter 5 also the drainage behaviour and the equilibrium thicknesses of PMA-pe films, made at different values of the degree of neutralization α, were discussed. The measured equilibrium thicknesses correlated well with ellipsometric measurements of an adsorbed layer. The drainage pattern changes if α is varied. At low α the films are rigid, whereas at high α they are mobile. Also the dilatational modulus decreased from $\alpha = 0.1$ to $\alpha = 1.0$. Probably the interaction forces between the polyelectrolyte segments which are responsible for these phenomena, are the same as those which induce the conformational transition in the molecule or which are responsible for the drastic changes in the rheological properties of emulsions stabilized by PMA-pe if α is varied.

A more elaborate discussion of the rheological properties of PMA-pe stabilized emulsions is given in chapter 6. Both dynamic and creep measurements were reported.

In the dynamic experiments the storage modulus G' and the loss modulus G'' were measured as a function of the frequency ω. The degree of neutralization, the polyelectrolyte supply and the salt concentration were variables. By comparing the gel point concentration of free PMA-pe with the polyelectrolyte concentration in the layer between two emulsion droplets, it was concluded that there also a gel could be formed if attractive forces between the polyelectrolyte segments dominate. This conclusion is supported by analyses of the $G'(\omega)$ and $G''(\omega)$ curves. In cases where such a kind of gel is formed, it is possible to relate G' to the number of polyelectrolyte cross-links between two droplets. Equations were given for the case of an ideal network model and for an aggregate model of the emulsion structure. For both models equations were also derived relating G' to the VAN DER WAALS attraction between the droplets. It was found that the ideal network model was good enough to interpret semi-quantitatively the results obtained for the viscoelastic emulsions. The VAN DER WAALS attraction between the emulsion droplets proved to be much less important than the interactions between the polyelectrolyte sheets. It was calculated that at α PMA-pe = 0.1, about 400–1000 polyelectrolyte bonds were formed between two emulsion droplets at interparticle distances of 30 to 50 nm. It implies that about 10–20% of the polyelectrolyte molecules, present in the contact region between two emulsion droplets, are directly involved in the formation of these bonds.

A short discussion was given of the unusually high values of the loss factor tg δ. The suggestion was put forward that these high values follow from the fact that liquid must move in and out of the micro gels between adjacent emulsion droplets or from the relaxation of the polyelectrolyte cross-links, during a deformation cycle.

The creep curves were analysed by assuming the existence of both strong and weak bonds between the emulsion droplets. If measured under the proper conditions the weaker (secondary) bonds are broken, but the stronger (primary) bonds are not. Then it is possible to calculate from a non-linearity in the deformation as a function of the shear stress, if any, the contribution of the secondary bonds to the shear stress. The secondary bonds were identified as VAN DER WAALS attraction between the emulsion droplets and the primary bonds as interactions between polyelectrolyte molecules adsorbed on different droplets. Again it was found that the VAN DER WAALS attraction is relatively unimportant. From the found contribution to the shear modulus of an emulsion due to VAN DER WAALS attraction and steric repulsion between the droplets the interparticle distance was calculated to be 25–30 nm. This value was of the same order of magnitude as the results of the film thickness measurements. A semiquantitative assessment of the activation energy necessary to break a polyelectrolyte-polyelectrolyte bond showed that the interactions between the methyl groups must have a cooperative character.

It was concluded that the results of creep and dynamic measurements support each other.

In conclusion, this study shows that both rheological measurements of sterically stabilized dispersions and the investigation of polymer stabilized thin liquid films are excellent tools for investigating the interactions between adsorbed macromolecules. Intramolecular interactions and interactions between macromolecules adsorbed on different interfaces are very similar. The latter interactions are dominated by the outer part of the adsorbed macromolecule layers.

SAMENVATTING

Het doel van het beschreven onderzoek was meer inzicht te verkrijgen in de inter- en intra-molekulaire wisselwerkingen tussen geadsorbeerde macromolekulen. Teneinde dit te bereiken werden verschillende experimentele methodes en theoretische benaderingen gebruikt. Uiteengezet werd dat zowel reologische metingen aan emulsies als de bepaling van de eigenschappen van door polymeer gestabiliseerde vrije vloeistoffilms goede perspectieven bieden om wisselwerkingen tussen geadsorbeerde macromolekulen te onderzoeken. Daarbij werden twee verschillende macromolekulen gebruikt, nl. het niet-ionogene polyvinyl alcohol (PVA) en een polyelektrolyt: een copolymeer van methacrylzuur en de methyl ester van methacrylzuur (PMA-pe).

De karakterisering van de gebruikte stoffen is beschreven in hoofdstuk 2. De conformatie-overgang die plaatsvindt in opgeloste polymethacrylaten werd kort bediscussieerd. Deze polyelektrolyten komen bij een lage pH voor in een uitzonderlijk compacte conformatie. Boven een pH van ongeveer 6 komen de molekulen voor in de normale meer uitgestrekte conformatie. Via viskositeitsmetingen aan PVA oplossingen werden conformatie parameters zoals de middelbare eindpuntsafstand, de lengte van een statistisch ketenelement en de lineaire expansiefactor bepaald. De conformatieparameters werden bepaald in 1 M glycerol oplossing. Ze worden namelijk gebruikt bij de berekeningen aan door PVA gestabiliseerde vrije vloeistoffilms. Bij deze experimenten was 1 M glycerol in de PVA oplossingen aanwezig teneinde de waterdampdruk te verlagen.

De experimentele methoden zijn beschreven in hoofdstuk 3. In het eerste deel werd de bereiding van de emulsies en het bepalen van eigenschappen ervan, zoals specifiek oppervlak en geadsorbeerde hoeveelheid, behandeld. Verschillende reologische meetmethoden werden in het tweede deel besproken. Een uitgebreidere beschrijving werd gegeven van de apparatuur waarmee de dynamische en de kruipmetingen werden uitgevoerd.

De diktemetingen van door polymeer gestabiliseerde vrije vloeistoffilms is behandeld aan het eind van hoofdstuk 3. Na een beschrijving van de apparatuur en de experimentele procedure volgde een discussie over de berekening van de dikten uit de intensiteit van het gereflecteerde licht. Het bleek dat voor de berekening van de correctie die toegepast moet worden op de equivalente vloeistoffilmdikten de uitgesmeerde geadsorbeerde polymeer-segmentlagen vervangen mogen worden door een blok-distributie.

De inter- en intra-molekulaire wisselwerkingen tussen de segmenten van het PMA-pe molekuul en het effekt van deze wisselwerkingen op de conformatie van de polyelektrolyt molekulen en op de reologische eigenschappen van emulsies gestabiliseerd door PMA-pe is behandeld in hoofdstuk 4. In de literatuur worden als oorzaak van de compacte conformatie bij lage pH, VAN DER WAALS aantrekking en hydrophobe binding tussen de methyl groepen in de hoofdketen

genoemd. Verder speelt COULOMBSE wisselwerking tussen de carboxyl groepen een rol bij de conformatie-overgang.

De conformatie-overgang tussen de uitzonderlijk compacte kluwen en de uitgestrektere conformatie van het polyelektrolyt molekuul werd bestudeerd met behulp van potentiometrische titratie aan opgelost en geadsorbeerd PMA-pe. Gegevens voor geadsorbeerd PMA-pe werden verkregen door titratie van een door dit polyelektrolyt gestabiliseerde emulsie. Aangetoond werd dat de conformatie-overgang ook plaatsvindt bij geadsorbeerd PMA-pe. Deze conformatie-overgang is terug te vinden in de reologische eigenschappen van paraffine – in – water emulsies gestabiliseerd door PMA-pe. Zowel uit de viskositeits- als uit de dynamische metingen kon geconcludeerd worden dat een sterke aantrekking tussen de emulsiedruppels alleen plaatsvindt als het PMA-pe molekuul in de compacte vorm geadsorbeerd is. Zowel de dynamische moduli als de viskositeit zijn dan uiterst hoog. Daarentegen zijn bij een hoge pH (hoge neutralisatiegraad α van het PMA-pe) de emulsies dun vloeibaar. Er is geen enkele aanwijzing dat dan ook aantrekking tussen de geadsorbeerde polyelektrolytlagen optreedt.

De belangrijkste conclusies van de genoemde experimenten waren:

a. de netto aantrekking tussen de PMA-pe segmenten bij lage α vindt ook plaats tussen de lussen en/of staarten geadsorbeerd op *een* emulsiedruppel;
b. de hoge waarden van de viskositeit en de dynamische moduli bij lage α worden veroorzaakt door aantrekking tussen de lussen en/of staarten geadsorbeerd op *verschillende* emulsiedruppels;
c. de twee typen van wisselwerkingskrachten zijn waarschijnlijk gelijk.

Deze conclusie werd bevestigd door de invloed van methanol op de viskositeit van door Na-PMA-pe gestabiliseerde emulsies en het effect van een verandering in de temperatuur na te gaan. Bovendien kon uit deze proeven geconcludeerd worden dat waarschijnlijk de uitzonderlijk compacte kluwen bij lage α in belangrijke mate het gevolg is van hydrophobe binding.

In hoofdstuk 4 werden ook enkele experimenten gerapporteerd waarmee de invloed van Ca^{++} ionen op de polyelektrolyt eigenschappen werd onderzocht. Uit potentiometrische titraties bleek dat in aanwezigheid van Ca^{++} ionen de conformatie-overgang is verschoven naar een hogere α. De overgang was weer terug te vinden in de reologische eigenschappen van emulsies gestabiliseerd door Ca-PMA-pe. De balans tussen de inter- en intra-molekulaire wisselwerkingskrachten en de wisselwerking zelf is gecompliceerder dan bij Na-PMA-pe het geval is. Dit ingewikkelder karakter is terug te vinden in de reologische eigenschappen van door Ca-PMA-pe gestabiliseerde emulsies.

De wisselwerkingen tussen geadsorbeerde macromolekulen werden nader onderzocht door de eigenschappen van door polymeer gestabiliseerde vrije vloeistoffilms te bestuderen. In hoofdstuk 5 werden zowel metingen gerapporteerd aan films gestabiliseerd door het niet ionogene PVA als aan films gestabiliseerd door het polyelektrolyt PMA-pe.

De wisselwerkingskrachten die in een PVA-film een rol spelen zijn: VAN DER WAALS aantrekking, hydrostatische druk en sterische wisselwerking. De VAN

DER WAALS aantrekking over een film kan berekend worden. De evenwichtsdikten van de PVA-films werden gemeten bij verschillende hydrostatische drukken. De sterische repulsiekracht F_S tussen twee geadsorbeerde PVA-lagen is dan te bepalen door $-F_S$ gelijk te stellen aan de hydrostatische druk en de VAN DER WAALS aantrekking. Op deze wijze is de sterische repulsiekracht voor verschillende evenwichtsdikten te berekenen. De vrije energie van sterische wisselwerking wordt vervolgens verkregen door grafische integratie van de kracht-afstand curven. Deze waarden kunnen vergeleken worden met theoretische voorspellingen.

Teneinde de vrije energie van sterische wisselwerking theoretisch te kunnen berekenen moest een model voor de segment-dichtheidsdistributie ontwikkeld worden. Het voorgestelde semikwantitatieve model was gebaseerd op het gegeven dat de molekuulgewichtsverdeling van het gebruikte PVA breed is en de veronderstelling dat een groot gedeelte van de segmenten is geadsorbeerd in de vorm van staarten. Aanwijzingen dat deze veronderstelling juist is, volgden uit een vergelijking van de naar $F_S \rightarrow 0$ geëxtrapoleerde filmdikte met de ellipsometrische dikte van een geadsorbeerde laag. Het model houdt in essentie in dat de eigenschappen van de buitenste delen van een geadsorbeerde laag bepaald worden door slechts enkele staarten. De vrije energie van sterische repulsie tussen twee geadsorbeerde PVA ($M_v = 27.000$ of 86.000) – lagen die berekend werd door gebruik te maken van dit model en de sterische repulsie theorie van HESSELINK e.a. (1971b) klopt goed met de experimenteel gevonden waarden voor redelijke staartlengten.

Naast de door PVA gestabiliseerde films werd in hoofdstuk 5 ook het drainage gedrag en de evenwichtsdikten van door PMA-pe gestabiliseerde films behandeld. De neutralisatiegraad α werd gevarieerd. De bij de verschillende α's gemeten evenwichtsdikten correleerden goed met ellipsometrische metingen aan een geadsorbeerde laag. Het drainage patroon was volkomen verschillend bij $\alpha = 0{,}1$ en 1,0. Bij een lage α zijn de films stijf terwijl ze bij $\alpha = 1{,}0$ beweeglijk zijn. Ook de dilatatie modulus nam af met toenemende α. Waarschijnlijk zijn dezelfde wisselwerkingskrachten tussen de polyelektrolyt segmenten verantwoordelijk voor de genoemde verschijnselen als die welke de conformatie-overgang in het molekuul en de drastische veranderingen in de reologische eigenschappen van door PMA-pe gestabiliseerde emulsies veroorzaken, bij verandering van α.

De reologische eigenschappen van door PMA-pe gestabiliseerde emulsies zijn meer in detail besproken in hoofdstuk 6. Zowel dynamische als kruipmetingen werden behandeld.

Bij de dynamische experimenten werd de opslagmodulus G' en de verliesmodulus G'' gemeten als functie van de frekwentie ω. Ook de neutralisatiegraad, de polyelektrolytconcentratie en de zoutconcentratie werden gevarieerd. Onder die omstandigheden dat de aantrekkingskrachten in het polyelektrolyt overheersen, geleert PMA-pe in oplossing. Een vergelijking van de geleringsconcentratie met de PMA-pe concentratie tussen twee naast elkaar gelegen emulsiedruppels wijst erop dat tussen die druppels een micro-gel gevormd kan worden.

Deze aanwijzing wordt ondersteund door een nadere beschouwing van de $G'(\omega)$ en $G''(\omega)$ curven. Het is mogelijk voor die gevallen dat een gel gevormd wordt, een vergelijking af te leiden waarin G' gerelateerd wordt aan het aantal polyelektrolyt-polyelektrolyt bindingen tussen twee emulsiedruppels. Vergelijkingen werden afgeleid voor het geval dat een emulsie beschreven kan worden met een ideaal netwerk model of met een aggregaat model. Daarnaast werden overeenkomstige relaties afgeleid tussen G' en de VAN DER WAALS aantrekking tussen de emulsiedruppels. Een semikwantitatieve berekening toonde aan dat de eigenschappen van de visko-elastische emulsies verklaard kunnen worden met het ideale netwerk model. De VAN DER WAALS aantrekking tussen de emulsiedruppels bleek veel minder belangrijk dan de wisselwerkingen tussen de geadsorbeerde polyelektrolyt molekulen. Berekend werd dat bij α PMA-pe = 0,1 ongeveer 400–1000 polyelektrolyt-polyelektrolyt bindingen gevormd worden tussen twee emulsiedruppels. Dit betekent dat ongeveer 10–20% van de polyelektrolyt molekulen die in het contact gebied tussen twee emulsiedruppels aan een van beide grensvlakken geadsorbeerd zijn, direct betrokken zijn bij de vorming van deze bindingen.

De verwachting is dat de gemeten grote waarden van de verliesfactor tg δ veroorzaakt worden, doordat tijdens elke deformatie cyclus, vloeistof in en uit het micro-gel tussen twee emulsiedruppels moet bewegen, of door de relaxatie van een aantal polyelektrolyt-polyelektrolyt bindingen.

Bij de interpretatie van de kruipmetingen werd aangenomen dat tussen de emulsiedruppels zwakke en sterke bindingen bestaan. Kruipmetingen kunnen in principe zo uitgevoerd worden dat de zwakke (secondaire) bindingen breken, maar de sterke (primaire) bindingen niet. Het is dan mogelijk uit een eventuele niet-lineariteit van de deformatie als functie van de afschuifspanning, de bijdrage van de secondaire bindingen aan de afschuifspanning te berekenen. Een essentiële voorwaarde is dat tijdens de metingen de samenhang van de monsters bewaard blijft. De secondaire bindingen werden geidentificeerd als de VAN DER WAALS aantrekkingskrachten tussen de emulsiedruppels en de primaire bindingen met de wisselwerkingen tussen de polyelektrolyt molekulen geadsorbeerd op verschillende emulsiedruppels. Uit de berekeningen volgde weer dat de VAN DER WAALS aantrekking relatief onbelangrijk is. De afstand tussen twee emulsiedruppels kon berekend worden als zijnde 25–30 nm. Deze waarden kloppen redelijk met de resultaten van de filmdiktemetingen. Uit een grootteorde berekening van de activeringsenergie, nodig om een polyelektrolyt-polyelektrolyt binding te breken, volgde dat de wisselwerkingen tussen de methyl groepen een coöperatief karakter moeten hebben.

De resultaten van de dynamische en de kruipmetingen bleken goed met elkaar te kloppen.

Als conclusie van dit onderzoek kan gesteld worden dat zowel reologische metingen aan sterisch gestabiliseerde dispersies als het bestuderen van door polymeer gestabiliseerde vrije vloeistoffilms uitstekende methoden zijn om de wisselwerkingen tussen geadsorbeerde macromolekulen te bestuderen. De

intramolekulaire interacties en die tussen macromolekulen geadsorbeerd op verschillende grensvlakken bleken zeer sterk met elkaar overeen te komen. De laatst genoemde interacties worden in sterke mate bepaald door de eigenschappen van het buitenste deel van de geadsorbeerde laag. De staarten kunnen hierbij een relatief zeer belangrijke rol spelen.

ACKNOWLEDGEMENTS

The investigation described in this thesis was carried out in the Laboratory for Physical and Colloid Chemistry of the Agricultural University, Wageningen, and was financially supported by Unilever Research Laboratory, Vlaardingen.

The author is very much indebted to Prof. Dr. J. Lyklema and to Dr. M. van den Tempel for their stimulating interest and constructive criticism during this study.

The development and the construction of the electronic part of the apparatus for thickness measurements on polymer stabilized films was the work of Mr. R. A. J. Wegh. The mechanical part of this apparatus was built by Mr. S. Maasland and Mr. H. E. van Beek. These essential contributions to the investigations dealing with polymer stabilized films are much appreciated.

Thanks are due to Mr. J. Benjamins of the Department of Physical Chemistry of Unilever Research Laboratory, Vlaardingen for carrying out the ellipsometric and surface dilatational modulus measurements.

Many of the rheological measurements have been carried out by students. The author wishes to express his thanks to Miss J. Bakker, Mr. M. A. J. S. van Boekel, Ir. R. G. van Driel, Miss Ir. J. Hamoen, Ir. A. C. M. van Hooydonk and Ir. G. J. Mocking.

Thanks are also due to Mrs. M. Heitkamp-Rijckaert, who typed the manuscript and Mr. G. Buurman, who prepared the drawings.

The friendship and helpfulness of the members of the Department of Physical and Colloid Chemistry is gratefully mentioned.

Finally Mr. H. Chabot is kindly acknowledged for correcting the English text of this thesis.

REFERENCES

AGTEROF, W. G. M. (1975). Personal communication.

ANUFRIEVA, E. V., BIRSHTEIN, T. M., NEKRASOVA, T. N., PTITSYN, O. B. and SHEVELEVA, T. V. (1968). J. Polym. Sci. C. **16**, 3519.

ARNOLD, R. and OVERBEEK, J. Th. G. (1950). Recl. Trav. Chim. Pays Bas **69**, 192.

BAGCHI, P. (1974). J. Colloid Interface Sci. **47**, 100.

BARRY, B. W. (1975). Adv. Colloid Interface Sci. **5**, 37.

BEGALA, A. J. and STRAUSS, U. P. (1972). J. Phys. Chem. **76**, 254.

BELTMAN, H. (1975). Thesis, Agricultural University, Wageningen, The Netherlands; Meded. Landbouwhogeschool Wageningen 75-2 (1975) (in Dutch).

BENJAMINS, J., FEYTER, J. A. DE, EVANS, M. T. A., GRAHAM, D. E. and PHILLIPS, M. (1975). Faraday Discussions Chem. Soc. **59**, 218.

BISWAS, B. and HAYDON, D. A. (1962). Kolloid Z.-Z. Polym. **185**, 31.

BOER, J. H. DE (1936). Trans. Faraday Soc. **32**, 10.

BÖHM, J. Th. C. (1974). Thesis, Agricultural University, Wageningen, The Netherlands; Meded. Landbouwhogeschool Wageningen 74-5 (1974).

BÖHM, J. Th. C. and LYKLEMA, J. (1975). J. Colloid Interface Sci. **50**, 559.

BÖHM, J. Th. C. and LYKLEMA, J. (1976). In: Theory and Practice of Emulsion Technology, A. L. Smith, Ed., Academic Press, London/New York, 23.

BOOTSMA, G. A. and MEYER, F. (1969). Surf. Sci. **14**, 52.

BRUIL, H. G. (1970). Thesis, Agricultural University, Wageningen, The Netherlands; Meded. Landbouwhogeschool Wageningen 70-9 (1970).

CASIMIR, H. B. G. and POLDER, D. (1948). Phys. Rev. **73**, 360.

CASPER, J., BERLINER, C., RUYSSCHAERT, J. M. and JAFFE, J. (1974). J. Colloid Interface Sci. **49**, 433.

CLAYFIELD, E. J. and LUMB, E. C. (1966). J. Colloid Interface Sci. **22**, 269.

CLAYFIELD, E. J. and LUMB, E. C. (1968). Macromolecules **1**, 133.

CLUNIE, J. S., GOODMAN, J. F. and INGRAM, B. T. (1971). In: Surface and Colloid Sci., E. Matijevic, Ed., John Wiley & Sons, New York **3**, 167.

CONIO, G., PATRONE, E., RUSSO, S. and TREFILETTI, V. (1976). Makromol. Chem. **177**, 49.

CRESCENZI, V., QUADRIFOGLIO, F. and DELBEN, F. (1972). J. Polym. Sci. A-2 **10**, 357.

CUTNELL, J. D. and GLASEL, J. A. (1976). Macromolecules **9**, 71.

DAVIS, S. (1971). J. Pharm. Sci. **60**, 1351.

DBP 947 115 (1956). Assigned to Röhm and Haas GmbH., Darmstadt.

DELBEN, F., CRESCENZI, V. and QUADRIFOGLIO, F. (1972). Eur. Polym. J. **8**, 933.

DERYAGIN, B. V. (1934). Kolloid Z. **69**, 155.

DOROSZKOWSKI, A. and LAMBOURNE, R. (1971). J. Polym. Sci. C **34**, 253.

DOROSZKOWSKI, A. and LAMBOURNE, R. (1973). J. Colloid Interface Sci. **43**, 97.

DUBIN, P. L. and STRAUSS, U. P. (1970). J. Phys. Chem. **74**, 2842.

DUISER, J. A. (1965). Thesis, State University, Leiden, The Netherlands (in Dutch).

DUYVIS, E. M. (1962). Thesis, State University, Utrecht, The Netherlands.

DZYALOSHINSKII, I. E., LIFSHITS, E. M. and PITAEVSKII, L. P. (1959). Zhur. Eksp. i. Teor. Fiz. **37**, 229.

ECCLESTON, G. M., BARRY, B. W. and DAVIS, S. S. (1973). J. Pharm. Sci. **62**, 1954.

ELIASSAF, J. and SILBERBERG, A. (1962). Polymer **3**, 555.

ELIASSAF, J. (1965). J. Polym. Sci. B **3**, 767.

EVANS, R. and NAPPER, D. H. (1973a). Kolloid Z.-Z. Polym. **251**, 409.

EVANS, R. and NAPPER, D. H. (1973b). Kolloid Z.-Z. Polym. **251**, 329.

FENYO, J. C., BEAUMAIS, J. and SELEGNY, E. (1974). J. Polym. Sci. A-1 **12**, 2659.

FERRY, J. D. (1970). Viscoelastic properties of polymers, 2nd Ed., John Wiley & Sons, New York/London.

FINCH, C. A. (1968). Properties and Applications of Polyvinyl Alcohol, S.C.I. Monograph **30**, Soc. Chem. Ind., London.
FINCH, C. A. (1973). Polyvinyl Alcohol, Monograph, John Wiley & Sons, London.
FISCHER, E. W. (1958). Kolloid Z. **160**, 120.
FISCHER, S. and KUNIN, R. (1956). J. Phys. Chem. **60**, 1030.
FLEER, G. J. (1971). Thesis Agricultural University, Wageningen, The Netherlands; Meded. Landbouwhogeschool Wageningen 71-20 (1971).
FLORY, P. J. (1953). Principles of Polymer Chemistry, Cornell University Press, Ithaca.
FRANKEL, S. P. and MYSELS, K. J. (1966). J. Appl. Phys. **37**, 3725.
FRANKS, F. (1973). Water, Plenum Press, New York/London, **2**, chapter 1.
FRIEND, J. P. and HUNTER, R. J. (1971). J. Colloid Interface Sci. **37**, 548.
FRISCH, H. L. and SIMHA, R. (1954). J. Phys. Chem. **58**, 507.
FRISCH, H. L. (1955). J. Phys. Chem. **59**, 633.
FRISCH, H. L. and SIMHA, R. (1957). J. Chem. Phys. **27**, 702.
GOULDEN, J. D. S. (1958). Trans. Faraday Soc. **54**, 941.
GRAHAM, D. E. and PHILLIPS, M. C. (1976a). In: Theory and Practice of Emulsion Technology, A. L. Smith, Ed., Academic Press, London/New York, 75.
GRAHAM, D. E. and PHILLIPS, M. C. (1976b). In: Foams, R. J. Akers, Ed., Academic Press, London/New York.
GREGOR, H. P. and FREDERICK, M. (1957a). J. Polym. Sci. **23**, 451.
GREGOR, H. P., GOLD, D. C. and FREDERICK, M. (1957b). J. Polym. Sci. **23**, 467.
HAMAKER, H. C. (1937). Physica **4**, 1058.
HESSELINK, F. Th. (1969). J. Phys. Chem. **73**, 3488.
HESSELINK, F. Th. (1971a). J. Phys. Chem. **75**, 65.
HESSELINK, F. Th., VRIJ, A. and OVERBEEK, J. Th. G. (1971b). J. Phys. Chem. **75**, 2094.
HESSELINK, F. Th. (1972). J. Electroanal. Chem. **37**, 317.
HESSELINK, F. Th. (1975). J. Colloid Interface Sci. **50**, 606.
HILDEBRAND, J. H. (1968). J. Phys. Chem. **72**, 1841.
HOEVE, C. A. J. (1965). J. Chem. Phys. **43**, 3007.
HOEVE, C. A. J., DIMARZIO, E. A. and PEYSER, P. (1965). J. Chem. Phys. **42**, 2558.
HOEVE, C. A. J. (1966). J. Chem. Phys. **44**, 1505.
HOEVE, C. A. J. (1970). J. Polym. Sci. C **30**, 361.
HOEVE, C. A. J. (1971). J. Polym. Sci. C **34**, 1.
HOWARTH, O. W. (1975). J. Chem. Soc., Faraday Trans. I **71**, 2303.
HUGLIN, M. B. (1975). In: Polymer Handbook, J. Brandrup and E. H. Immergut, Eds., John Wiley & Sons, New York.
HUPPENTHAL, L. (1963). Rocz. Chem. **37**, 1001.
INOKUCHI, K. (1955). Bull. Chem. Soc. Jap. **28**, 453.
JENKEL, E. and RUMBACH, B. (1951). Z. Electrochem. **55**, 612.
KANNER, B. and GLASS, J.E. (1969). Ind. Eng. Chem. **61**, 31.
KATCHALSKY, A. and GILLIS, J. (1949). Rec. Trav. Chim. Pays Bas **68**, 879.
KATCHALSKY, A. and EISENBERG, H. (1951a). J. Polym. Sci. **6**, 145.
KATCHALSKY, A. (1951b). J. Polym. Sci. **7**, 393.
KATCHALSKY, A. (1971). Pure Appl. Chem. **26**, 327.
KAUZMAN, W. (1959). Advan. Protein Chem. **14**, 1.
KAY, P. J., KELLY, D. P., MILGATE, G. I. and TRELOAR, F. E. (1976). Makromol. Chem. **177**, 885.
KEDEM, O. and KATCHALSKY, A. (1955). J. Polym. Sci. **15**, 321.
KITCHENER, J. A. and MUSSELWHITE, P. R. (1968). In: Emulsion Science, P. Sherman, Ed., Academic Press, London.
KLENIN, V. J., KLENINA, O. V., SHVARTSBURD, B. I. and FRENKEL, S. Ya. (1974). J. Polym. Sci. C **44**, 131.
KOOPAL, L. K. and LYKLEMA, J. (1975). Faraday Discussions Chem. Soc. **59**, 230.
KUHN, W. (1934). Kolloid Z. **68**, 2.

KURATA, M., TSUNASHIMA, Y., IWEMA, M. and KAMADA, K. (1975). In: Polymer Handbook, J. Brandrup and E. H. Immergut, Eds., John Wiley & Sons, New York.
LANDO, J. B., KOENIG, J. L. and SEMEN, J. (1973). J. Macromol. Sci., Phys. B **7**, 319.
LANKVELD, J. M. G. (1970). Thesis, Agricultural University, Wageningen, The Netherlands; Meded. Landbouwhogeschool Wageningen, 70-21 (1970).
LANKVELD, J. M. G. and LYKLEMA, J. (1972a). J. Colloid Interface Sci. **41**, 454.
LANKVELD, J. M. G. and LYKLEMA, J. (1972b). J. Colloid Interface Sci. **41**, 466.
LANKVELD, J. M. G. and LYKLEMA, J. (1972c). J. Colloid Interface Sci. **41**, 475.
LEYTE, J. C. and MANDEL, M. (1964). J. Polym. Sci. A **2**, 1879.
LEYTE, J. C. (1966). J. Polym. Sci. B **4**, 245.
LEYTE, J. C., ARBOUW-VAN DER VEEN, H. M. R. and ZUIDERWEG, L. H. (1972). J. Phys. Chem. **76**, 2559.
LIFSHITS, E. M. (1955). Zhur. Eksp. i. Teor. Fiz. **29**, 94.
LIPATOV, Y. S., ZUBOV, P. I. and ANDRYUSHCHENKO, E. A. (1959). Colloid J. USSR **21**, 57.
LODGE, A. S. (1964). Elastic Liquids. An Introductory Vector Treatment of Finite Strain Polymer Rheology, Academic Press, London.
LONDON, F. (1930). Z. Physik **63**, 245.
LONDON, F. (1937). Trans. Faraday Soc. **33**, 8.
LUCASSEN, J. and TEMPEL, M. VAN DEN (1972). J. Colloid Interface Sci. **41**, 491.
LUCASSEN-REYNDERS, E. H. and LUCASSEN, J. (1969). Adv. Colloid Interface Sci. **2**, 347.
LYKLEMA, J. and MYSELS, K. J. (1965a). J. Am. Chem. Soc. **87**, 2539.
LYKLEMA, J., SCHOLTEN, P. C. and MYSELS, K. J. (1965b). J. Phys. Chem. **69**, 116.
LYKLEMA, J. (1968). Adv. Colloid Interface Sci. **2**, 65.
MACKOR, E. L. (1951). J. Colloid Sci. **6**, 492.
MACKOR, E. L. and WAALS, J. H. VAN DER (1952). J. Colloid Sci. **7**, 535.
MACRITCHIE, F. (1976). J. Colloid Interface Sci. **56**, 53.
MANDEL, M. and STADHOUDER, M. G. (1964). Makromol. Chem. **80**, 141.
MANDEL, M., LEYTE, J. C. and STADHOUDER, M. G. (1967). J. Phys. Chem. **71**, 603.
MANDEL, M. (1970). Eur. Polym. J. **6**, 807.
MANDEL, M. and STORK, W. H. J. (1974). Biophys. Chem. **2**, 137.
MCCRACKIN, F. L. and COLSON, J. P. (1964). In: Ellipsometry in the Measurement of Surface and Thin Films, Symp. Proceedings, Washington 1963, E. Passaglia, R. R. Stromberg and J. Kruger, Eds., Nat. Bur. Stand. Misc. Publ. **256**, 61.
MEIER, D. J. (1967). J. Phys. Chem. **71**, 1861.
MICHAELI, I. (1960). J. Polym. Sci. **48**, 291.
MORAWETZ, H. (1965). Macromolecules in Solution, Interscience Publ. New York.
MORAWETZ, H. and KANDANIAN, A. Y. (1966). J. Phys. Chem. **70**, 2995.
MOTOMURA, K. and MATUURA, R. (1969). J. Chem. Phys. **50**, 1281.
MULLER, G. (1974). J. Polym. Sci. B **12**, 319.
MUSSELWHITE, P. R. and KITCHENER, J. A. (1967). J. Colloid Interface Sci. **24**, 80.
MUSSELWHITE, P. R. and PALMER, J. (1968). Vth Intern. Congr. Surface Activity, Barcelona, Proceedings **2**, 505.
MYSELS, K. J., SHINODA, K. and FRANKEL, S. (1959). Soap Films, Studies of Their Thinning and a Bibliography, Pergamon Press, New York.
NAGASAWA, M., MURASE, T. and KONDO, K. (1965). J. Phys. Chem. **69**, 4005.
NAGASAWA, M. (1971). Pure Appl. Chem. **26**, 519.
NEDERVEEN, C. J. (1963). J. Colloid Sci. **18**, 276.
NÉMETHY, G. and SCHERAGA, H. A. (1962a). J. Chem. Phys. **36**, 3401.
NÉMETHY, G. and SCHERAGA, H. A. (1962b). J. Phys. Chem. **66**, 1773.
NEVILLE, P. C. and HUNTER, R. J. (1974). J. Colloid Interface Sci. **49**, 204.
NIELSEN, L. E., WALL, R. and ADAMS, G. (1958). J. Colloid Sci. **13**, 441.
NORDE, W. (1976). Thesis, Agricultural University, Wageningen, The Netherlands; Meded. Landbouwhogeschool Wageningen 76-6 (1976).
OAKENFULL, D. G. and FENWICK, D. E. (1974). J. Phys. Chem. **78**, 1759.
OAKENFULL, D. G. and FENWICK, D. E. (1975). Aust. J. Chem. **28**, 715.

OKAMOTO, H. and WADA, Y. (1974). J. Polym. Sci. A-2 **12**, 2413.
O'NEILL, J. J., LOEBL, E. M., KANDANIAN, A. Y. and MORAWETZ, H. (1965). J. Polym. Sci. A **3**, 4201.
OOSAWA, F. (1971). Polyelectrolytes, Marcel Dekker, Inc., New York.
OSMOND, D. W. J., VINCENT, B. and WAITE, F. A. (1973). J. Colloid Interface Sci. **42**, 262.
OSMOND, D. W. J., VINCENT, B. and WAITE, F. A. (1975). Colloid Polym. Sci. **253**, 676.
OTTER, J. L. DEN (1967). Thesis, State University, Leiden, The Netherlands.
OVERBEEK, J. Th. G. (1948). Bull. Soc. Chim. Belg. **57**, 252.
OVERBEEK, J. Th. G. (1952). In: Colloid Science, H. R. Kruyt, Ed., Elsevier, Amsterdam, **I**, chapter 10.
PAPENHUIZEN, J. M. P. (1971). Rheol. Acta **10**, 493.
PAPENHUIZEN, J. M. P. (1972). Rheol. Acta **11**, 73.
PATAT, F., KILLMAN, E. and SCHLIEBENER, C. (1964). Fortschr. Hochpolym. Forsch. **3**, 332.
PRIEL, Z. and SILBERBERG, A. (1970a). J. Polym. Sci. A-2 **8**, 689.
PRIEL, Z. and SILBERBERG, A. (1970b). J. Polym. Sci. A-2 **8**, 705.
PRINS, A. and TEMPEL, M. VAN DEN (1970). Special Discussions Faraday Soc. **1**, 20.
PRITCHARD, J. G. (1970). Polyvinyl Alcohol, Basic Properties and Uses, Polymer Monographs **4**, Gordon and Breach, London.
ROBERTS, R. T. (1976). In: Foams, R. J. Akers, Ed., Academic Press, London/New York.
ROE, R. J. (1965). J. Chem. Phys. **43**, 1591.
ROE, R. J. (1966). J. Chem. Phys. **44**, 4264.
ROWLAND, F. W. and EIRICH, F. R. (1966). J. Polym. Sci. A-1 **4**, 2401.
SAKAI, T. (1968). J. Polym. Sci. A-2 **6**, 1659.
SCHOLTENS, B. J. R. (1977). Thesis, Agricultural University, Wageningen, The Netherlands; Meded. Landbouwhogeschool Wageningen, in course of preparation.
SHELUDKO, A. (1962). Proc. Koninkl. Ned. Akad. v. Wetenschap. B **65**, 87.
SHELUDKO, A. (1967). Adv. Colloid Interface Sci. **1**, 391.
SHERMAN, P. (1968). Emulsion Science, A. C. S. Monograph, Academic Press, London.
SILBERBERG, A., ELIASSAF, J. and KATCHALSKY, A. (1957). J. Polym. Sci. **23**, 259.
SILBERBERG, A. (1962a). J. Phys. Chem. **66**, 1872.
SILBERBERG, A. (1962b). J. Phys. Chem. **66**, 1884.
SILBERBERG, A. (1967). J. Chem. Phys. **46**, 1105.
SILBERBERG, A. (1968). J. Chem. Phys. **48**, 2835.
SILBERBERG, A. and MIJNLIEFF, P. F. (1970). J. Polym. Sci. A-2 **8**, 1089.
SILBERBERG, A. (1975). Faraday Discussions Chem. Soc. **59**, 203.
SONNTAG, H. (1968). Tenside **5**, 188.
SONNTAG, H. (1976). Personal communication.
STOCKMAYER, W. H. and FIXMAN, M. (1963). J. Polym. Sci. C **1**, 137.
STRENGE, K. and SONNTAG, H. (1974). Colloid Polymer Sci. **252**, 133.
STRENGE, K. and SONNTAG, H. (1975). Intern. Conf. Colloid and Surface Sci., Budapest, Proceedings, E. Wolfram, Ed., Akadémiai Kiadó, Budapest **1**, 397.
STROMBERG, R. R. (1967). In: Treatise on Adhesion and Adhesives, R. L. Patrick, Ed., Dekker, New York.
TAN, J. S. and GASPER, S. P. (1974). J. Polym. Sci. A-2 **12**, 1785.
TAN, J. S. and SCHNEIDER, R. L. (1975). J. Phys. Chem. **79**, 1380.
TANFORD, C. (1961). Physical Chemistry of Macromolecules, John Wiley & Sons, New York.
TANFORD, C. (1973). The Hydrophobic Effect, John Wiley & Sons, New York.
TEMPEL, M. VAN DEN (1958). Rheol. Acta **1**, 115.
TEMPEL, M. VAN DEN (1961). J. Colloid Sci. **16**, 284.
TEMPEL, M. VAN DEN (1963). In: Rheology of Emulsions, P. Sherman, Ed., Pergamon Press, London, chapter 1.
TEMPEL, M. VAN DEN (1974). Personal communication.
TEMPEL, M. VAN DEN (1976). Personal communication.
TOBOLSKY, A. and EYRING, H. (1943). J. Chem. Phys. **11**, 125.

TOYOSHIMA, K. (1968). In: Properties and Applications of Polyvinyl Alcohol, S.C.I. Monograph **30** Soc. Chem. Ind., London.
VAŠIČEK, C. J. (1960). Optics of Thin Films, North-Holland Publishing Co., Amsterdam.
VERWEY, E. J. W. and OVERBEEK, J. Th. G. (1948). Theory of the Stability of Lyophobic Colloids, Elsevier, Amsterdam.
VINCENT, B. (1974). Adv. Colloid Interface Sci. **4**, 193.
VISSER, J. (1972). Adv. Colloid Interface Sci. **3**, 331.
VLIET, T. VAN and LYKLEMA, J. (1975). Intern. Conf. Colloid and Surface Sci., Budapest, Proceedings, E. Wolfram, Ed., Akadémiai Kiadó, Budapest **1**, 197.
VÖLKER, Th. (1961a). Makromol. Chem. **XLIV-XLVI**, 107.
VÖLKER, Th. (1961b). Oesterreichische Chem. Z. **62**, 345.
VRIES, A. J. DE (1958). Rec. Trav. Chim. **77**, 383.
VRIJ, A. (1966). Faraday Discussions Chem. Soc. **42**, 23.
VRIJ, A. and OVERBEEK, J. Th. G. (1968). J. Am. Chem. Soc. **90**, 3074.
VRIJ, A., HESSELINK, F. Th., LUCASSEN, J. and TEMPEL, M. VAN DEN (1970). Proc. Koninkl. Ned. Akad. v. Wetenschap. **B 73**, 124.
WALSTRA, P. (1965). Neth. Milk Dairy J. **19**, 93.
WALSTRA, P. (1968). J. Colloid Interface Sci. **27**, 493.
WALSTRA, P. and OORTWIJN, H. (1969). J. Colloid Interface Sci. **29**, 424.
WOJTCZAK, Z. (1965). J. Polym. Sci. A **3**, 3613.
WOJTCZAK, Z. (1966). J. Polym. Sci. A-1 **4**, 969.
YAACOBI, M. and BEN-NAIM, A. (1973). J. Solution Chem. **2**, 425.
YAMAKAWA, H. (1971). Modern Theory of Polymer Solutions, Harper & Row Publ., New York.

LIST OF SYMBOLS

PVA	polyvinyl alcohol
PVAc	polyvinyl acetate
PMA	polymethacrylic acid
PMA-pe	copolymer of methacrylic acid and the methyl ester of methacrylic acid
PAA	polyacrylic acid
PAA-pe	copolymer of acrylic acid and the methyl ester of acrylic acid
MeOH	methanol
EtOH	ethanol
a	exponent in the MARK-HOUWINK equation (eq. 2.2.)
A	HAMAKER constant
A_{eff}	effective contact region between two emulsion droplets, m^2
b	number of polymer bonds between two emulsion droplets
c'	number of elastically effective chains per bond (cross-link)
c_p	polyelectrolyte concentration
d	droplet diameter, m
D	rate of shear, s^{-1}
f'	retardation correction factor to the short range VAN DER WAALS attraction energy
f''	ibid to the force
F	force between two emulsion droplets
F_A	VAN DER WAALS attraction force, Nm^{-2}
F_H	hydrostatic pressure, Nm^{-2}
F_S	steric repulsion force, Nm^{-2}
$\Delta_{hb}F^0$	standard free energy of formation of a hydrophobic bond
g_1	average resilience of primary bonds, Nm^{-1}
g_2	ibid for secondary bonds, Nm^{-1}
G	shear modulus, Nm^{-2}
G'	storage shear modulus, Nm^{-2}
G''	loss shear modulus, Nm^{-2}
G'_g	storage modulus of the micro-gel formed between two emulsion droplets, Nm^{-2}
G_0	instantaneous shear modulus, Nm^{-2}
G_{pol}	contribution to the shear modulus of an emulsion attributable to the interaction between polyelectrolyte molecules adsorbed on different droplets, Nm^{-2}
G_{vdW}	contribution to the shear modulus of an emulsion due to VAN DER WAALS attraction and steric repulsion between the droplets, Nm^{-2}
ΔG^0	standard free energy change of dissociation
ΔG_{el}	electrostatic contribution to the free energy change of dissociation of a polyacid

h	thickness of a free liquid polymer film, nm
h_f	equivalent aqueous solution thickness, nm
h_s	film thickness at which maximum reflection occurs (silvery film), nm
h_1	thickness of the equivalent polymer surface layer, nm
h_2	thickness of the aqueous core of the film, nm
h^*	correction to be applied to the equivalent aqueous solution thickness in order to obtain the real thickness, nm
H	distance between two emulsion droplets, nm
H_0	shortest, distance in equilibrium between two emulsion droplets, nm
ΔH	elongation of the distance between two emulsion droplets upon deformation, nm
i	number of statistical chain elements in a loop or tail
$\bar{i}$	average number of statistical chain elements per loop or tail
I_0	intensity of incident light beam
I_r	intensity of reflected light beam
I_s	reflected intensity from the silvery film (first maximum)
J	shear compliance, $N^{-1}m^2$
k'	HUGGINS constant
k_1	MARK-HOUWINK constant
K	apparent ionization constant
K_0	intrinsic ionization constant
K_{av}	averaged ionization constant in the HENDERSON-HASSELBALCH equation (eq. 4.8.)
l	height difference between the film and the level of the bulk solution
l_s	length of a statistical chain element
m	number of chains connecting two aggregates (Ch. 6)
M_v	viscosity average molecular weight
M_1	contribution of primary bonds to the shear modulus, Nm^{-2}
M_2	ibid for secondary bonds, Nm^{-1}
$M(\bar{i},h)$	dimensionless osmotic function (eq. 5.17.)
n	number of emulsion droplets per aggregate (Ch. 6)
n_f	refractive index of a film consisting solely of aqueous solution
n_0	refractive index of air
n_1	refractive index of the equivalent polymer surface layer
n_2	ibid of the aqueous core of the film
n_1	number of primary bonds per unit of length in the direction of the stress (Ch. 6), m^{-1}
n_2	ibid for secondary bonds (Ch. 6), m^{-1}
N	number of emulsion droplets per unit volume, m^{-3}
N_1	number of primary bonds in a cross section normal to the direction of the stress, m^{-2}
N_2	ibid for secondary bonds, m^{-2}
N_A	number of aggregates per unit volume, m^{-3}

N_t	total number of polymer segments adsorbed per unit area
r	FRESNEL coefficient
$(\overline{r^2})^{1/2}$	root mean square end-to-end distance
$(\overline{s^2})^{1/2}$	root mean square radius of gyration
t_{el}	ellipsometric thickness of an adsorbed layer
t_{rms}	root mean square thickness of an adsorbed layer
ΔU_2	mean energy of activation for breaking a secondary bond
V_A	VAN DER WAALS attraction energy, Jm^{-2}
V_S	steric repulsion energy, Jm^{-2}
V_{VR}	free energy of repulsion due to volume restriction
V_M	free energy of repulsion due to the mixing term
w	number of polymer molecules adsorbed on A_{eff}
$W(\bar{\imath},h)$	dimensionless volume restriction function (eq. 5.15.)
x	distance to the interface (Ch.5)
X_t	percentage of segments adsorbed as tails
α	degree of neutralization
α'	degree of ionization
α''	angle of refraction
α	linear expansion factor (sections 2.5., 5.2. and 5.3.)
α_η	hydrodynamic expansion factor
β	LONDON constant, Jm^6
γ	shear strain
γ_0	instantaneous shear strain (creep measurements)
γ_0	maximum shear strain (dynamic measurements)
Γ	amount of polymer adsorbed per unit area, mg m^{-2}
δ	phase angle between stress and strain
δ	thickness of the first polymer layer on the surface (Ch. 5)
ε	surface dilatational modulus, mN m^{-1}
η	viscosity, Nsm^{-2}
η_{re}	viscosity ratio excess
$[\eta]$	intrinsic viscosity, dl g^{-1}
η_ω	dynamic viscosity, Nsm^{-2}
Θ	theta temperature
λ	wavelength, nm
λ_2	distance across which two droplets must be moved apart to break bonds of type 2
ν	number of elastically effective chains, m^{-3}
$\rho(x)$	polymer segment density distribution
$\Delta\rho$	density difference between the film phase and the outer phase
σ	shear stress Nm^{-2}
σ_0	instantaneous shear stress (creep measurements)
σ_0	maximum shear stress (dynamic measurements)
τ	relaxation time
υ	number of tails or loops per unit area

ϕ	volume fraction of dispersed phase
Φ	FLORY constant
ω	angular frequency, s^{-1}

ENKELE PERSOONLIJKE GEGEVENS

De middelbare schoolopleiding volgde ik op de Marnix M.U.L.O. te Maassluis, waarna ik de Hogere Landbouwschool te Dordrecht bezocht. In 1966 werd de studie aan de Landbouwhogeschool te Wageningen begonnen. Het kandidaatsexamen Levensmiddelentechnologie (chemisch-biologische specialisatie) werd afgelegd in januari 1971 en het ingenieursexamen in juni 1973. De ingenieursstudie omvatte naast het hoofdvak Levensmiddelenchemie de bijvakken Fysische en Kolloidchemie (verzwaard) en Technische Microbiologie.

Vanaf januari 1974 tot januari 1977 was ik werkzaam als promotieassistent op het Laboratorium voor Fysische en Kolloidchemie van de Landbouwhogeschool te Wageningen.